Settlement calculation for lime/cement column improved clay

Analytical and numerical analyses related to a case study

Hulumtaye Kefyalew

Master of Science Thesis 18/01
Division of Soil and Rock mechanics
Department of Civil and Architectural Engineering
Royal Instituet of Technology
Stockholm, Sweden 2018

Master of Science Thesis 18/01

Division of Soil and Rock mechanics

Royal Institute of Technology

ISSN 1652-599X; 18:02

Forward

This master thesis doesn't mean only the achievement regarding fulfillment of the academic criteria instead it was a great chance to get an exposure with the practical project. I have gained a good experience through discussions and advices from different experts in the area of Geotechnical Engineering.

I would like to express my gratitude to some individuals those who encouraged, motivated, advised and helped me during my thesis work.

First and foremost, I would like to express my sincere gratitude to my adviser and examiner Stefan Larsson, Professor in Geotechnology and Head of the Division of soil and rock mechanics in the Department of Civil and Architectural Engineering at Royal Institute of Technology, for giving me a chance to work on this fascinating topic.

Besides to my adviser, my sincere thanks go to Dr. Kenneth Viking (Trafikverket) and Caesar Kardan (Skanska), for their dedicated consultation, advice, and motivation throughout the entire time of my work.

My sincere thanks to my supervisors Mats Oscarsson (Ramböll) and Professor Fredrik Johansson (KTH) for their help and support at each step that enhanced the quality of this work. I would also thank Razvan Ignat for his advice regarding the Plaxis simulation.

I would also like to thank Pia Andersson (Trafikverket), Abebe Aschalew (NCC) and Jan-Erik Andersson (Trafikverket) for their cooperation in relation with collecting data in the case study project. I would also like to thank all stuff in Geotechniques department of Ramböll Stockholm for their collaboration and friendly approaches.

Finally, I would like to thank the consulting company Ramböll Sverige AB which arranged the office and all the necessary facilities during my work.

Stockholm, December 2017

Hulumtaye Kefyalew

Summary

The dry deep mixing method is widely used to improve a soft clay soil to increase the shear strength as well as to reduce the time for consolidation. It is a mechanical mixing process that makes parts of the soil stiffer than its original strength. It is mainly applicable to soft clay or peat soil.

In this master thesis, the objective was set to perform a comparative analysis on the prediction of the settlements of a clay soil improved by lime/cement columns (LCC). The theoretical settlement predictions were made using two analytical and numerical modeling. A case study was carried out on a part of Stockholm bypass project where LCC was applied to improve soft clay for a foundation of a concrete trough. Field measurements of the vertical deformation of the improved soil were performed using settlement plates to compare the analytical and numerical results.

The first analytical method was performed based on the recommendation of TK Geo 13 (2013) while the second method was performed based on the concept of a composite ground. In the case of the numerical method, FEA was performed using 2D plane strain model in Plaxis simulation. The performance of the geometry and combined matching models were investigated to convert the axisymmetric to plane strain model. The variation in stiffness of the columns were taken into consideration by applying two stiffness values 30 and 33 MPa for the upper and lower half of the column respectively. A preload of 58 kPa was applied on the improved clay soil to simulate the time-dependent consolidation settlement due to the stress addition.

A comparison was carried out between the results obtained from the analysis and a field measurement. The two analytical methods produced a better agreement with the field measurement regarding long-term consolidation settlement and a reasonable agreement concerning the rate of consolidation. The numerical analysis showed a good agreement with the benchmark concerning both the long-term consolidation settlement as well as the rate of consolidation. The geometry matching model gave a reasonable result regarding correctness of the result compared with the combined matching. Based on the results obtained in this study, the numerical methods had a better agreement with the measurements.

Key words: LCC, deep mixing, consolidation settlement, rate of consolidation, numerical analysis, analytical analysis, field measurement.

Sammanfattning

Jordförstärkning med kalkcementpelare är en vanlig metod för förstärkning av lösa jordar genom ökning av den blandade jordens hållfasthet samt minskning av konsolideringstiden. Metoden är en mekanisk process som ökar jordens styvhet och är främst tillämpbar i lös leror men även organiska jordar.

Detta examensarbete har syftat till att jämföra sättningsberäkningar i lera som är förstärk med KC-pelare. De teoretiska beräkningarna har utförts genom två analytiska modeller samt numerisk modellering. En fallstudie har utförts på del av Förbifart Stockholm där jordförstärkning av lös lera med KC-pelare har använts inför grundläggning av ett betongtråg. Resultat från fältmätningar av installerade markpeglar har jämförts med resultat från de teoretiska sättningsberäkningarna.

Den första beräkningsmetoden utfördes i enlighet med rekommendationer från TK Geo 13 (2013) och den andra metoden är baserad på principer för kompositjordar. Den numeriska beräkningen har utgjorts av FEM-modellering i 2D i programmet Plaxis. För att anpassa en plan-töjningsmodell till en axialsymmetrisk modell har inverkan av geometrin samt kombinerad anpassning av modell studerats. Hänsyn har tagits till KC-pelarnas styvhet genom att använda två olika värden (30 resp. 33 MPa) för KC-pelarnas övre respektive undre del. En överlast om 58 kPa applicerades på KC-pelarförstärkt området för att påskynda den tidsberoende konsolideringssättningarnas förlopp som orsakas av överlastens tillskottspänningar.

Baserat på resultat från uppmätta sättningar jämfört med beräkningar, har följande slutsatser dragits. Jämförelser mellan resultaten har visat på en rimlig överrensstämmelse mellan de två analytiska metoderna och utförda fältmätningar avseende långtids konsolideringssättningar. Den numeriska beräkningen har visat en god överensstämmelse med fältmätningar med hänsyn till både konsolideringssättningar och konsolideringsgraden. Den geometriskt anpassade modellen visade ett rimligare resultat i förhållande till den kombinerade anpassade modellen. Sammanfattningsvis bedöms det att den numeriska modelleringen stämmer bättre överens med resultaten från uppmätta sättningar i förhållande till analytiska beräkningar.

Nyckelord: KC-pelare, djupstabilisering, konsolideringssättningar, konsolideringsgrad, numerisk analys, analytisk analys, fältmätningar

List of notations

Greek Letters

α	Area replacement ratio
α_{cz}, β_c	Displacement parameters
β	Depth replacement ratio
γ_w	Unit weight of water
γ	Unit weight
γ'	Effective unit weight
γ_{rz}	Shear strain
ε	Strain
ε_z	Vertical strain
ε_v	Volumetric strain
ε_{col}	Vertical strain of the column
ε_{soil}	Vertical strain of the soil
$\varepsilon_{col,max}$	Maximum vertical strain of the column
η_{LC}	Load distribution factor
λ^*	Modified compression index
λ_i	Slope of virgin compression
μ	Factor in equivalent permeability calculation
μ_z	Depth reduction factor
μ_c	Ratio of stress in the column to average stress
μ_s	Ratio of stress in the soil to average stress
ν	Poisonous ratio
ν_i	Poisonous ratio of layer i
ν_c	Poisonous ratio in the column
ν_s	Poisonous ratio in the soil
σ	Normal stress
σ_h	Horizontal stress
σ_{col}	Vertical stress in the column
σ_{soil}	Vertical stress in the soil
σ_{creep}^{col}	Creep stress of the column
σ_c'	Pre-consolidation stress
σ_L'	Limiting stress
σ_{vi}'	Initial effective stress
σ_{avi}'	Average effective stress
$\overline{\sigma_c}$	Average total stress of the column
$\overline{\sigma_{s1}}$	Average total stress of the surrounding soil
$\sigma_{h,col}'$	Effective horizontal stress in the column
$\sigma_{ho,soil}'$	Initial horizontal stress in the column
$\sigma_{LCC,max}'$	Compressive strength of LCC
$\Delta\sigma_{v,col}'$	Vertical stress increase in the column
$\Delta\sigma_{v,soil}'$	Vertical stress increase in the soil
$\Delta\sigma_{col,max}$	Maximum vertical stress increase in the column

$\Delta\sigma_{LC}$	Vertical stress increase on improved soil block
τ_{rz}	Shear stress
τ_{rz}	Undrained shear strength of the column
τ_{rz}	Characteristic undrained shear strength of the column
φ'	Effective angle of friction
φ'_{col}	Effective angle of friction of the column
ω_N	Natural water content
ω_{LCC}	Water content of LCC
ω_L	Liquid limit

Roman Letters

a	Column area ratio
a_{pl}	Area improvement ratio in plane strain model
a_{ax}	Area improvement ratio in axisymmetric model
A	Area of improved soil
A_{col}	Area of the column
A_{prob}	Area of the probe
B	Half of the influence width in plane strain model
b_c	Width of the wall in plane strain model
cc_{col}	Center to center distance between columns
$c_{uk,col}$	Characteristics undrained shear strength of the column
c_{crit}	Critical shear strength of the column
c_u	Undrained shear strength
c_v	Coefficient of vertical consolidation
c_r	Coefficient of radial consolidation
c_{vv}	Coefficient of vertical consolidation flow in the vertical direction
c_{vh}	Coefficient of vertical consolidation flow in the horizontal direction
c_{v1}	Coefficient of vertical consolidation of layer 1
c_{v2}	Coefficient of vertical consolidation of layer 2
c_g	Geometry factor
c'_{col}	Effective cohesion of the column
d	Depth of zone A
d_c	Diameter of the column
d_e	Diameter of the unit cell
d_s	Diameter of smear zone
D	Weighted average constrained modulus
D_{ci}	Constrained modulus of column
D_{si}	Constrained modulus of the surrounding soil
E	Young's elastic modulus
E_i	Elastic modulus of layer i
E_c	Constrained modulus of soil cement column
E_s	Constrained modulus of the soil
$E4$	European highway
E_{col}	Elastic modulus of the column

E_{col-1}	Elastic modulus of the upper half column
E_{col-2}	Elastic modulus of the lower half column
$E_{c,pl}$	Elastic modulus of the column in the plane strain model
$E_{s,pl}$	Elastic modulus of the soil in the plane strain model
$E_{c,ax}$	Elastic modulus of the column in the axisymmetric model
$E_{s,ax}$	Elastic modulus of the soil in the axisymmetric model
$E_{s1}(r)$	Constrained modulus in the disturbed zone
E_{s2}	Constrained modulus of the surrounding soil in layer 2
$\overline{E}_{s1}$	The average constrained modulus of the surrounding soil layer 1
$\overline{E}_{s2}$	The average constrained modulus of the surrounding soil layer 2
E_{50}^{u}	Undrained secant modulus
e_i	Void ratio of layer i
e_{oi}	Initial void ratio
e_s	Void ratio in the soil
e_c	Void ratio in the clay
σ'_{LCC}	Compression strength of the LCC
h_1	Depth of layer 1
h_2	Depth of layer 2
H	Thickness of soft soil
H_L	Length of column
H_c	Thickness of parts of improved soil
H'_1	Thickness of improved layer 1
H'_2	Thickness of improved layer 2
H_{1i}	Thickness of sub soil layer of H'_1
H_{2i}	Thickness of sub soil layer of H'_2
I	Influence factor
k	Coefficient of permeability
k_{v1}	Coefficient of vertical permeability of layer 1
k_{v2}	Coefficient of vertical permeability of layer 2
k_{v}	Coefficient of vertical permeability
k_{h}	Coefficient of horizontal permeability
$k_{v,pl}$	Coefficient of vertical permeability in plane strain model
$k_{v,ax}$	Coefficient of vertical permeability in axisymmetric model
$k_{h,pl}$	Coefficient of horizontal permeability in plane strain model
$k_{h,ax}$	Coefficient of horizontal permeability in axisymmetric model
k_{col}	Coefficient of permeability of the column
k_{soil}	Coefficient of permeability of the soil
$k_{v1}(r)$	Coefficient of permeability in the radial direction
k_{block}	Coefficient of permeability LC soil block
K_o	Coefficient of lateral earth pressure
K^*	Modified swelling index
L_{col}	Length of column
m	Modular ratio
M	Compression modulus
M'	Modulus number

M_{col}	Modulus of the column
M_{block}	Modulus of the improved soil block
M_{soil}	Modulus of the unimproved soil
M_L	Modulus at the limiting stress level
m_v	Coefficient of volume compressibility
m_{v1}	Coefficient of volume compressibility of layer 1
m_{v2}	Coefficient of volume compressibility of layer 2
m_{vs}	Coefficient of volume compressibility of the soil
m_{vc}	Coefficient of volume compressibility of the column
n_s	Stress concentration ratio
N	Bearing factor
P	Force on the probe
P'	Mean effective consolidation stress
Δp_{1i}	Total vertical stress increments in layer H_1'
Δp_{2i}	Total vertical stress increments in layer H_2'
q	Applied load
$q_{ö}$	Fictitious load on the upper part of the block
q_u	Fictitious load on the lower part of the block
R	Influence radius in axisymmetric model
r_e	Radius of the surrounding soil
r_c	Radius of the column in axisymmetric model
r_s	Radius of the surrounding soil
$S(t)$	Total compression
S_1	Compression of improved layer 1
S_2	Compression of improved layer 2
S_c	Column spacing
S_o	Settlement of clay soil
S_t	Top surface settlement
S_f	Final settlement
T_v	Time factor
T_m, T_c	Factors determined in consolidation calculation
U	Degree of consolidation
U_v	Vertical degree of consolidation
U_r	Radial degree of consolidation
U_{vr}	Average degree of consolidation
σ_o	Uniformly distributed load on the column
u_0	Initial excess pore water pressure
u_t	Excess pore water pressure at time t
u_{s1}	Excess pore water pressure of layer 1
u_{s2}	Excess pore water pressure of layer 2
$\bar{u}_{s1}$	Average excess pore water pressure of layer 1
$\bar{u}_{s2}$	Average excess pore water pressure of layer 2
u_s	Excess pore water pressure in the clay
u_c	Excess pore water pressure in the column
w_{rz}	Displacement of soil element at depth z
w_{cz}	Displacement of column element at depth z

x	Distance from the center of the load
z	Depth from ground surface
z_{fic}	Fictitious depth

Abbreviations

CRS	Constant rate of strain
DM	Deep mixing
FSE	Förbifart Stockholm Enterprenad (Stockholm bypass agreement)
FEA	Finite element analysis
FEM	Finite element method
GK	Geoteknisk klass (Geotechnical Class)
LC	Lime/cement
LCC	Lime cement column
MC	Mohr Coulomb
MWL	Mean water level
OCR	Over consolidation ratio
OTB	Objektspecifik teknisk beskrivning (Object specific technical description)
TK Geo	Trafikverkets tekniska råd för geokonstruktioner (Swedish transportation Administration Technical Advice for geo structueres)
2D	Two-dimensional
3D	Three dimensional

Table of Contents

1 Introduction

1.1 Background

It is clear that there is no easy way to select the most suitable ground condition for the construction of structures. Instead, we may build on areas by avoiding grounds with difficult characteristics, such as areas covered by soft clay or peat. Such soils will exhibit a very large deformation or settlement as a result of a change in stresses due to applied loads. So, soils like soft clay or peat usually need an improvement to carry loads from buildings, roads, and other structures.

One of the most common methods used for soil improvement is the dry/wet deep mixing (DM) method. Deep mixing is a general name of different methods used for soil improvement, which is a mechanical mixing process that mixes a binding agent mostly lime or cement with soil. In the Scandinavian countries, this method has different names such as "lime-cement column", "deep improvement", "dry jet mixing method" or "column improvement" (Larsson 2003). Improvement of soil using lime/cement column (LCC) is a widely applicable in Sweden and Finland to improve the stability of a road and railway embankments constructed on soft soil (Kivelö & Broms 1999). This method is often more economical compared with other conventional methods such as excavation and replacement and embankment piles.

However, the deep mixing process is not simple concerning the chemical reactions between the binder and the soil. It is very complex and will contain different phases that influence the results and the properties of the improved soil (Larsson 2003). Due to the complexity of the mixing process and the variation of the soil properties, it is difficult to make a fairly uniform distribution of the binders. Hence this will result in variability in the strength as well as the settlement properties of the LCC (Bergman 2015). The uncertainties in settlements calculation and how the settlements develop with time have been rather significant. Using a simplified method of analysis for the calculation may result in a moderately conservative design (Baker 2000).

1.2 Objective of the study

The purpose of this study is to perform a comparative analysis in prediction of settlements of a clay soil improved by LCC using analytical and numerical methods and field measurements. Regarding the analytical method, it is aimed to examine the already established procedure in TK Geo 13 (2013) for the calculation of settlements in deep mixing. The numerical analyses were performed using a finite element method using 2D Plaxis commercial software. A comparison of results from the analytical calculation and numerical analysis was performed to check their agreement with field measurements. Furthermore, a case study has been performed in conjunction with the installation of LCC on parts of Stockholm bypass project, particularly on site FSE502 (Förbifart Stockholm Enterprenad). The settlement of the LCC measured from the field was compared with results of the theoretical analyses.

The literature review in this thesis is dedicated to previous studies that are concerned with different methods used to predict the rate of consolidation and settlements of a soft clay soil which is improved with cement, lime and LCC.

1.3 Scope and limitations

In this study, it is limited to calculate the settlement due to consolidation when LCC is used for ground improvement. The settlement, in this case, is the deformation of the column and the surrounding soil due to consolidation only in the vertical direction as a result of the application of load at the surface level. The settlement due to creep effect hasn't been studied. The geometrical models used for the analysis are similar to the real project selected for the case study. All the geometrical data's and soil parameters used as an input for both analyses are identical with the real project since it is targeted to make a comparison between the theoretical results with measured from the field. In the 2D numerical analysis, the undrained material model of Soft Soil and Mohr-Coulomb were used for the clay and the LCC respectively. Deformation of the column in the radial direction and stability analysis of the structure on top of the column were not included.

1.4 Outline of the thesis

The first chapter is the introduction part that briefly discusses the deep mixing method as background information, the objective of the study, the scope and its limitations. In the second chapter, previous studies on deep mixing methods focusing on settlement calculations are briefly reviewed. The third chapter describes the case study that is used as a reference project. The description of the project, the geological condition and the input parameters used in the analysis are parts of this chapter. The methodology and procedures applied for the analyses are described in chapter four. Chapter five presents the results from both theoretical analysis and field measurements. The discussion on results obtained from each method is presented in the sixth chapter. Finally, the conclusion from this particular study and suggestions to be considered in a further study are presented in chapter seven and eight respectively.

2 Literature review

This chapter reviews previous studies related to deep mixing methods related with the prediction of settlements. A brief historical background and deep mixing methods based on binder application are presented at the beginning.

2.1 Historical background

The deep mixing method was first developed in 1970's both in Sweden and Japan around in the same period. However, the research and development related with deep mixing were started a few years earlier in both countries. In Sweden, in 1967 Kjeld Paus a vice president of the Swedish construction company BPA proposed a new method using a lime column to improve a soft clay soil (Broms 1984). The first trial was done by mixing in situ soft clay with unslaked lime (CaO). The purpose was to use the lime column as ground improvement in place of preloading and vertical drain, lightweight fill and as a lightweight foundation for light structures, etc. In 1971 the first lime columns were manufactured by Linden-Alimak and the first full-scale practical field tests were started in 1972 at Skå-Edeby, which is the test field of the Swedish Geotechnical Institute. The lime column method used for practical application in the first time is in 1974 for road embankment and deep trench at Huddinge located south of Stockholm (Broms 1984). The first machine used for the installation of the lime column was drill rigs mounted on a Volvo tractor see Figure 2.1.

Simultaneously with the development of deep mixing method in Sweden a research and development had been carried out in Japan since 1967 (Larsson 2003). Port and Harbor Institute of the Japanese Ministry of Transportation that is aiming to develop a method for deep mixing of marine clay performed a test in the laboratory. Later in 1975 a research and development on deep mixing using dry binder started in Japan. The Ministry of Construction led this development, and the first project was done in 1981 (Larsson 2003). This method used in this new development was similar to the Swedish lime column method.

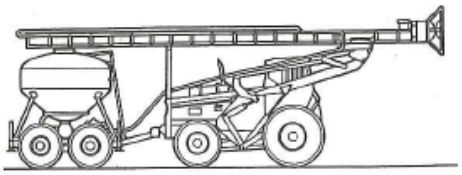

Figure 2.1-lime column machine Volvo BM LM 641 (after Broms 1984)

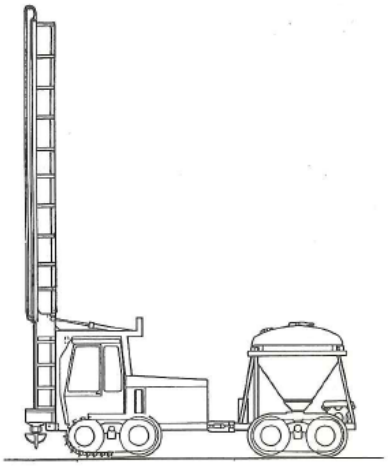

Figure 2.2 lime column machine Linden-Alimak after (after Broms 1984)

Improvement of soil using lime columns was extensively used until the end of 1980's, at the time in which LCC first introduced. It is also the first time that lime cement/column introduced in Sweden. The main purpose of adding the cement is to increase the shear strength of the soil and to increase the ability to improve organic soils that were not effective by using lime only (Kivelö & Broms 1999). The addition of cement will affect the mechanical properties of the column material and the behavior of the column itself. The shear strength and the modulus of elasticity of the column will be higher than the lime column whereas the permeability is reduced.

2.2 Application and mixing process

Ground improvement using deep mixing method is a mechanical process that mixes binders (lime, cement or lime/cement) into a soft soil to form columns to strengthen the soil. The mixing process can be applied in two different ways depending on how the binders mixed with the soil (Larsson 2003). The first one is the dry deep mixing method which uses a rotary machine to mix a dry powder of binder into the soil. In this method, the dry binder blown into the soil through the nozzles in mixing tools with compressed air, see Figure 2.4 the mixing tool used in the case study project. Then the binder will react with the natural water of the soil and binder mixture. So, it is very suitable for soft soil with high natural water content. The mixing process is very complex and contains different phases and factors that can affect the process and the results. Its main purpose is to make an even distribution of binders throughout the column length. The illustrative diagram of the mixing process of the dry method is shown in Figure 2.3. In Sweden, only the dry mixing method is used (Larsson 2006).

The second application method is a wet deep mixing method. In this method, the binder will mix with water before the installation of the column then the suspension will pump into the soil during mixing. It is more suitable to use in a soil with low natural water content since it facilitates the mixing of cement. The dry deep mixing method was applied for the installation of LCC in the case study project.

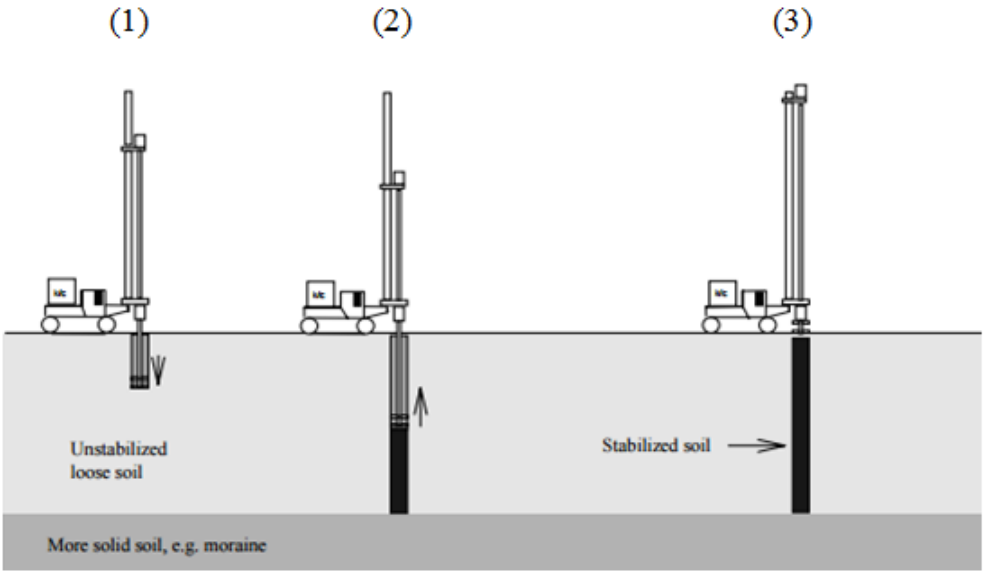

Figure 2.3 Mixing process in dry deep mixing of LCC installation (1) Penetration of mixing tool to the required depth (2) Dispersion of binder agent into the soil and (3) Installation completed but mixing will continuous by molecular diffusion (after Larsson 2003).

Figure 2.4 Mixing tools used in the case study FSE502 project (Photo Hulumtaye.K)

2.3 Settlement prediction

The most known models in the analysis of deformation of composite materials are established based on two assumptions. Those are the assumption of equal stress and equal strain distribution within the material. Equal stress distribution means the stress at the surface of the material will be spread uniformly with the same magnitude. Similarly, in the case of the equal strain, it is assumed that the strain distribution will be the same throughout the materials. In most methods that are used for calculations of settlements of a soil improved using deep mixing columns are under the assumption of the equal strain on the column and on the surrounding soil without distribution of load into improved soil area. Commonly the settlements are controlled on the construction site to check whether the improved soil functions as expected or not.

In deep mixing improved soil, the settlement and its change in time mainly depend on the modulus of compressibility and the permeability of both the improved and unimproved soil (Baker 2000). Hence it is very important to have a good knowledge regarding those two parameters to select the method to be applied for the analysis of settlement and degree of consolidation of the improved soil. Different techniques have been used to improve the soft soil by deep mixings, like cement column, lime column, and LCC. The common thing in all these methods is making part of the soil stiffer than its original strength. According to Baker (2000) this process results in a variation of hydraulic properties of the composite material and needs to set different boundary conditions to calculate the time-dependent settlement. Various methods have been established using analytical and numerical solutions to calculate settlements of improved soil. In this section, some of the previous studies that are mainly focused on settlement prediction are briefly presented.

2.3.1 Settlement prediction analytical

Several theoretical methods have been developed for the prediction of settlements of improved soil by deep mixing columns. The concept of a unit cell is the base and often used for the analytical model in the estimation of settlements of the improved soil.

Chai & Pongsivasathit (2010)

Chai & Pongsivasathit (2010) presented a method for estimating a consolidation settlement-time curve of the clayey subsoil modified by a ground improvement using a floating soil-cement column. The new proposal in this method is a relative penetration of the column in the underlying soft soil was considered during the consolidation process.

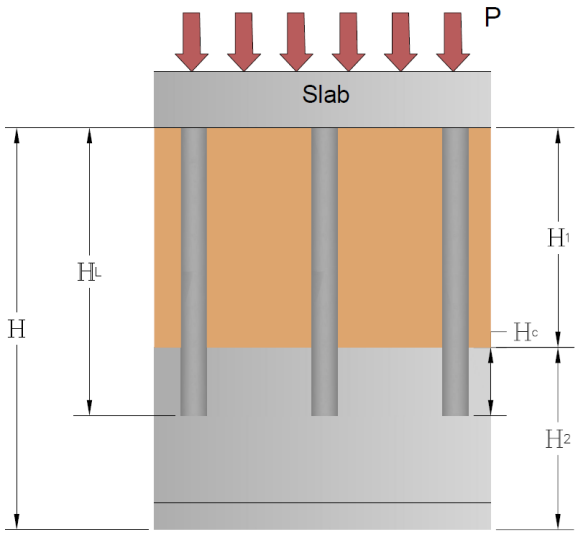

Figure 2.5 Improved clayey sub soil by floating column (after Chai & Pongsivasathit 2010)

Due to this the stress concentration ratio (stress on the column to stress on the surrounding soil) will vary with time and depth. In addition to this, the relative penetration of the column is influenced by the area replacement ratio (α) and the depth replacement ratio (β), which is used to describe the relative improvement of the soft soil by the column. The load intensity (P) and the stiffness of the soft soil (E_s) also have an impact on the relative penetration.

$$\alpha = \frac{d_c}{d_e} \tag{2.1}$$

$$\beta = \frac{H_L}{H} \tag{2.2}$$

Where: d_c, d_e = diameter of the column and diameter of the unit cell which represent the column and the surrounding soil, respectively.
H= thickness of the soft clay soil excluding the slab thickness
H_L= length of the column

As shown in Figure 2.5 (H_c) is part of the improved soil but for the purpose of settlement calculation it is considered as unimproved soil. The thickness of the improved soil which is considered as unimproved can be expressed as a function of (α) and (β):

$$H_c = H_L f(\alpha) g(\beta) \tag{2.3}$$

According to the author's definition the functions f (α) and g (β) are bilinear functions which are chosen based on results of numerical studies and mathematically written as:

$$f(\alpha) = \begin{cases} \frac{8}{15} - \frac{\alpha}{75} & (10\% \leq \alpha \leq 40\%) \\ 0 & (\alpha > 40\%) \end{cases} \tag{2.4}$$

$$g(\beta) = \begin{cases} 1.62 - 0.016\beta & (20\% \leq \beta \leq 70\%) \\ 0.5 & (70\% \leq \beta \leq 90\%) \end{cases} \tag{2.5}$$

The value of area and depth replacement ratio (α) and (β) should be in percentage. After defining the two functions the settlement of the soft soil was calculated in two different parts: the first one is (s_1) the compression of the improved layer with thickness H_1' and the second part is (s_2) the compression of unimproved layer with a thickness of H_2'. Then to calculate settlements in each defined layer a formula have been proposed as expressed in Eq. 2.6 and 2.7.

For improved layer (H_1'):

$$(s_1) = \sum_{i=1}^{n} \frac{\Delta p_{1i} H_{1i} U(t)}{D_{ci}\alpha + (1-\alpha) D_{si}} \tag{2.6}$$

For unimproved layer (H_2'):

$$(s_2) = \sum_{i=1}^{n} H_{2i} \frac{\lambda_i}{1+e_{0i}} \ln\left(1 + \frac{\Delta p_{2i}}{\sigma_{vi}'} U(t)\right) \tag{2.7}$$

Where: H_{1i}, H_{2i}= Thickness of the sub soil layers in layers of H_1' and H_2' respectively
σ_{vi}'=The initial vertical effective stress in sub layer H_{2i}
e_{0i}= Initial void ratio
λ_i= The slope of virgin compression line in $e - \ln(p')$ plot
p'= The mean effective consolidation stress
$\Delta p_{1i}, \Delta p_{2i}$=The total vertical stress increments in layers H_1' and H_2' respectively
D_{ci}, D_{si}=The constrained moduli of the column and the surrounding soil of the layer H_{1i} can be calculated as:

$$D_{ci} = \frac{E_i(1-v_i)}{(1+v_i)(1-2v_i)} \tag{2.8}$$

$$D_{si} = \frac{(1-e_i)\sigma_{avi}'}{\lambda_i} \tag{2.9}$$

Where: E_i elastic modulus, v_i Poisson's ratio, e_i the void ratio, σ_{avi}' the average effective vertical stress including stress increment by the embankment of the corresponding sub-layer of the soil. For Eq. 2.7 and 2.9 in using the $e - \ln(p')$ it is recommended to use k_i instead of λ_i when the subsoil layer is over consolidated. Accordingly, the final settlement (compression) can be calculated as:

$$s(t) = s_1(t) + s_2(t) \tag{2.10}$$

In this settlements prediction method Chai & Pongsivasathit (2010) considered the improved clay subsoil as a two-layer system as shown in Figure 2.6. Then a theoretical solution proposed by Zhu et al. (1999) was applied to estimate the degree of consolidation. In addition to the coefficient of consolidation (c_v), the degree of consolidation (U) could be influenced by the permeability (k) and the coefficient of volume compressibility (m_v) individually.

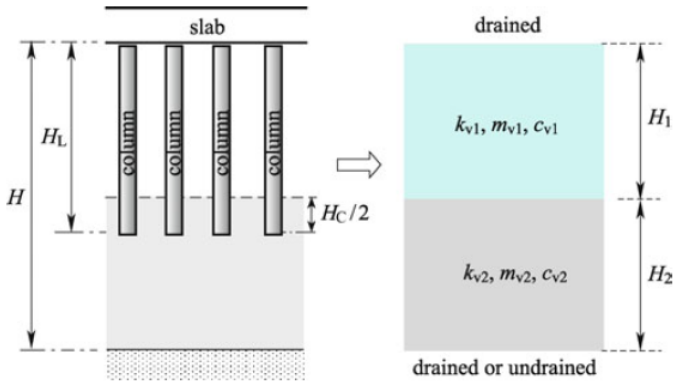

Figure 2.6 Two-layer systems for calculation of degree of consolidation (after Chai & Pongsivasathit 2010)

So, the value of the volume compressibility m_{v1} could be evaluated using the area weighted average of the constrained moduli of the column (D_c) and the soil in the unit cell (D_s)

$$m_{v1} = \frac{1}{\alpha D_c + (1-\alpha) D_s} \tag{2.11}$$

Regarding the value of the column permeability in most cases, it is almost closer or same to the permeability of the surrounding soil, but due to a higher stiffness of the column it's coefficient of consolidation could be much larger than the soil in the cell and this results in a flow in the radial direction. Hence the permeability of the improved soil was determined by introducing the concept of equivalent vertical permeability of the prefabricated vertical drain. So, the value of (k_{v1}) can be evaluated from the following equation:

$$k_{v1} = \left(1 + \frac{2.5H_1^2}{\mu d_e^2}\left(\frac{k_h}{k_v}\right)\right) k_v \tag{2.12}$$

Where: k_v, k_h= permeability of the soft soil in the vertical and horizontal direction respectively
H_1=the thickness of layer-1 and μ described as follows:

$$\mu = \ln\left(\frac{n}{s}\right) + \frac{k_h}{k_s}\ln(s) - \frac{3}{4} + \frac{8H_1^2 k_h}{3d_c^2 k_c} \tag{2.13}$$

Where: $n = d_e/d_c, s = d_s/d_c$, d_s = diameter of the smear zone
k_c, k_s= Coefficient of permeability of the column and the smear zone, respectively

The other issue resolved in this proposal is the thickness of layer-1 and layer-2. Through comparison of results from a finite element analysis (FEA) using unit cell model and by trial and error the thickness of layer-1 obtained as $H_1 = H_L - H_c/2$ which gives a good result. But in the case of layer-2 due to large consolidation strain its thickness completely different before and after consolidation since it is unimproved soil. The new proposal in this case is to take the average thickness of layer-2.

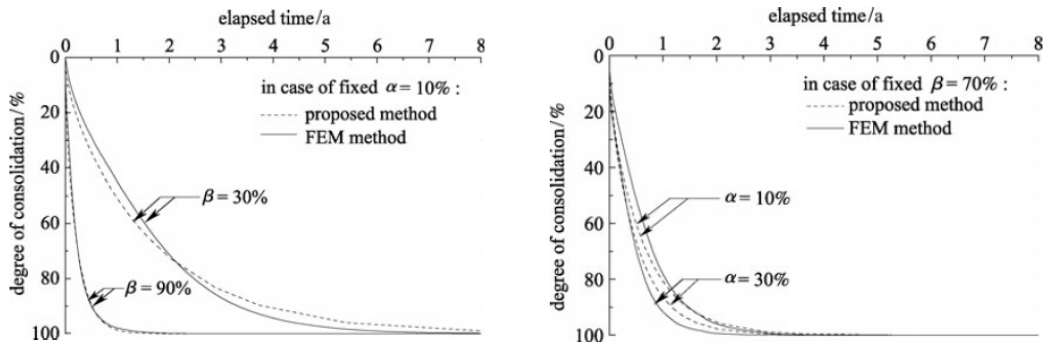

(a) (b)

Figure 2.7 Result comparison of proposed method with FEA a) for α=10% and b) for β =70% (after Chai & Pongsivasathit 2010)

The validation of this newly proposed method was done by using a finite element analysis (FEA) for a reference condition of soft clayey soil with a soil deposit of 12 m thick. It is analyzed using a unit cell model for different values of α and β which range $10\% \leq \alpha \leq 30\%$ and $10\% \leq \beta \leq 30\%$, as shown in Figure 2.7(a) and 2.7(b), respectively. The calculated degree of consolidation compared with different values of α and β, and the proposed method shows a good prediction of the degree of consolidation. The effectiveness of the method was verified by comparing measured results from lab and case histories from the site and suggested to use for designing of a soft soil improvement by floating soil-cement column.

Gong et al. (2015)

Gong et al. (2015) proposed a simplified analytical method for the estimation of the settlement of a soil improved by a floating soil-cement column based on double soil layer consolidation theory. This method also developed based on the concept of a unit cell model and the interaction between the soil and the column were idealized as shown in Figure 2.8. The simplified analytical solution was obtained based on the following assumptions.

- The vertical strain on the column and the surrounding soil will be equal, equal vertical strain assumption adopted.
- Flow and consolidation not allowed in the soil-cement column and an impervious column soil interface was assumed.
- The addition of stress on the unit cell assumed to be a function of depth (z) and elapsed time (t), that is $\sigma = \sigma\ (z, t)$.
- The coefficient of permeability in the radial direction $k_{v1}(r)$ and the constrained modulus $E_{s1}(r)$ in the disturbed soil zone can vary depending on the radial distance from the column.
- Also, the same assumptions in Terzaghi's one-dimensional consolidation theory even considered in here.

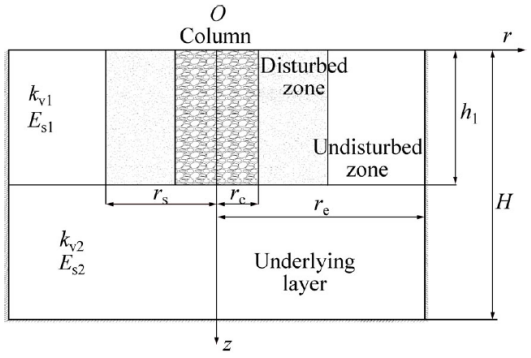

Figure 2.8 Diagram for consolidation of a soft ground with floating soil-cement column (after Gong et al. 2015)

Both the column and the surrounding soil share the total stress at any time means:

$$\pi(r_e^2 - r_c^2)\bar{\sigma}_{s1} + \pi r_c^2 \bar{\sigma}_c = \pi r_e^2 \sigma \tag{2.14}$$

Where $\bar{\sigma}_c$ and $\bar{\sigma}_{s1}$ are the average total stress of the column and the surrounding soil for $0 \le z \le h_1$, respectively, r_c is the radius of the column and r_e radius of the surrounding soil. Then the equal strain assumption yields:

$$\frac{\bar{\sigma}_{s1} - \bar{u}_{s1}}{\overline{E_{s1}(r)}} = \frac{\bar{\sigma}_c}{E_c} = \varepsilon_z = \varepsilon_v \tag{2.15}$$

Where: $\bar{u}_{s1} = \frac{1}{\pi(r_e^2 - r_c^2)} \int_{r_c}^{r_e} 2\pi r u_{s1}(r)\, dr$ is the average excess pore water pressure within the soil in the unit cell for $0 \le z \le h_1$; $\overline{E_{s1}(r)}$ the average constrained modulus of the surrounding soil; E_c is the constrained modulus of the soil-cement column; $\varepsilon_z, \varepsilon_v$ are the vertical strain and the volumetric strain at any depth of the surrounding soil and the column.

The author described that the permeability of the soil-cement column (k_c) is much lower than the surrounding soil (k_s). Therefore, no flow and consolidation were considered in the soil-cement column as a result flow will not happen in the radial direction. Based on this the governing equation was given according to the principle of mass conservation:

$$\frac{\partial \varepsilon_v}{\partial t} + \frac{k_{v1}}{\gamma_w} \frac{\partial^2 \bar{u}_{s1}}{\partial z^2} = 0 \tag{2.16}$$

Where k_{v1}=coefficient of permeability in the vertical direction of the soil layer ($0 \le z \le h_1$) and γ_w=the unit weight of water.
The penetration of the column into the underlying layer was ignored in the derivation of the governing equation of consolidation for the underlying layer i.e. ($h_1 \le z \le H$) for simplification. Then Terzaghi's one-dimensional consolidation theory adopted as follows.

$$\frac{\partial^2 \bar{u}_{s2}}{\partial t} - c_{v2} \frac{\partial^2 \bar{u}_{s2}}{\partial z^2} = \frac{\partial \sigma}{\partial t} \tag{2.17}$$

Where: $\bar{u}_{s2} = \frac{1}{\pi r_e^2} \int_0^{r_e} 2\pi r u_{s2}(r) dr$ is the average excess pore water pressure in the underlying soil layer; c_{v2}=$k_{v2}E_{s2}/\gamma_w$ is the consolidation coefficient of the underlying layer; k_{v2}, E_{s2}= the coefficient

of permeability in the vertical direction and the constrained modulus of the soil respectively in ($h_1 \leq z \leq H$).

Based on Eq. 2.16 and 2.17 after derivation and rearrangements the new governing equation for consolidation of a soil improved by a floating soil–cement column proposed as follows:

$$\begin{cases} \frac{\partial \bar{u}_{s1}}{\partial t} = A\frac{\partial^2 \bar{u}_{s1}}{\partial z^2} + \frac{n^2}{n^2-1}\frac{\partial \sigma}{\partial t}, & 0 \leq z \leq h_1 \\ \frac{\partial \bar{u}_{s2}}{\partial t} = c_{v2}\frac{\partial^2 \bar{u}_{s2}}{\partial z^2} + \frac{\partial \sigma}{\partial t}, & h_1 \leq z \leq H \end{cases} \tag{2.18}$$

Where: A is the equivalent consolidation coefficient of the soft soil improved by soil-cement column it is defined through the derivation process.

Linear vertical total stress increments were assumed with depth and time and remain constant after time t_0. The initial boundary condition was modified since the top surface of the soil considered as permeable and the bottom as impermeable. To obtain the analytical solution of the proposed equation some parameters are transformed and also additional dimensionless parameters were defined and then the solution for Eq. 2.18 derived as:

$$\begin{cases} \bar{u}_{s1} = \frac{1}{n^2-1}\sum_{m=1}^{+\infty} T_m(T_v)Z_m(z), & 0 \leq z \leq h_1 \\ \bar{u}_{s2} = \frac{1}{n^2}\sum_{m=1}^{+\infty} T_m(T_v)Z_m(z), & h_1 \leq z \leq H \end{cases} \tag{2.19}$$

Where: $T_m(T_v)$ is a factor defined by Zhu et al. (1999).

Finally, the average degree of consolidation defined as the ratio of the settlement at time *t* to the final settlement. The settlement of soil improved by soil-cement floating column at a time *t* can be expressed as:

$$S_t = \int_0^H \varepsilon(z,t)dz = \int_0^{h_1}[\sigma(z,t) - \bar{\bar{u}}_{s1}(z,T_v)]\hat{m}_{v1}dz + \int_{h_1}^{h_2}[\sigma(z,t) - \bar{u}_{s2}(z,T_v]\hat{m}_{v2}dz \tag{2.20}$$

Where: $\bar{\bar{u}}_{s1} = \frac{\bar{u}_{s1}\pi(r_e^2 - r_c^2)}{\pi r_e^2} = \frac{\bar{u}_{s1}(n^2-1)}{n^2}$ is the average pore water pressure at the cross-sectional area of the improved soil.

In similar way, the final settlement of the improved soil when the pore water pressure reaches to zero can be expressed as:

$$S_t = \int_0^H \varepsilon(z, t=\infty)dz = \int_0^{h_1} \sigma(z, t=\infty)\hat{m}_{v1}dz + \int_{h_1}^{h_2} \sigma(z, t=\infty)\hat{m}_{v2}dz \tag{2.21}$$

Therefore, the average degree of consolidation derived as:

$$U(T_v) = \min\left(1, \frac{T_v}{T_c}\right) - \sum_{m=1}^{+\infty} \frac{2\hat{m}_{v1}h_1 T_m(T_v)}{\{\lambda_m \alpha \sin(\lambda_m \alpha) n^2[\hat{m}_{v1}h_1(\sigma_0+\sigma_1)+m_{v2}h_2(\sigma_1+\sigma_2)]\}} \tag{2.22}$$

A parametric analysis was performed using this simplified method to investigate the consolidation behavior of the soft soil improved by the floating soil cement column. The results showed that the consolidation behavior is strictly related with the depth replacement ratio of the column. The rate of consolidation increases when thickness ratio (h_1/H) increases. The influence of the permeability of the upper soil (k_{v1}) on the consolidation was observed even though the consolidation coefficient on the upper (c_{v1}) and the underlying layer (c_{v2}) are the same.

Alamgir et al. (1996)

A theoretical approach has been developed by Alamgir et al. (1996) to predict the deformation behavior of a soft ground improved by a columnar inclusion. The improvement by the columnar inclusion can be stone columns/granular piles, sand compaction piles, lime or cement columns or others that are stiffer than the surrounding soil. The analysis considers the phenomena of different deformation of the composite ground and the interaction between the column and the soil to determine the load distribution and the resulting settlement. The proposed approach considers only the elastic solution to make the analysis very simple. The unit cell that consists of the column and the surrounding soil used to obtain the solution from the analysis see Figure 2.9. The column is considered as cylindrical with height (H) and diameter (d_c). The unit cell with diameter (d_e) and uniformly loaded with (σ_0). The unit cell the diameter d_e relates with the column spacing S_C as:

$$d_e = c_g S_C$$

Where: c_g is a factor depending on the geometry equal to 1.05, 1.13 and 1.29 for triangular, square and hexagonal column patterns respectively. The soil and the material in the column assumed to behave a linearly deformable homogenous material with a constant elastic modulus (E) and Poisson's ratio (ν).

The analysis was done by dividing both the column and the surrounding soil into a number of elements that are uniformly loaded. The interaction between the column and the soil will remain elastic since the only elastic analysis was considered. In displacement analysis, the compatibility of the column and the soil was considered along with the depth for no-slip condition between the column and the soil. As a result, the displacement of the column and the surrounding soil will be equal at the interface. In this analysis, only the vertical displacement is considered the displacement in the radial direction is neglected. The main point that is intended to present in this analysis is to define the shape of the deformation of the column and the surrounding soil. The displacement of the column is the same over its cross-sectional area whereas the displacement of the surrounding soil is the same value with the column displacement at the column–soil interface and decreases radially and become minimum outside the unit cell.

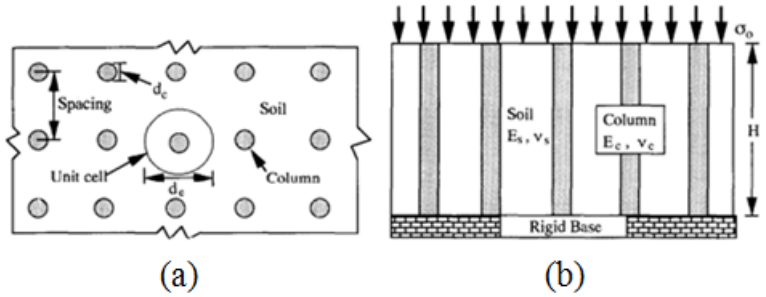

Figure 2.9. The foundation system to be analyzed: a) plan b) elevation (after Alamgir et al. 1996)

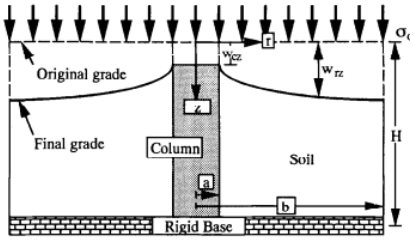

Figure 2.10. Mode of deformation of the column-soil system (after Alamgir et al. 1996)

This shape of deformation is supported by experiments and the mode of deformation for ground reinforced column expressed as:

$$w_{rz} = w_{cz} + \alpha_{\square z}\left[\frac{r}{a} - e^{\beta_c\left(\frac{r}{a}-1\right)}\right] \quad for \;\; a \le r \le b \tag{2.23}$$

Where: a, b=radii of the column and the unit cell respectively
r=the radial distance measured from the center of the column
w_{rz}=displacement of the soil element at depth z and radial distance r
w_{cz}=displacement of the column element at depth z
α_{cz} and β_c=are the displacement parameters

Eq. 2.23 indicates as the vertical displacement of the column and the surrounding soil varies with depth and radial distance accordingly the mobilized shear strain and shear stress vary in both directions. Then the shear strain γ_{rz} and the shear stress τ_{rz} were derived from Eq. 2.23 and expressed as:

$$\gamma_{rz} = \frac{\delta w_{rz}}{\delta r} = \frac{\alpha_{cz}}{a\left[1-\beta_c e^{\beta\square\left(\frac{r}{a}-1\right)}\right]} \tag{2.24}$$

$$\tau_{rz} = \frac{E_s \alpha_{cz}}{2a(1+v_s)}\left[1 - \beta_c e^{\beta_c\left(\frac{r}{a}-1\right)}\right] \tag{2.25}$$

The shear stress outside the unit cell becomes zero at $r=b$, due to symmetry of the load and geometry and results:

$$\beta_c e^{\beta_c(n-1)} - 1 = 0 \tag{2.26}$$

Eq. 2.26 shows that as β_c is a function of the spacing ratio $n=b/a$ of the columns.

To evaluate the deformation of the soil column system using Eq. 2.23, it is important first to find the values for deformation of the column $w_{\square z}$ and the deformation factor α_{cz}. The vertical deformation of the column w_{cz} can be obtained by using equilibrium of forces on the elements of the column; the normal stress derived first then the deformation obtained by relating the elastic modulus of the material. A similar procedure was applied to find the deformation of the soil. Finally, the deformation factor α_{cz} derived through displacement compatibility analysis between the column and the surrounding soil. A finite element analysis was performed to make a comparison of results from the proposed method and a reasonable agreement was achieved.

TK Geo 13 (2013)

The TK Geo 13 (2013) is a guide for design and construction of geo-structures which is published by Swedish Transportation Administration. This guide consists of the criteria and requirements how to use a deep mixing method for ground improvement. In this section, a summary of the method is presented.

- **Material characteristics**

The material model of the improved soil is assumed to have ideal elastoplastic properties, where the elastic part of the shear is limited by the critical shear stress c_{crit} and the plastic stress in the uniaxial compressive load.

According to Larsson (2006), characteristic values are carefully selected on the bases of laboratory results and empirical experiences. In the conversion of laboratory values to field conditions, various uncertainties need to be observed. The presence of disturbed zone under the column and lower strength on the upper part of the column should be considered in the selection of characteristics strength.

The maximum value of the undrained shear strength of the LCC in the design of GK2 is selected $c_{uk,col} = 150\ kPa$ which is independent of the laboratory and field test results. But for the stability analysis, the shear strength of the column is adapted 100 kPa.

- **Deformation characteristics**

The elastic modulus of the column is the most significant parameter for evaluation of its deformability during the application of load. The modulus of the column is not determined in the field, but the model is assumed to be a function of $c_{uk,col}$ or its undrained compressive strength, $q_{uk,col}$, (Larsson 2006). According to TK Geo 13 (2013) for stress value below c_{crit} , the elastic modulus of the column E_{col} estimated using Eq. 2.27. In this case, the unit for critical stress is kPa.

$$E_{col} = 13.\, c_{crit}^{1.6} \tag{2.27}$$

The time dependent settlement of the improved soil influenced by how the column functions as a vertical drain, the stiffness difference between the column and the unimproved soil and the stiffness of the column through time. The relationship between these factors is not yet clarified. A method that considers the strength of the column in the process of the consolidation has not been developed. On the other hand, a method for calculation of consolidation process for a vertical drain is well established. So, the method for calculation of consolidation process of improved soil was developed by considering the column as a vertical drain. This method includes a fictitious permeability of the column that compensates the stiffness difference between the column and unimproved soil and strength development in the column.

The actual permeability of the column may vary through time. But for a soil improved by LCC recommended to estimate the permeability of the LCC 500 times the permeability of unimproved soil. The permeability of the soil volume improved by a deep mixing column k_{block} calculated according to Eq. 2.28.

$$k_{block} = a.k_{col} + (1 - a)k_{soil} \quad (2.28)$$

Where: k_{col}= permeability of the column, k_{soil}=permeability of unimproved soil.

- **Zones for settlement calculation**

The calculation of settlements of the improved soil is based on the performance of three different zones of the soil as shown in Figure 2.11, based on calculation model described in TK Geo 13 (2013).

Zone A: is a transition zone between the embankment and the lime/cement (LC) block. Since it is the upper part of the columns the compression strength is not adequate to carry the proportional elastic part of the applied load hence the column is in plastic failure.
Zone B: is LC block. It is the main lower zone and improved as a composite material; its material properties are obtained by taking the weighted mean value of the properties of the column and the soil.
Zone C: is unimproved clay under the LC block.

In this calculation method, different assumptions have been considered. The load distribution model assumes Boussinesqs solution for an infinite half space (Alen et al. 2006). The influence of limited depth at the bottom and stress concentration caused by the improved clay is taken into consideration.

In the calculation of settlement in zone A the first task is to determine the limiting depth between the plastic and elastic zones. The thickness of zone A, (d) is determined by the depth where the critical shear strength is not exceeded or the depth at which the weight Q2 of the pyramid in Figure 2.12 is balanced by adhesion along the adjacent column. According to Alen et al. (2006), a simple equilibrium analysis will use by considering the load distribution as shown in Figure 2.12. Part of the embankment load Q1 taken up by the bridging effect and the remaining embankment load Q2 is taken by the shear stress along the perimeter of the column which controls the extension of the zone with depth. Then the equilibrium equation is simplified to get the depth of the transition zone d.

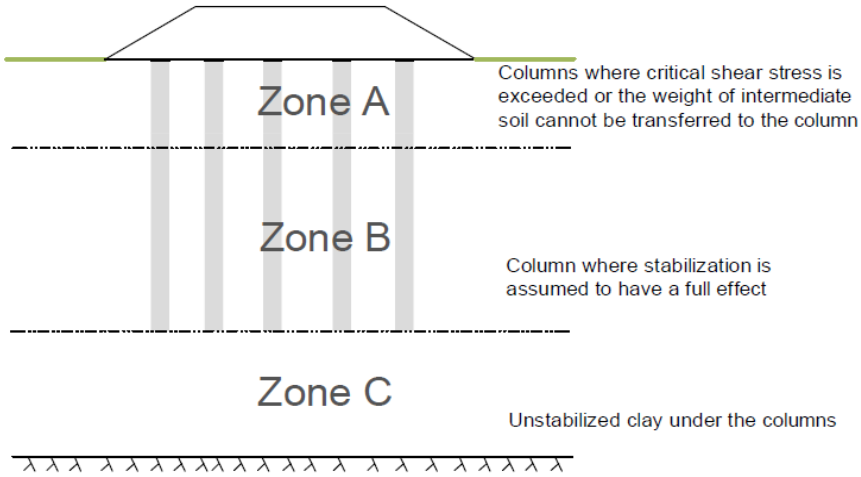

Figure 2.11 Zoning of improved soil block, (TK Geo 13 2013)

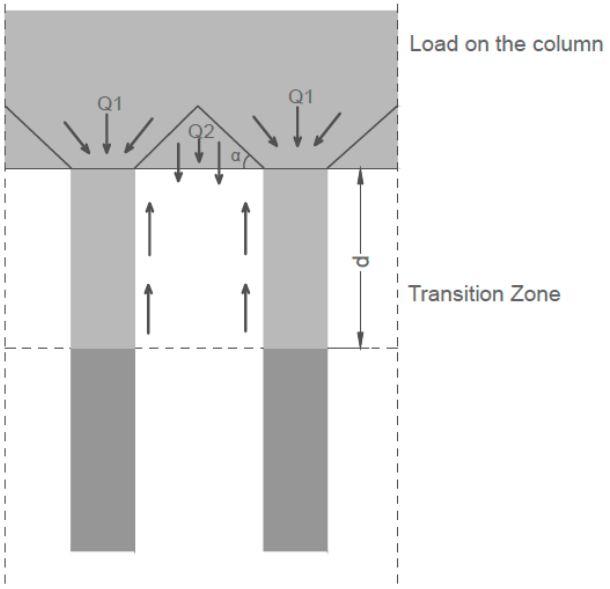

Figure 2.12 Schematic diagram of load transfer to the column for calculation of depth of transition zone (after Alen et al. 2006)

In the method introduced in TK Geo 13 (2013) the stress increment on the column due to the applied surface load is calculated by considering the load distribution as shown in Figure 2.13. The load acting on the improved soil volume q is divided into two fictional loads. The load ($q_{ö}$) is assumed to act at the top surface level of the improved soil block and the other load (q_U) will act at the lower edge of the improved soil block.

To estimate the two loads described in the model, the first step is to determine the load distribution factor. (η_{LC}) is a function of M_{block} and M_{soil}. It also depends on the depth of the block (L_{col}) and the depth of the soil up to the firm layer (d). Then the distributed load within the improved soil block as illustrated in Figure 2.13 can be calculated as:

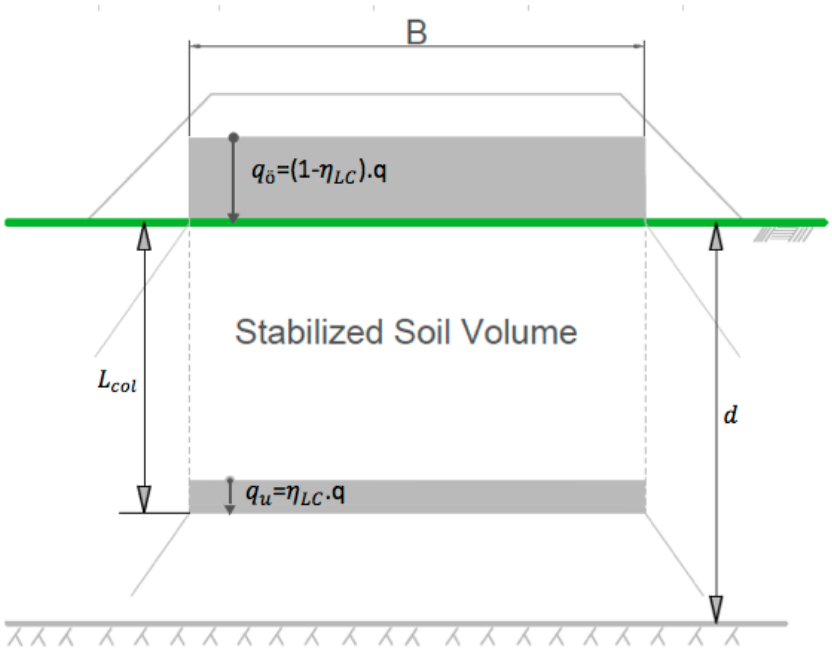

Figure 2.13 Load distribution model for calculation of stress addition (TK Geo 13 2013)

$$q_{ö} = (1 - \eta_{LC}).q \quad (2.29)$$

$$q_U = \eta_{LC}.q \quad (2.30)$$

$$\eta_{LC} = \left(\frac{L_{col}}{d}\right)^{\beta} \quad (2.31)$$

$$\beta = \frac{1}{\left(\frac{M_{block}}{M_{soil}}\right)^{0.1} - \left(\frac{M_{soil}}{M_{block}}\right)^{0.1}} \quad (2.32)$$

M_{block} is compression modulus of the improved soil block as considered a composite material and M_{soil} is compression modulus of unimproved soil between the columns. Both are selected as a representative average value with in the block.

As it has mentioned earlier the influence of the load spreading is based on the Boussinesqs solution for infinite half space. According to Alen et al. (2006) the influence factor for a stress intensity of an infinitely long embankment with width B can be determined as:

$$I(B,x,z) = \begin{bmatrix} 2z.\frac{B+2x}{4z^2+(B+2x)^2} + \text{atan}\left(\frac{B+2x}{2z}\right) \\ +2z.\frac{B-2x}{4z^2+(B-2x)^2} + \text{atan}\left(\frac{B-2x}{2z}\right) \end{bmatrix} \quad (2.33)$$

Where *x* is the distance from the center of the load in the horizontal direction perpendicular to the soil and *z* is the depth under the load.

The load distribution on the above is applied for isotropic and semi-infinite soil volume and using a restricted depth to the firm layer causes stress concentration towards the center. Then it is proposed to use a reduced depth to account this problem. So, a depth reduction factor is applied to calculate the fictitious depth z_{fic} as expressed in Eq. 2.34.

$$\mu_z = \left(1 - \frac{0.4B}{d}\right) \quad and \quad z_{fic} = \mu_z z \quad (2.34)$$

By combining the load distribution described in the model shown in Figure 2.13 the stress increment on the LCC can be calculated as described in Eq. 2.35 and 2.36, (Alen et al. 2006).

$$\Delta\sigma_{LC}(z) = (1 - \eta_{LC}).\sigma(q, \mu_z.z) + \eta_{LC}.q \quad for\ z < L_{col} \quad and\ x < B/2 \quad (2.35)$$

$$\Delta\sigma_{LC}(z) = (1 - \eta_{LC}).\sigma(q, \mu_z.z) \quad for\ z < L_{col} \quad and\ x > B/2 \quad (2.36)$$

$$\Delta\sigma_{LC}(z) = (1 - \eta_{LC}).\sigma(q, \mu_z.z) + \eta_{LC}.\sigma(q, \mu_z.(z - L_{col}) \quad for\ z > L_{col} \quad (2.37)$$

Where: - $\Delta\sigma_{LC}$ is the vertical stress increase on the block, L_{Col} is the length of the column, B is the width of the area to be improved.

- **Compression in improved soil**

In the development of the basic analytical model it is assumed that plane section will remain plane for any stress changes. Based on this the compression of the column and the soil are equal and the compression of the improved soil block (ε) calculate as:

$$\varepsilon = \frac{\Delta\sigma_{LC}}{M_{block}} = \varepsilon_{col} = \frac{\Delta\sigma_{v,col}}{E_{col}} = \varepsilon_{soil} = \frac{\Delta\sigma_{soil}}{M_{soil}} \quad (2.38)$$

Where: - $M_{block} = a.E_{col} + (1-a).M_{soil}$, $\Delta\sigma_{v,col}$ = is the vertical increase of stress in the column, $\Delta\sigma_{soil}$= is the vertical increase of stress in the soil.

Replacing the expression for M_{block} in Eq. 2.38 and rearranging resulted Eq. 2.39 to calculate the stress increment on the column.

$$\Delta\sigma'_{v,col} = \frac{\Delta\sigma_{LC}}{\left[(1-a).\frac{M_{soil}}{E_{col}}+a\right]} \quad (2.39)$$

Similarly, Eq. 2.40 was derived from Eq. 2.39 to calculate the stress increment on the soil.

$$\Delta\sigma'_{soil} = \frac{M_{soil}}{M_{block}}\Delta\sigma_{LC} \quad (2.40)$$

The calculation of the compression was done in an iterative process since the response of the materials in the load distribution model is influenced by the effective stress (σ'). This is because the column can't carry load greater than the critical stress ($\sigma'_{LCC,max}$). For compressive strength of the column, an analogy was proposed based on active triaxial tests. If a change in horizontal stress is caused due to additional vertical stress, the compressive strength of the column can be drawn based on Mohr-Coulomb rupture hypothesis as expressed in Eq. 2.41.

$$\sigma'_{LCC,max} = 2.\frac{cos\phi'_{col}}{1-sin\phi'_{col}}.c'_{col} + \frac{1+sin\phi'_{col}}{1-sin\phi'_{col}}.\sigma'_{h,col} \quad (2.41)$$

Where: - c'_{col} and ϕ'_{col} are inner strength parameters. The horizontal stress of the column calculated according to Eq. 2.42 assuming that the installation of the column doesn't affect the stress situation.

$$\sigma'_{h,col} = \sigma'_{h,0,soil} + 0.5\Delta\sigma'_{v,soil} \quad (2.42)$$

Where: $\sigma'_{h,0,soil} = K_0.\sigma'_{v,soil}$

Then the maximum vertical stress increment from the column contribution calculated as:

$$\Delta\sigma_{col,max} = \sigma'_{LCC,max} - \sigma'_{v,0} \quad (2.43)$$

The strain in the column due to the maximum stress increment becomes:

$$\varepsilon_{col,max} = \frac{\Delta\sigma_{col,max}}{E_{col}} \quad (2.44)$$

- **Long term settlements**

The stress increments in Eq. 2.39 and 2.40 are long term increments which are increment of the effective stress after deduction of pore water pressure. Based on this the long-term settlement on the

improved soil block can be calculated in a conventional way by integrating the strain of the block due to the applied load as expressed in Eq. 2.45.

$$s = \int_0^{L_{col}} \varepsilon dz = \int_0^{L_{col}} \frac{\Delta\sigma'_{v,col}}{E_{col}} dz \quad or \int_0^{L_{col}} \frac{\Delta\sigma'_{soil}}{M_{soil}} dz \tag{2.45}$$

- **Time dependent settlement**

The time dependent settlements of LCC improved soil block with consideration of flow in the radial direction estimated from Eq. 2.44. As per TK Geo 13 (2013) recommendation, this estimation can be valid under the provision of the diameter of the column (D_{col}) is between $0.5 \leq D_{col} \leq 1.0\ m$ and the center-to-center distance (cc_{col}) is between $0.8 \leq cc_{col} \leq 2.0\ m$.

So, the consolidation of the LC soil block calculated by considering the column as a vertical drain. Hence the degree of consolidation estimated using Eq. 2.46.

$$U = 1 - \exp\left[\frac{2.c_{vh,block}.t}{R^2.f(n)}\right] \tag{2.46}$$

Where *t*- is the time of consolidation $c_{vh,block}$ is the coefficient of consolidation in horizontal direction and flow in the vertical direction of the block, *R* is the influence radius. Since the column is installed in a square pattern *R=0.55.* cc_{col}. The Factor $f(n)$ can be calculated as:

$$f(n) = \frac{n^2}{n^2-1}\left[\ln(n) - 0.75 + \frac{1}{n^2}.\left(1 - \frac{1}{4.n^2}\right)\right] + \left[\frac{n^2-1}{n^2}.\frac{1}{r^2}.\frac{k_{soil}}{k_{col}}.L_{col}^2\right] \tag{2.47}$$

The value of $c_{vh,block}$ is taken $2c_{vv,block}$ and the k_h is assumed $3k_v$.

Chai & Carter (2011)

Chai & Carter (2011) had been developed a method for calculation of settlements of a clay soil improved by fully penetrated column. The method was originally proposed for a soil improvement using soil cement column. The basic concept of this method is similar with various studies done for calculation of settlements of a composite ground. This method is adapted for calculation of settlements of a soil improved by deep mixing column. So, Chai & Carter (2011) suggested two methods for calculation of the final settlement of a soil improved applying fully penetrated column. The two methods are the equilibrium and the composite modulus.

- **The equilibrium method**

The equilibrium method allows calculating one-dimensional settlement of the improved soil by considering the effect of the stress concentration between the clay soil and the column as illustrated in Figure 2.14(a). In the unit cell concept, it is assumed that all the columns can behave the same. The vertical displacement on any horizontal level is considered as uniform.

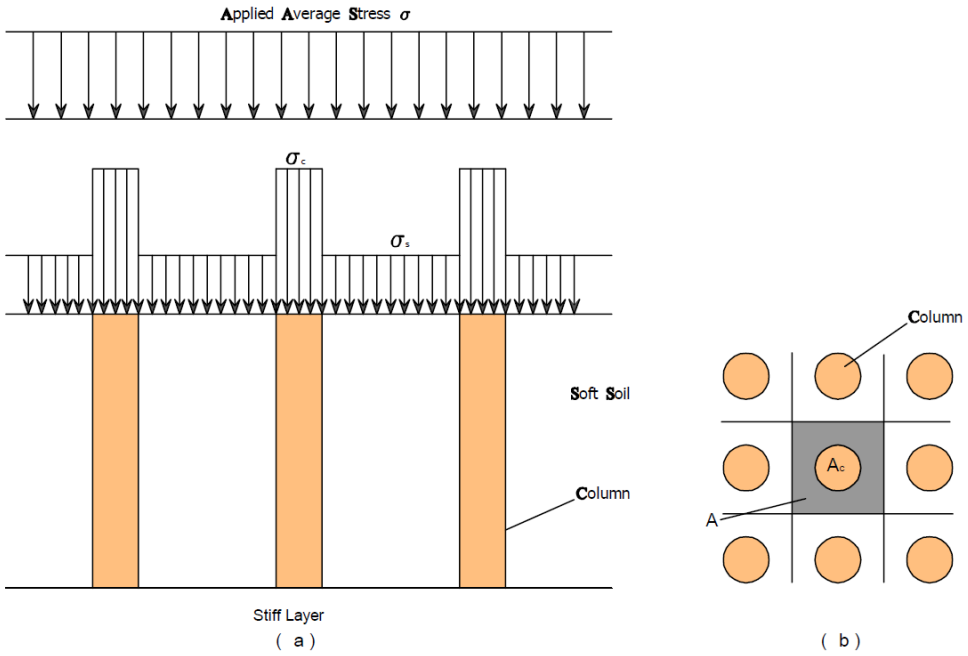

Figure 2.14 Illustration of a) stress concentration b) cross section of the column (after Chai and Carter 2011)

According to Chow (1996) the equilibrium of forces in Figure 2.14(a) can be expressed as:

$$\sigma A = \sigma_{col} A_{col} + \sigma_{soil}(A - A_{col}) \tag{2.48}$$

Where: σ is the average applied vertical stress, σ_{soil} is the stress acting on the surrounding soil, σ_{col} the stress acting on the LCC, A is the total area to be improved by a single column and A_{col} is the cross-sectional area of the column.

The strain compatibility between the LCC and the surrounding soil will result

$$\varepsilon = \varepsilon_{col} = \varepsilon_{soil} \tag{2.49}$$

Where ε is strain in the unit cell, ε_{col} strain in the surrounding soil and ε_{soil} strain in the column. The assumption of one dimensional confined compression gives

$$\frac{\sigma_{soil}}{M_{soil}} = \frac{\sigma_{col}}{M_{col}} \tag{2.50}$$

Where M_{soil} is the compression modulus of the surrounding soil and M_{col} is the compression modulus of the LCC. This approach can be applied when the clay is considered as drained since it is related with long term settlement. So, Eq. 2.50 can be written as

$$\frac{M_{col}}{M_{soil}} = \frac{\sigma_{col}}{\sigma_{soil}} = m \tag{2.51}$$

Where: m is stress concentration or modular ratio.
According to Chai & Carter (2011) the vertical stresses acting on the column and the surrounding soil can be obtained as expressed in Eq. 2.52 and 2.53 respectively, by substituting Eq. 2.51 in to Eq. 2.48.

$$\sigma_{col} = \frac{m\sigma}{[1+(m-1)a]} = \mu_c\sigma \quad (2.52)$$

$$\sigma_{soil} = \frac{\sigma}{[1+(m-1)a]} = \mu_s\sigma \quad (2.53)$$

Where μ_c and μ_s are the ratio of the stress in the column and the surrounding soil to the average applied stress respectively, a is the improvement area ratio which is calculated as $a = A_{col}/A$.
The settlement before improvement S_0 of a clay sub soil can be calacualted by the following equation.

$$S_0 = m_{vs}.\sigma.H \quad (2.54)$$

Where m_{vs} is the cofficent of volume compressibility of the soft soil, H is the thickness of the soft soil. The final settlement of the improved soil can be estimated by the following equation by taking into the effect of stress concentration into consideration.

$$S = m_{vs}.\mu_s.\sigma.H \quad (2.55)$$

The settlement reduction ratio between improved and unimproved soil can be obtained by Comparing Eq. 2.54 and 2.55, which is

$$\frac{S}{S_0} = \beta = \mu_s.$$

- **The composite modulus method**

In the composite modulus method, the improved soil zone was assumed as a uniform mass with an improvement area ratio a. The constrained modulus of the mass D can be obtained from weighted average of the constrained moduli or from the volume compressibility of the column and the surrounding soil. So D can be calculated from two approaches. The first approach is calculating using the volume compressibility.

$$D = \frac{1}{m_{vs}(1-a)+m_{vc}a} \quad (2.56)$$

Where m_{vc} is the coefficient of volume compressibility of the column. The second approach to calculate D is from the constrained moduli of the column D_c and the soil D_s.

$$D = a.D_c + (1-a).D_s \quad (2.57)$$

The value of D calculated using Eq. 2.56 is much smaller than the one obtained from Eq. 2.57. In this regard, it is recommended to use Eq. 2.56 in a case of equal stress condition at the ground surface aiming on settlement of the clay soil. It is recommended to use Eq. 2.57 in the case of equal strain condition aiming settlement of the column.

According to Lambe & Whitman (1979) the constrained modulus is the ratio of the axial stress to the axial strain in a case of confined compression. So D_c and D_s can be computed using Eq. 2.58 and 2.59 respectively.

$$D_c = \frac{E_c(1-\nu_c)}{(1+\nu_c)(1-2\nu_c)} \quad (2.58)$$

$$D_s = \frac{E_s(1-\nu_s)}{(1+\nu_s)(1-2\nu_s)} \quad (2.59)$$

Where ν_c and ν_s are the possinous ratio of the column and the soil respectively.

The strain in the unit cell can be determined by Eq. 2.60

$$\varepsilon = \frac{\sigma A}{A_{col}M_{col}+(A-A_{col})M_{soil}} \quad (2.60)$$

Eq. 4.34 can be simplified to

$$\varepsilon = \frac{\sigma}{M_{soil}}\left(\frac{1}{1+(m-1)a}\right) \quad (2.61)$$

Then the final settlement of the improved clay soil can be calculated as

$$S = \frac{\sigma H}{M_{soil}}\left(\frac{1}{1+(m-1)a}\right) \quad (2.62)$$

The method proposed by Chai & Carter (2011) calculates the degree of consolidation of the improved soil by considering the effect of flow in both the vertical and radial directions. The final degree of consolidation could be the average of the vertical and the horizontal. For a fully penetrated column, a formula for degree of consolidation was derived based on the illustrative diagram shown in Figure 2.15.

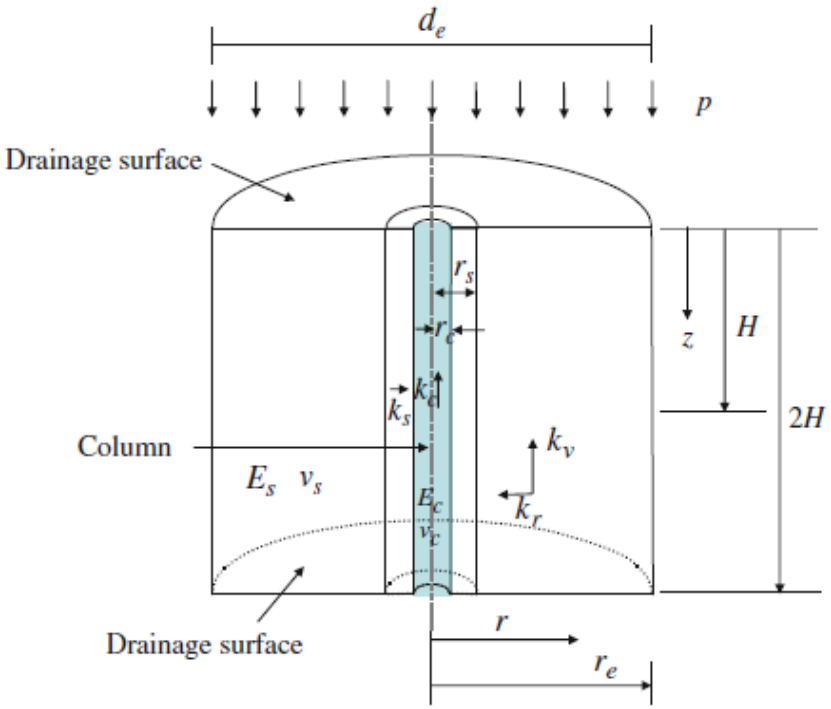

Figure 2.15 Illustrative diagram and definition of terms for unit cell model (after Chai & Carter 2011)

Hence the average degree of consolidation due to a flow in the radial direction (U_r) can be expressed as:

$$U_r = 1 - e^{-\left(\frac{8}{F'_m}\right)T_{rm}} \tag{2.63}$$

Where:$T_{rm} = \frac{c_{rm}}{d_e^2}t$, $c_{rm} = c_r\left(H - n_s\left(\frac{1}{n^2-1}\right)\right)$ and

$$F'_m = \left(\frac{n^2}{n^2-1}\right)\left(\ln\left(\frac{n}{s}\right) + \frac{k_r}{k_s}\ln(s) - \frac{3}{4}\right) + \left(\frac{s^2}{n^2-1}\right)\left(1 - \frac{k_c}{k_s}\right)\left(1 - \frac{s^2}{4n^2}\right) + \left(\frac{k_r}{k_s}\right)\left(\frac{1}{n^2-1}\right)\left(1 - \frac{1}{4n^2}\right) + \frac{32}{\pi^2}\left(\frac{k_r}{k_c}\right)\left(\frac{H}{d_c}\right)^2$$

Where c_r= is coefficient of consolidation of the soft soil due to radial flow, n_s= the stress concentration ratio between the vertical stress in the column and in the surrounding soil, t= time, $n = r_e/r_c$, $d_c = 2r_c$, and $s = r_s/r_c$. The effect of the vertical flow of the natural clay soil was evaluated by using Terzaghi's one-dimensional consolidation theory. Then it is combined with the effect of the radial flow due to the presence of the column and vertical flow of the clay soil. Finally, by using a solution of (Carrillo 1942) the average degree of consolidation (U_{vr}) can be obtained from Eq. 2.64.

$$U_{vr} = 1 - (1 - U_v)(1 - U_r) \tag{2.64}$$

For prediction of final settlements of a soil improved by LCC the current design method in Sweden is based on the assumption that plane section will remain plane. Similarly, it is assumed that the horizontal section of the ground will remain horizontal during the entire course of the settlement (Baker 2000). The assumption was originally introduced by (Broms 1984) in a model for ground improvement using lime column. Based on this the soil in the column soil system was assumed to behave as an elastic material whereas the column inclusion behaves as elastoplastic material. The relationship between the load and the deformation in a binder improved soil is assumed to be ideal elastoplastic as shown in Figure 2.16. The empirical formula described in Eq. 2.65 can be used to estimate the failure strength of the LCC.

$$\sigma_{failure}^{col} = 2.c_{uk} + 3.\sigma_h \tag{2.65}$$

Where: c_{uk}- characteristics undrained shear strength of the column, σ_h=total horizontal stress at the column – soil boundary.

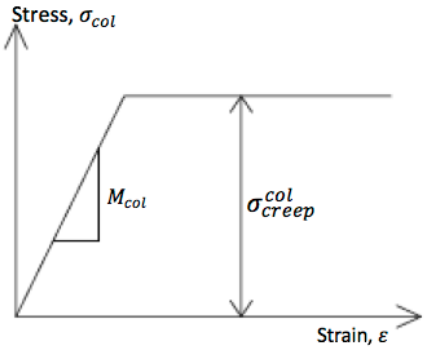

Figure 2.16 Assumed load deformation relationship for improved soil linear elastic plastic behavior, (after Baker 2000)

According to Figure 2.11, the relationship is linear elastic up to the column creep strength σ_{creep}^{col} and the slope represents the elastic modulus of the column, E_{col}. Once the creep strength reached, it is assumed that the load will be constant. This load-deformation relationship can be used for analysis of load distribution between the column and the unimproved soil.

2.3.2 Settlement prediction numerical

Jiang et al. (2013)

Jiang et al. (2013) have presented a study on numerical analysis for consolidation of soft soil, which is improved by a fully penetrated deep mixed column. The study mainly focused on the analysis of the effect of different parameters on the consolidation process of a soft soil that result in a settlement. A mechanically and hydraulically coupled three-dimensional numerical method was employed for the study, and a unit cell concept was implemented by assuming the column and the surrounding soil as an elastic material. To verify the three-dimensional, model a case study have been carried out on the consolidation of the fully penetrated stone column before the numerical analysis of the deep mixed column. Then the consolidation of the deep mixed column foundation was examined by replacing the stone column with the deep mixed column. The verification of the model of the unit cell of stone column studied by (Tan et al. 2008) was selected and a quarter of the unit cell which have the same size, material properties and boundary condition with (Tan et al. 2008). Commercial finite element soft wares ABAQUS and PLAXIS were used for the numerical analysis and comparison was made between the results from each to assure the correctness of the numerical simulation.

In this numerical analysis, a baseline case study was designated as a typical case to establish a base for comparison when the parameters vary from the baseline case. The model for the baseline case was considered as linearly elastic, similar to the quarter of the unit cell of the deep mixed column mentioned earlier. But as the schematic model in Figure 2.17 shows the stone column was replaced by the deep mixing column with different material properties. So, the following assumptions were made to adopt the model for the numerical analysis of the deep mixed column. The elastic modulus of the column is assumed to be ten times the surrounding soil, and the load was applied after the completion of the column hardening; both the vertical and radial permeability of the column were assumed the same with surrounding soil.

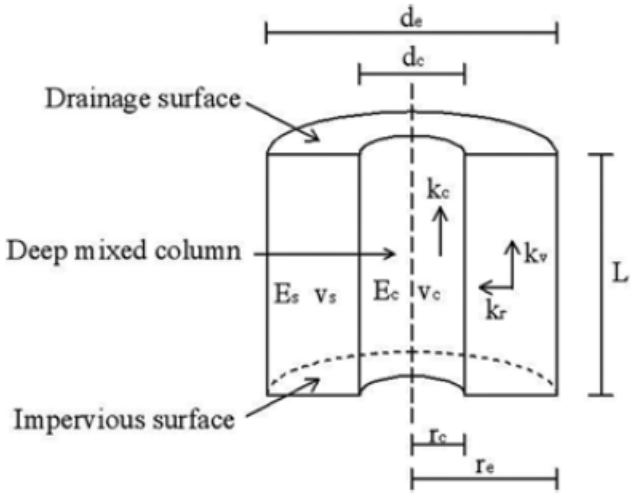

Figure 2.17. Schematic model of the unit cell of the fully penetrated deep mixed column (after Jiang et al.2013)

The vertical stress distribution of the baseline model under a rigid plate was analyzed after the end of consolidation. Relatively uniform distribution of stress obtained on the top of the column. The stress concentration ratio at the end of the consolidation ($n = \sigma_c/\sigma_s$) which is the average vertical stress on the column to the average vertical stress on the surrounding soil was calculated. This value is less than the calculated value of the modular ratio. But from the theoretical background, the stress concentration ratio and the modular ratio should be the same if the column and the surrounding soil considered as a one-dimension settlement. So, the difference between the stress concentration ratio and the modular ratio indicates as the column deforms not only one-dimensionally also deforms laterally.

The settlement of the column and the surrounding soil was calculated from the numerical analysis as well as from Eq. 2.66, which is developed based on the concept of the composite foundation. A comparison was made between the two results and the result from Eq. 2.66 become larger than results from the numerical analysis. The cause for larger settlement from the simplified method proves that the surrounding soil is not in a one-dimensional constrained condition. So according to Han & Ye (2001), the column can deform in the lateral direction, and due to this reason, the vertical settlement (compression) of the surrounding soil will decrease.

$$S = \frac{\sigma}{[1+a_s(n-1)]D_s} H \tag{2.66}$$

Where: S= the consolidation settlement, σ= average vertical stress on the rigid plate, a_s= area replacement ratio, n= the stress concentration ratio, H= the thickness of the soft soil and D_s= the constrained modulus of the surrounding soil can be computed using Eq. 2.67 (Mayne & Poulos 1999).

$$D_s = \frac{E_s(1-v)}{(1+v)(1-2v)} \tag{2.67}$$

Where: E_s= is the elastic modulus of the surrounding soil, v= is the poisson's ratio of the surrounding soil.

As the author proved that the average degree of consolidation could be calculated from the known definition expressed in Eq. 2.68 but it is not suitable to do it during the whole consolidation process using this equation from the numerical results. Because the average excess pore water pressure profile needs to be calculated at every moment.

$$U = 1 - \frac{\int_0^H u_t dz}{\int_0^H u_0 dz} \tag{2.68}$$

Where: u_0 is the initial pore water pressure, u_t excess pore water pressure at time t, z is the depth of the foundation from the ground surface and H is the thickness of the soft soil.

The other way to calculate the average degree of consolidation is based on the calculated settlement at a time t as expressed in Eq. 2.69.

$$U = \frac{S_t}{S_f} \tag{2.69}$$

Where: S_t is the top surface settlement at time t and S_f is the final settlement at the end of consolidation.

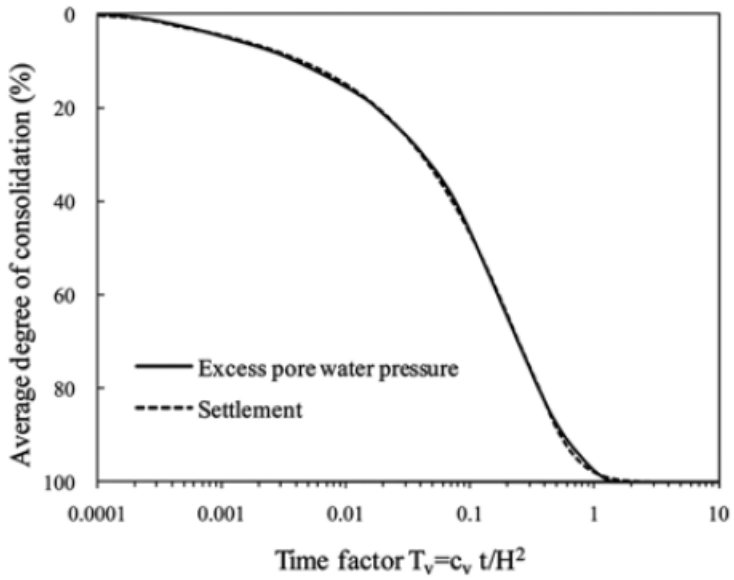

Figure 2.18. Average degree of consolidation based on settlement and excess pore water pressure (after Jiang et al. 2013)

To make a comparison between the two definitions, a plot of average degree of consolidation versus time was presented. Both definitions in Eq. 2.68 and 2.69 produce an identical average degree of consolidation as shown in Figure 2.18. This conclusion works under the assumption of both the column and the surrounding soil behave as linear elastic.

Finally, a parametric study was conducted to examine the effect of the predefined four different factors on the stress concentration ratio, settlement and degree of consolidation. As the result of the analysis shows the factors the soil thickness to the unit cell diameter ratio, the area replacement, and permeability ratios are don't have a significant effect on the stress concentration ratio. But the stress concentration increases with modulus and time. The analysis also proved that the settlement of the deep mixed foundation column increases as the thickness of the soft soil increase but settlement decrease as modulus and area replacement ratio increases. Moreover, in this study, it is also observed the increase in the average degree of consolidation of the deep mixed column foundation as an increase in the elastic modulus of the column, the area replacement, and permeability ratio.

Tan et al. (2008)

Tan et al. (2008) have been developed plane strain modeling of a stone-column improved ground. The analysis was mainly focused on the method to convert axisymmetric to plane strain model. The conversion method was developed based on the analytical solution for consolidation, and the matching includes the derivation of the equivalent plane strain parameter and geometry. The matching scheme categorized into two parts, the geometry-matching scheme, and the parameter-matching scheme.

- **Parameter matching scheme**

The parameter matching scheme is one of the methods to convert from axisymmetric to plane strain model as proposed by (Tan et al. 2008). In this case, the column width in the plane strain model is taken as equal to the column diameter in the axisymmetric model, to have equal flow path along the column perimeter. Hence as shown in Figure 2.19(a) and (b) the relation can be expressed as: -

$$b_c = r_c \tag{2.70}$$

Compatibly, the radius of the drainage zone R is also taken as equal to the equivalent plane strain width B as shown in Figure 2.19(a) and (b).

$$R = B \tag{2.71}$$

This method allows an easy transition from axisymmetric to plane strain model since the same basic geometrical input data were used. As the geometric configuration is unchanged in both axisymmetric and plane strain model, it falls into a category of parametric matching scheme model. Thus, some parameters in the plane strain model need to be adjusted by taking the change in geometry into consideration. The stiffness of the material of the plane strain can be described by the following relation which is based on the matching of the composite stiffness of the soil and the column.

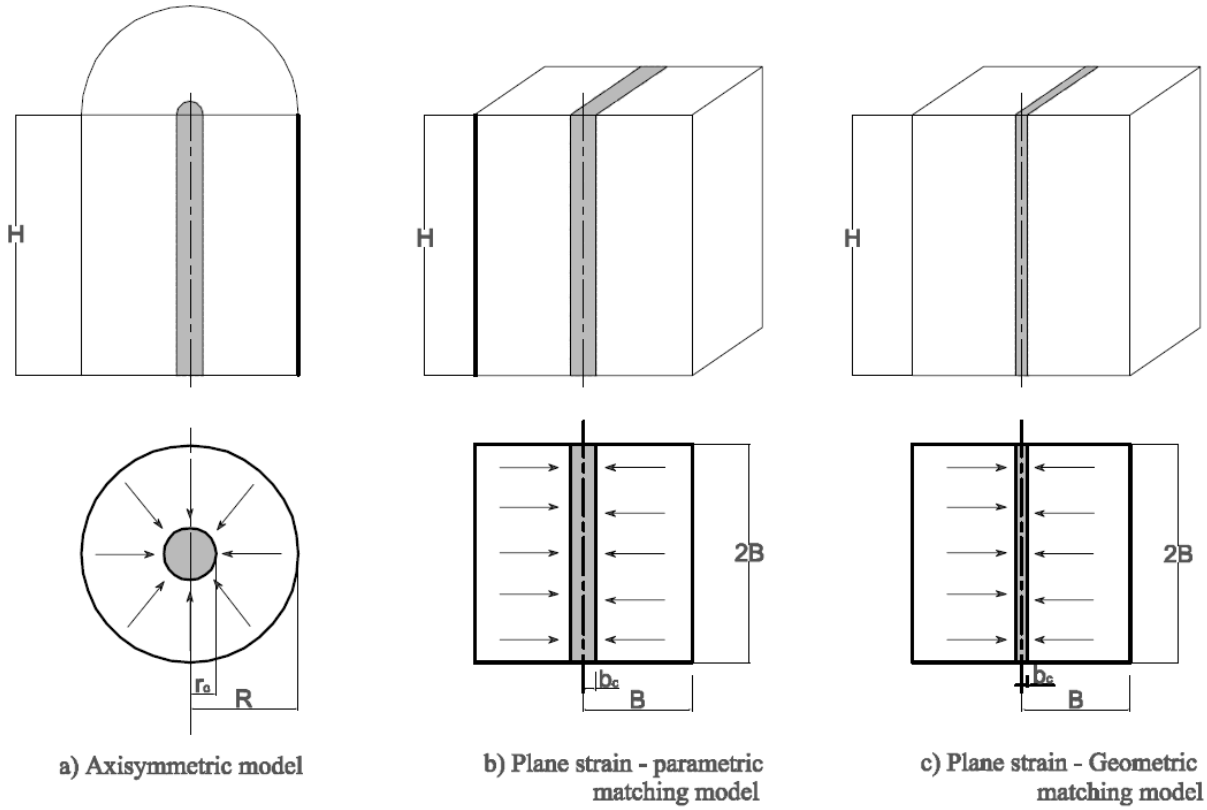

Figure 2.19 Cross section of a unit cell LCC and plane strain conversion (after Tan et al. 2008)

$$E_{c,pl}a_{pl} + E_{s,pl}(1 - a_{pl}) = E_{c,ax}a_{ax} + E_{s,ax}(1 - a_{ax}) \tag{2.72}$$

Where: - E_c and E_s are the elastic modulus of the column and the surrounding soil respectively and subscripts pl and ax represents the plane strain and axisymmetric model respectively. And a is the area replacement ratio, $a = A_{col}/(A_{col} + A_{soil})$, where A_{col} and A_{soil} are area of the column and the soil respectively. In this method $E_{s,pl} = E_{s,ax}$ to simplify the analysis and $E_{c,pl}$ can be calculated using Eq. 2.72.

The matching of the permeability was done by using the Eq. 4.40 which is derived by (Tan & Oo 2005).

$$\frac{k_{h,pl}}{k_{h,ax}} = \frac{F(N)_{pl}}{F(N)_{ax}} \left[\frac{m_{vs}m_{vc}(1-a)}{m_{vc}(1-a)+m_{vs}a}\right]_{pl} \left[\frac{m_{vc}(1-a)+m_{vs}a}{m_{vs}m_{vc}(1-a)}\right]_{ax} \left(\frac{B^2}{R^2}\right) \tag{2.73}$$

Where k_h= is coefficient of permeability of the soil in the horizontal direction;

$$F(N) = \left[\frac{N^2}{N^2-1}\right] \ln(N) - \frac{3N^2-1}{4N^2} \tag{2.74}$$

Where N is the diameter ratio $N = R/r_c$ for axisymmetric and $N = B/b_c$ for plane strain model;

$$m_{vs} = \frac{\alpha_{vs}}{1+e_s} \tag{2.75}$$

$$m_{vc} = \frac{\alpha_{vc}}{1+e_c} \tag{2.76}$$

Where $\alpha_{vc} = (1 + e_c)/E_c$ and $\alpha_{vs} = (1 + e_s)/E_s$ are coefficients of compressibility of the column and the surrounding soil respectively; and e_c and e_s are void ratios in the column and in the soil respectively.

Since the water flows mainly in the horizontal direction a small influence of the vertical permeability will be expected on the rate of consolidation and it is assumed to have equal vertical permeability value both in the axisymmetric and plane strain model $k_{v,pl} = k_{v,ax}$. So, the horizontal permeability of the plane strain model can be calculated from Eq. 2.73.

- **Geometry matching scheme**

This method is established based on the equivalent drainage capacity of the column in the axisymmetric and plane strain condition (Tan et al. 2008). The concept is originally developed for conversion of vertical drain system to equivalent plane strain drain walls. In this conversion method, it is assumed to have an equal total cross-sectional area (area of the column and the surrounding soil) in both axisymmetric and plane strain condition. The width of the column in the plane strain model can be obtained from the relation expressed in Eq. 2.77 which is derived based on the equivalent area ratio.

$$b_c = B\frac{r_c^2}{R^2} \tag{2.77}$$

Eq. 2.77 gives smaller plane strain column width and larger flow path length compared with the other method as shown in Figure 2.19 (b) and (c). Since the column are set in a square pattern R and B related as expressed in Eq. 2.78 (Barron 1948).

$$R = 1.13B \tag{2.78}$$

In the case with large column diameter and smaller spacing between columns this method is more preferable compared to the previous one; the first method gives excessive area replacement ratio and column drainage capacity in the plane strain condition because of unchanged geometrical configuration in both model. It might be possible to use Eq. 2.72 to determine the plane strain column stiffness but will get the same column stiffness in both models, that is $E_{c,pl} = E_{c,ax}$ it is given as $a_{pl} = a_{ax}$ and $E_{s,pl} = E_{s,ax}$ similar with the first method. To make the analysis simple both the vertical and the horizontal permeability in the axisymmetric and plane strain model are taken equal that is $k_{h,pl} = k_{h,ax}$ and $k_{v,pl} = k_{v,ax}$. So, in this conversion method the plane strain model keeps similar parameters with the axisymmetric model and it falls to the category of geometry matching scheme model.

Finally, those methods were tested to validate with comparison in unit cell simulation and comparison in field test results. In the case of the unit cell, both methods gave good agreement with the benchmark regarding long-term settlement, but the parametric matching model gave an over the estimated rate of consolidation. In the case of the field measurement, the parametric matching model gave an erroneous lower long-term settlement whereas the geometric matching model shows a good agreement with the benchmark.

2.4 Stiffness of LCC

The mixing of a binding agent like lime, cement or lime and cement into a loose or soft clay soil will change the strength as well as the deformation behavior of the clay very quickly. Then the improved soil became very stiff compared to the unimproved soil. The increase in strength of the improved soil (LCC) will lead to stress concentration on the column and reduction of additional stress on the unimproved soil. But as studies in Åhnberg (2006) show that the strength of the LCC depends on different factors such as type and amount of binder, the type of soil, the curing time and the stress condition. The strength of the LCC will not be considered as a constant value, and it has characteristics to increase over time. As it had been proved in field tests, the LCC strength will have a substantial growth up to 10 years (Larsson 2007a).

The shear strength of the LCC can be evaluated from field or laboratory tests. The most common method is the unconfined compression laboratory test which is the quickest and cheapest method to evaluate the shear strength of the improved soil. Whereas the stiffness of the LCC can be obtained from a combined triaxial and odometer tests which will enable to see as the stiffness of improved soil proportional to the shear strength (Baker 2000).

Table 1.1 Young's modulus of LCC based on laboratory mixed samples at 56 days age (after Baker 2000).

Depth	Unconfined compressive strength		Secant Young's Modulus	
	laboratory	field	$E_{50,laboratory}$	$E_{50,field}$
m	[kPa]	[kPa]	[MPa]	[MPa]
1	314	344	30.5	34.0
2	330	407	23.0	33.0
3	261	332	22.0	36.0
4	278	250	30.0	30.0
5	380	390	31.0	34.5

A laboratory test was carried out by (Baker 2000) to evaluate the stiffness of LCC. Two different samples have been used for this test one from the field and the second was prepared in the lab. The field sample was taken from a clay soil of depth at 1 to 5 meters and mixed with 92 kg/m3 of binding agent which consists of 50% lime and 50% cement. The test was conducted at the curing age of 56 days.

The results show that the secant modulus E_{50} of the LCC vary between 30 to 36 MPa with an average value of 32.5 MPa. And the ratio secant modulus to the compressive strength was obtained between 90 and 140. As results in Table 1.1 shows that the secant modulus value of the laboratory-prepared samples is lower than the average secant modulus of field samples.

In a triaxial test conducted by Steensen-Bach et al. (1996) a 50/50 percent mixture of LC was used to improve the soil with an amount of binder 23 kg/m. The soil sample used for the test had the undrained shear strength of 6 – 15 kPa. The test result shows that the drained Young's modulus of the LCC between 30 and 50 MPa whereas the undrained Young's Modulus at stress level 50% of the failure load was between 45 and 105 MPa. The ratio of the undrained secant modulus to the undrained shear failure was about 200 to 500.

2.5 Permeability of LCC

According to Åhnberg (2006), there are several reasons that need to study the permeability of the improved soil. Among those it affects the pore water pressure response during loading, influence the extent to which undrained or drained condition that govern the strength behavior depending on the rate of loading. The other effect related to permeability of the improved soil is its high influence on the rate of consolidation after construction. The permeability is very different when it is measured on the field compared to the laboratory measured. The permeability of the improved soil will decrease through time due to the continuous formation of different reactions in the improved soil. The rate and the extent will depend on the amount of binder and the type of soil. The initial change in permeability may link to the change in void ratio and might be related to the change in water content.

As Baker (2000) described that the addition of lime would increase the permeability of the soft clay, but the permeability of the clay soil will not increase or decrease due to the addition of LC or cement mixture into the soil. Similar to the mechanical properties of the LCC its permeability also depends on the type of soil, the binder and the procedure of the production of the column.

Quang & Chai (2016) have been conducted a laboratory test to evaluate the permeability of clayey soil improved by lime and cement. The test result shows that the permeability (k) of the cement improved soil is equal with the unimproved soil with similar void ratio (e) conditions. But the (k) value will decrease significantly when the amount of cement increase above 8%. The same phenomena happened in the case of lime improved soil, and a threshold value of 4% and 8% were determined for the amount of lime and cement respectively.

A field and laboratory tests had been conducted by Baker (2000) to measure the permeability of the LCC. The field test made on the first site shows that the permeability of the LC improved soil varies 10 and 100 times that of the unimproved soil with an average value of 50. The values of permeability measured for field mixed sample of LCC vary 1 and 90 times that of the original soil. The fields mixed LC samples were used to measure the permeability in the laboratory and a variation of 3 and 25 times that of the clay soil were obtained.

Summary

Both the analytical and numerical settlement prediction methods reviewed in this section have a similarity as well as differences in some basic assumptions and procedures. The analytical methods proposed by Chai & Pongsivasathit (2010) and Gong et al. (2015) used the same double soil layer consolidation theory and developed for soil improvement using a soil cement column. The difference in Chai & Pongsivasathit (2010) is a cement stabilized slab was placed on top of the column and the relative penetration of the column due to the stress concentration was considered. In Gong et al. (2015) studies there is no slab and the relative penetration of the column was ignored for simplicity of the analysis. The settlement prediction in Chai & Pongsivasathit (2010) method is a function of the degree of consolidation and the change in vertical stress. Whereas in Gong et al. (2015) the settlement of the improved clay soil was determined by integrating a time dependent equation with a function of the average excess pore water pressure and coefficient of volume compressibility. Both Chai & Pongsivasathit (2010) and Gong et al. (2015) used a double layer consolidation solution published by Zhu & Yin (1999). For the improved soil layer an equivalent vertical permeability was introduced and used in both analytical methods. But in Gong et al. (2015) proposal equal vertical and horizontal permeability was assumed for the column which is not in Chai & Pongsivasathit (2010). The permeability (k) and the coefficient of volume compressibility (m_v) are the main parameters which were considered that influence the degree of consolidation in addition to the coefficient of consolidation. This consideration was applied in both Chai & Pongsivasathit (2010) and Gong et al. (2015) analytical methods.

The TK Geo 13 (2013) assumed equal vertical strain on the column and the surrounding soil similar with analytical methods in Gong et al. (2015), Chai & Pongsivasathit (2010) and Chai & Carter (2011). But the mechanism that the load distributed in the improved soil is different in the case of TK Geo 13 (2013). All the applied load on the top of the improved soil block not transferred to the bottom of the block rather distributed at the top and bottom with a load distribution factor. This is the main difference of TK Geo 13 (2013) calculation model with analytical methods proposed by Gong et al. (2015), Chai & Pongsivasathit (2010) and Chai & Carter (2011). The consideration of the improved soil as a composite material is the same assumption in both TK Geo (2013) and (Chai & Carter 2011) analytical methods. However, TK Geo 13 (2013) predicts the compression of the improved soil block by calculating the ratio of the additional stress to the stiffness which is similar with the basic hooks law. In Chai & Carter (2011) the improved soil layer was considered as a composite ground, and the

settlement of the improved soil was determined by using the stress ratio and coefficient of volume compressibility of the soil as a factor. The coefficient of volume compressibility is a function of the constrained modulus which is determined by area weighted average of the constrained moduli of the column and the soil. In all analytical methods reviewed in this section the rate of consolidation was calculated based on the principle developed for vertical drain and hence the column considered as a vertical drain. In TK Geo 13 (2013) the degree of consolidation was determined using the permeability and the coefficient of consolidation as an input by considering flow only in the radial direction. The difference in Chai & Carter (2011) method is the degree of consolidation was calculated by taking the average of the radial and vertical degree of consolidation. The radial degree of consolidation was determined by using the stress concentration ratio as an input and the vertical degree of consolidation was calculated by the conventional method which uses the time factor as input.

The analytical approach developed by Alamgir et al. (1996) was targeted to study the different deformation behavior of the soft ground and the columnar inclusion. So, the column and the soft soil don't deform equally unlike the assumption considered in Gong et al. (2015), Chai & Pongsivasathit (2010) and Chai & Carter (2011). The consideration of compatibility between the column and the soil gave equal deformation only at the interface. The basic idea of the analysis was to define the shape of the deformation of the column and the soil, and the result showed that the column deforms uniformly in its all cross-sectional area whereas the deformation of the soil is the same with the column at the interface and increase along the radial direction. This approach looks more realistic when it is compared with the real phenomena that could happened due to the column soil interaction. Similar with studies performed in Gong et al. (2015), Chai & Pongsivasathit (2010) and Chai & Carter (2011) the deformation in the radial direction was neglected in Alamgir et al. (1996) for simplicity of the analysis.

The numerical analysis performed by Jiang et al. (2013) was done for a fully penetrated deep mixing column. As previous studies showed that in most cases the numerical methods were developed based on the analytical solution. Hence Jiang et al. (2013) used similar equations with Chai & Carter (2011) and Gong et al. (2015) to predict the settlement of the improved soil and for calculation of the degree of consolidation. Jiang et al. (2013) were modeled the column and the surrounding soil as an elastic material which is the same assumption with analytical approaches. In Jiang et al. (2013) method, a 3D numerical model was studied by considering the comparison of the real three-dimensional problem in future studies. The study was performed first for the stone column and then later replaced by deep mixing column and verified by selecting an axisymmetric model analyzed by Tan et al. (2008). Then a baseline case was chosen to study the variation of the parameters from the baseline. The numerical method developed by Tan et al. (2008) was mainly focused on the procedure to convert the axisymmetric to plane strain model. Tan et al. (2008) were used both the 2D and 3D models for prediction of a settlement of the improved soil and the development of the excess pore water pressure. For the 2D numerical analysis Tan et al. (2008) was proposed two different methods based on the parameters and the geometry of the improved soil. The analysis also performed by using the axisymmetric model to make a comparison with the 2D solutions. Two different material models were considered to represent the unit cell in the simulation and results from two cases. In the first case the soil and the column were modeled as a linear- isotropic –elastic material, and in the second case, the materials were modeled as MC with characteristics of linear elastic-perfectly plastic behavior.

3 Case Study

3.1 Introduction

The case study in this thesis is part of the ongoing infrastructure project named *E4*. The Stockholm bypass project, here abbreviated as (FS).*E4*. The Stockholm bypass (Förbifart Stockholm) is the new route for the European highway *E4* past the Swedish capital. Figure 3.1, illustrates the entire route of the bypass where 18 kilometers of the total 21 kilometers consists of tunnels.

The case study relates to the contract abbreviated (FSE502) – Förbifart Stockholm Entreprenad 502 which is located north of the traffic interchange Hjulsta. The red circle in Figure 3.1 indicates the location of the contract FSE502.

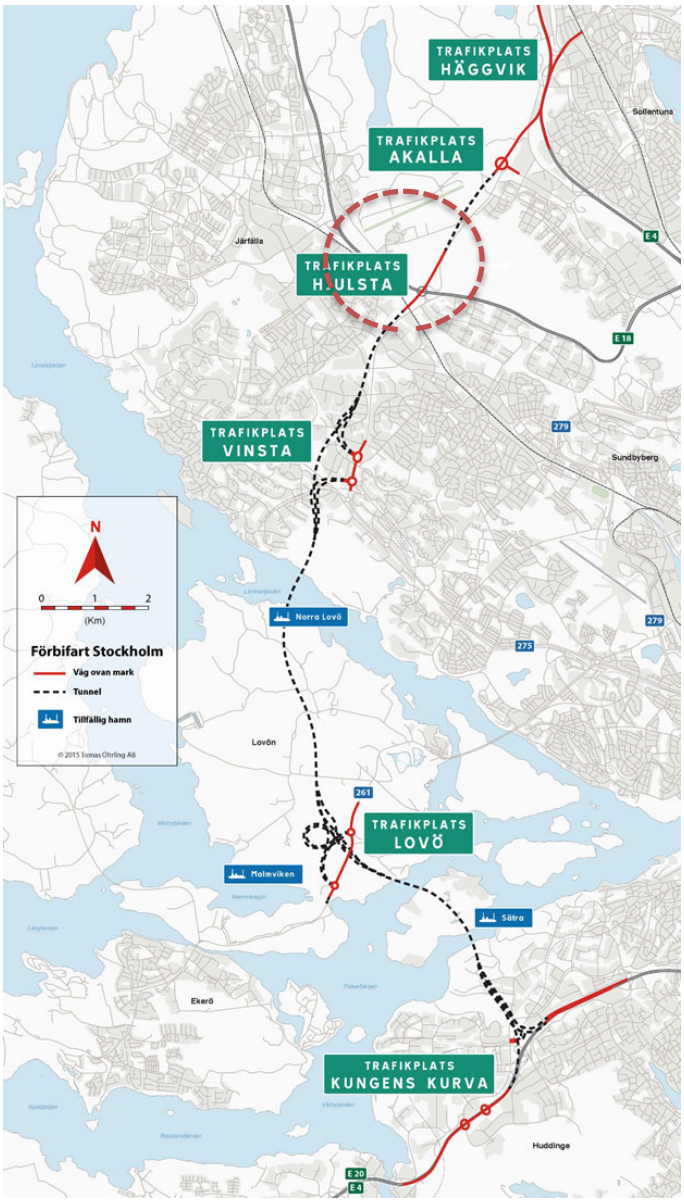

Figure 3.1 Schematic route of *E4 Stockholm bypass*, location of FSE502 in red circle, (source Trafikverket)

The FSE502 contract consists of a construction of tunnel, and trough as well as the construction of a road link towards Akalla. On parts of a section of this road, a concrete trough (Betongtråg) will be constructed to enable the flow of the groundwater towards to the bedrock. The place where the trough to be constructed is a soft clay soil which is not able to carry the design loads and is highly compressible. Due to this reason, deep mixing method using LCC has been proposed to strengthen the soft clay soil as well as to reduce the long-term settlement.

3.1.1 General

The FSE502 contract consists of two parts, one named *Akalla link* (Akallalänken) which is a design and build contract and the other named *Main road* (Huvudvägen) which is a turnkey contract. The existing Akalla link needs to be relocated so the main road can be built. The main road contract consists of totally 540 meters long excavation, from km 27/170 to km 27/740, starting at current ground level (+13) and ending approximately 23 meter (-11) below ground level. The initial 177 meters in length (km 27/170 to km 27/347) consists of an open concrete trough (tråg). The continuing 340 m will consist of a concrete tunnel and final 20 meters of rock tunnel. The main geotechnical challenge is to keep the ground water level intact. The initial 177 meters of the main road intended to be founded on LCC improved clay, see Figure 3.2 and the remaining part founded on bedrock.

3.1.2 Criteria's considered

Design lifespan of underground and substructure was considered as 40 years. Accordingly, the road design was done by considering the settlement during the lifespan of 40 years which satisfies the requirement in TK Geo 13 (2013). Based on the design analysis performed for LCC improvement a settlement of 13 cm was expected in a time of six months due to the application of a preloading. In this project, the reduction of groundwater that will occur due to load increment was planned not to exceed 1 m. The lowering of the groundwater was calculated from the mean water level (MWL). The geotechnical conditions and measures to be taken were considered into account in the calculation of settlements. The settlement of the structure will be monitor by measuring during the construction phase as well as at the end of the project.

3.1.3 Geotechnical condition

The topography of the area is characterized by higher elevation and valleys in the main northwest or eastern direction. In the vicinity of Hästa Klack, there are hills with thin moraine layers and valleys with thick soil layer. The ground surface that the LCC installed area has the lowest level of +13 and the highest +15 meters above sea level. The groundwater level is found 2.2 meters below the natural ground level. The eastern part of the concrete trough will build on the area where the existing Akalla link road runs; it is approximately between sections km 27/200-27/347. The LCC installation was performed after the demolition of the existing road embankment.

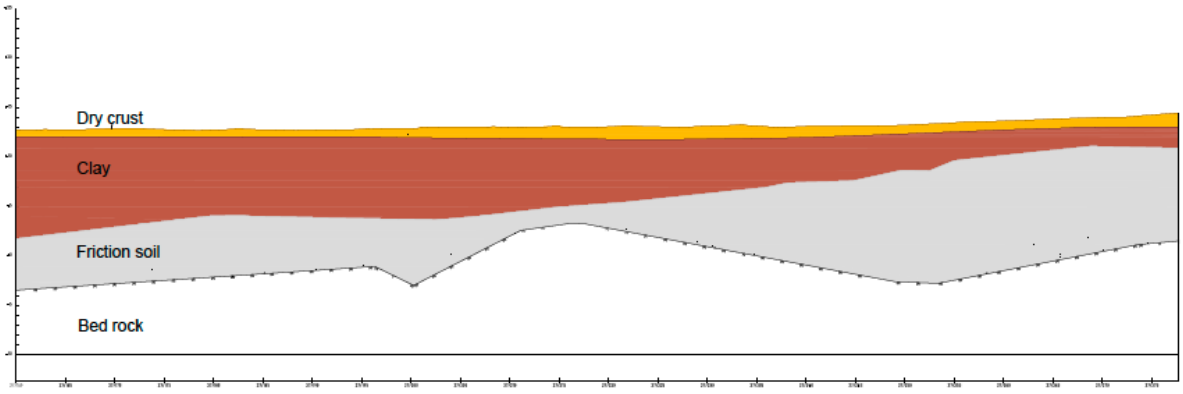

Figure 3.2 Soil profile of the site LCC to be installed (Trafikverket)

As shown in Figure 3.2 the area improved by a deep mixed LCC which is between km 27/170 – 27/235 consists of a clay soil with variable depth. The thickness of the clay layer varies between 6 and 10 meters. Under the clay soil friction soil and bedrock exist sequentially. The upper part of the clay has a dry crust character for a depth of 0.5 – 1.5 meters and the thickness of the friction soil vary between 4.2 and 11.7 meters. The rock model of the area shows that the depth of the bedrock varies between levels -3.0 and +2.0 meters above sea level, which means 10 and 16 meters below the ground surface respectively.

3.1.4 Geometry of structure

The installation pattern of the LCC was designed to use three different column center to center distances. The diameter of the column is 0.6 meter, and various center to center distances of the columns was set for an interval of a road section depending on the thickness of the clay. The spacing between columns corresponding to each section interval is presented in Table 3.1. In the case of column spacing 0.45 meters the entire clay act as a block since there is no unimproved soil in between the columns. The overall layout of the columns is as shown in Figure 3.3.

Table 3.1 Column spacing for corresponding road section, see Figure 3.3 (Trafikverket).

Road section (kms)	Column Spacing c/c (m)	Area ratio (%)
27/173 - 27/175	0,45	100
27/175 - 27/185	0,80	44
27/185 - 27/235	1,00	28

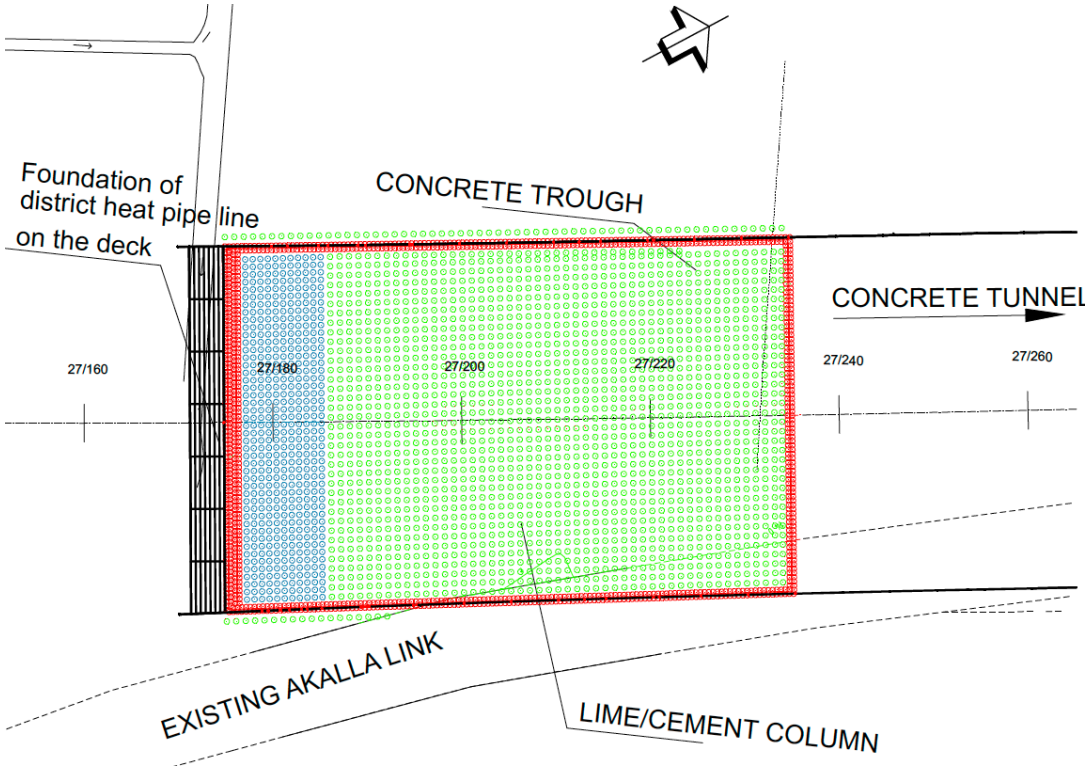

Figure 3.3 Plan of LCC under the concrete trough, the red with c/c 0.45m installed as a block, the blue are with c/c 0.8m and the green are with c/c 1.0 m (Trafikverket)

The permanent load that will act on the top of the LCC was calculated as per the size and material properties presented in Table 3.2.

Table 3.2 Type of material and thickness used for the foundation of the trough

Material	Thickness (m)	Unit weight (kPa
Crushed rock fill	1,70	20
Concret slab	0,50	25
Crushed rock fill	0,50	20

3.2 Input data's

3.2.1 Soil parameters

The input parameters of the soil, the undrained shear strength of the clay, compression modulus, density, liquid limit, pre-consolidation stress, limiting stress, modulus number, permeability and consolidation coefficient of the construction site of road project FSE502 were derived from geotechnical investigation report. The table of input data's is presented in Appendix A. The summary of the mean values for deformation and strength properties of the soil and LCC are presented in Table 3.3.

Table -3.3 Summary of applied deformation and strength properties of the soil in the case study.

Material	Parameters	Desigenation	Values	Level
Friction soil	Friction angle	φ'	37°	
	Unit weight	γ'/γ	12/20	
	Elastic Modulus	E	36 MPa	+ 2 - (-3)
Blasted material	Friction angle	φ'	45°	
	Unit weight	γ'/γ	12/22 kN/m^3	
Clay	Friction angle	φ'	32°	
	Density		16.5 kN/m^3	
	Undrained shear strength	c_u	15 kPa	+13 - +10
			10 kPa	+10 - +5
			15 kPa	+ 5 - 0.0
	Modulus	M_0	3000 kPa	+13 - +10
			2500 kPa	+10 - +5
			3500 kPa	+ 5 - 0.0
LCC	Friction angle	φ'	35°	
	Unit weight	γ	17	
	Elastic Modulus	E	20-40 MPa	

Since different input parameters are required for stability as well as settlement analysis, laboratory and field tests were conducted according to the criteria's and guides on TK Geo 13 (2013) and TR Geo 13 (2013), version 1. The laboratory test was performed in SWECO GEOLAB see results in Appendix A. On the road stretch that LCC planned to install, the final level of the concrete trough will be between +15.5 and +13.1 meters. The lowest natural ground level of this section is +13.0 meters.

Soil samples were taken from the site to check the shear strength of the soil and to determine other important parameters. The parameters that are required for further analysis, compression modulus (M), pre-consolidation stress (σ_c'), limiting stress (σ_L'), and permeability (k) were determined from the soil sample taken at levels +10 – +4.5 meters below the ground level. The derived parameters are presented in Figure 3.4. The clay below the natural ground level can be considered as an over-consolidated, but it became a normally consolidated as depth increases.

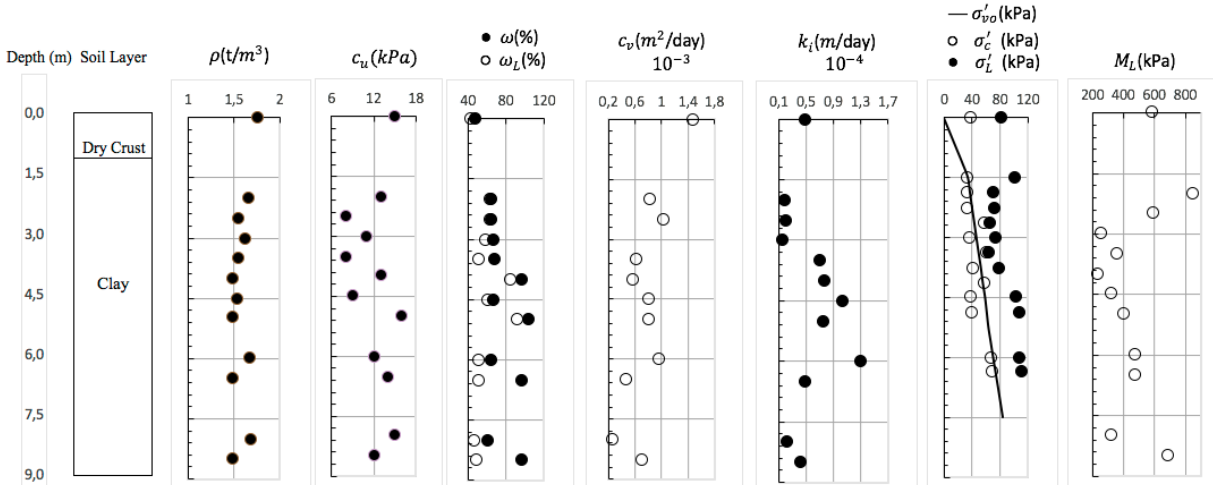

Figure 3.4 Summary of geotechnical properties of the soil at the location of the case study.

3.2.2 Laboratory strength tests

The strength development of a clay soil improved by LCC was investigated in the geotechnical laboratory. The result for a binder mixture of 90 kg/m3 shows means undrained shear strength increase of 81-88 kPa and 136-138 kPa after 7 and 28 days respectively. From another test with a binder mixture of 110 kg/m3, the result shows an average undrained shear strength increase of 95 kPa and 136-185 kPa at 7 and 28 days respectively; see results from laboratory experiments in Appendix A.

To get more reliable results field trial tests had been carried out by installing LCC to check the strength development. In total 18 columns were installed and the strength development was tested by column penetration test. Among these 10 of the columns were installed adjacent to the place where the concrete trough is planned to be construct. The columns were installed in the west direction 4.5 meters away from the outer edge of the trough. The remaining eight columns were installed in the place where the diversion of Akalla links planned, which is in the east 30 meters away from the trough. The columns were made with binder amount of 90 and 110 kg of LC per m3 of soil with a proportion of 50% lime and 50% cement, which are 25 and 31 kg/m of the column respectively. The number of columns was divided into two groups corresponding to the binder proportion; nine columns were performed with binder amount 90 kg/m3 and the other nine were performed with binder amount 110 kg/m3. The shear strength of the column was verified by using column penetration test, and the results are presented in Appendix A. The results from the field test shows good strength development regarding the amount of binder, increasing the binder amount from 25 to 31 kg/m will increase the strength of column at depth 2-4 meters. So, in the production of LCC, it is decided to use binder amounts of 25 kg/m in the lower half of the column and 31 kg/m in the upper half of the column.

3.2.3 LCC penetration test

The quality of the installed LCC was checked by performing a column penetration test. The test was carried out to control the continuity and the strength of the installed column throughout its length. In this project, the pre-drilled traditional column probing with penetration force registration FTPS (Förborrad Traditionell Pelarsondering med Spetskraftregistrering) test procedure was applied. The equipment that used for FTPS test is a probe with an area of 0.01 m2 which is fitted with vanes as shown in Figure 3.5. The size of the vane varies with the diameter of the column, but in this particular case, the column diameter and the vane size are 600 and 500 mm respectively.

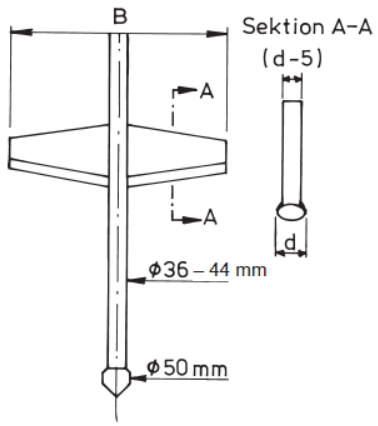

Figure 3.5 Column Probe for tradtional test (after Larsson R 2006)

The probe test was performed concerning strength through column probe with a separate registration of the tip pressure against the wing. To enable the assessment weather, the probe is controlled from the column or not the equipment includes an inclinometer. Drilling was performed with soil-rock probing equipment (58 mm crown diameter) by applying pressure and rotation before the column probing is carried out. The pre-drilling should be done carefully at the center of the column and vertically aligned. The production control test performed continuously during the production of the column. The tests were carried out at two different times the first one is in 12-16 days and the second in 26-34 days after the installation of the column. Then from the test results, it can be able to evaluate the undrained shear strength of the column. According to Axelsson & Larsson (2004) the undrained shear strength of the column can be calculated as expressed in Eq. 3.1.

$$\tau_{fu} = \frac{1}{N} * \frac{P}{A_{prob}} \tag{3.1}$$

Where: P is the force in the probe tip required to penetrate the column, A_{prob} is the cross-sectional area of the probe as shown in Figure 3.5, τ_{fu} is the undrained shear strength of the column and N is the bearing factor that is approximately 10.

The Swedish guidelines recommended to use N=10 as published in Axelsson & Larsson (2004) and A_{prob} is calculated based on the van size of 500x15 mm then a conversion factor of 12.5 obtained to simplify Eq. 3.1 to Eq. 3.2. In this case $\tau_{fu} = c_{u,col}$ since it is undrained condition.

$$c_{u,col} = 12.5 * P \tag{3.2}$$

As results presented in Appendix A the test result showed that the mean $c_{u,col}$ values vary between 120 to 200 kPa for the depth below the dry crust part. Based on the summary of the production control test results the $c_{u,col}$ values of 120 and 135 kPa were used for the upper and the lower half of the LCC respectively. Accordingly, the secant modulus of the column was calculated using the following empirical formula as recommended in TK Geo 13 (2013).

$$E_{50}^{u} = 250 * c_{u,col} \tag{3.3}$$

Where: E_{50}^{u} is the undrained secant modulus of the LCC.

3.2.4 Field measurements

The settlement of the improved soil was monitored by using a deep settlement plate (markpeglar). The deep settlement plates were placed on top of the improved ground prior to the preloading. According to Salem & El-sherbiny (2013) plates could be different in size, typically square plate their sides varying between 0.5 to 1 meter. The deep settlement plate consisted of a square plate size 0.5mx0.5m welded to a steel riser rod extended from bottom to the top of the preloading as shown in Figure 3.6. The riser rod was incased with a plastic pipe throughout the thickness of the preloading soil. The plastic pipe was filled with smaller size of pumice. A reading reflector was placed on top of the steel rod. Then surveying top of the riser elevation provided the settlement of the plate.

Figure 3.6 Pictures that shows what the deep settlement plate consists of. (Photo Hulumtaye. K.)

A total of 23 deep settlement plates were placed on the sides and in the middle of the road section as shown in Figure 3.7. The measurement of the settlement was started before the application of the first stage loading, and a zero measurement was recorded; see measurement Table in Appendix D. The preloading was performed using a material with a density of 18 kN/m^2 and a total height of 3.25 m. It was performed in two different stages; the first 1 m height was applied after ten days of the last column installation, and the remaining 2.25 m height was applied 30 days after the last column installation. Measurements from deep settlement plates P_11, P_12 and P_14, were taken to compare predicted settlements of the LCC at section 27/180, 27/200 and 27/220 respectively.

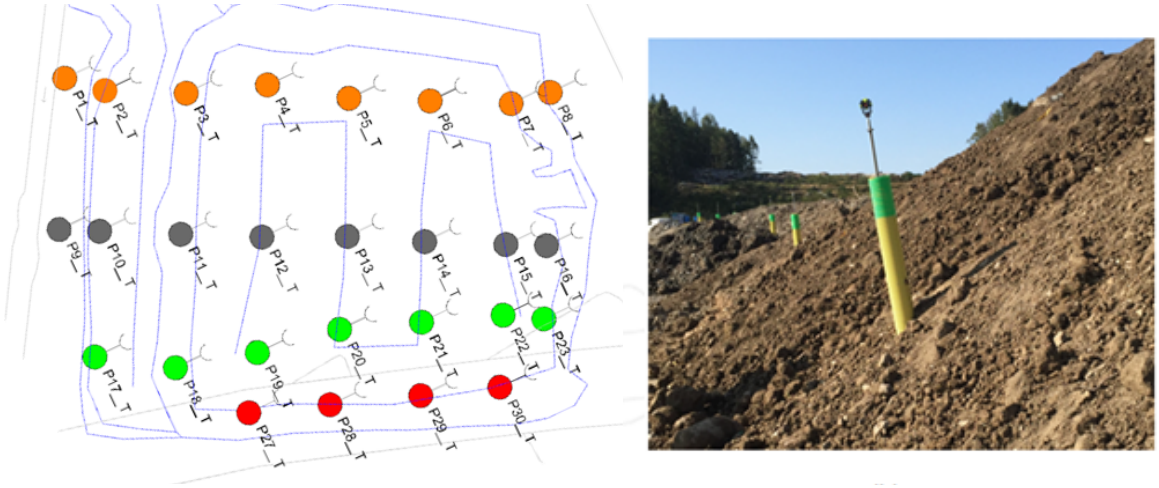

(a) (b)

Figure 3.7 Schematic diagram of the deep settlement plates for measuring of settlements; a) plan view of point location b) Location of units at the eastern edge of the preloading. (Photo Hulumtaye. K.)

4 Methodology

4.1 General

Three different methods were presented in this chapter for prediction of settlements in an improved soft clay soil. The first two are analytical methods in which an elastic model was considered for the representation of the material, and the third one is a numerical method. The settlement analysis in the first analytical calculation was performed by TK Geo 13 (2013) as reviewed in Chapter 2. The second analytical method was done based on the concept of a unit cell, and the settlement calculation was done by considering the improved soil as composite ground. In this case, a settlement calculation method for end bearing column improvement presented by Chai & Carter (2011) was adopted. The use of the analytical method will increase the understanding on long-term settlements and the effects of the stress due to the additional load. The third one is a finite element numerical method used to calculate the consolidation settlement of the lime /cement column. In this numerical method, Plaxis 2D commercial software was engaged for the prediction of the settlement of the improved soil. The conversion of the axisymmetric to the plane strain model was performed by using a method analyzed by Tan et al. (2008). The same input geotechnical data were used in all methods, which are derived from the field tests of the case study project.

4.2 Settlement prediction analytical

The TK Geo 13 (2013) is a technical advice that guides how to do a design for dry deep mixing in regard with serviceability as well as the ultimate limit state. The method was established based on the theories in Broms (1984) developed for lime cement column. All the detail information's required for the analyses were not included in this document, like the procedures how to calculate the stress increment as a function of depth. Hence additional information was taken from Alen et al. (2006) and Larsson (2006), as per the recommendation. The second analytical method was originally proposed by Abosh et al. (1979) for prediction of settlement in the composite ground and adopted by Chow (1996), Chai & Carter (2011), Beragdo et al. (1994) for settlement calculation of end bearing columns in soil improvement. In this section, the procedures how the analytical methods were used for prediction of a settlement of the improved soil are presented.

In both analytical methods, the settlement calculation was performed using an excel template. For analytical method 1 (TK Geo 13 2013) the clay soil was divided into sublayers with a thickness of 0.5 meter. All the required strength parameters of the clay and the column were determined in each sub-layer as presented in Appendix B. But in the second analytical method (Equilibrium approach) the clay layer was divided into two parts corresponding to the upper and lower half parts of the column. The details how the most influential parameters calculated are described in the following sections, and the main input parameters used in both analytical calculations are presented in Table 4.1.

Table 4.1 Basic input data for analytical calculations

For LCC

	$c_{col,u}[kPa]$	$E_{col,}[MPa]$	$E_{50}^{u}[MPa]$	$k_{col,}[m/s]$	$c_{vh,}[m^2/s]$
Upper half column	120	27582	30000	8,68E-07	1,70E-08
Lower half column	135	33303	33750	8,68E-07	1,70E-08

For the clay

	$M_0[kPa]$	$M_L[kPa]$	$k_{soil}[m/s]$	$c_{vv,}[m/s]$	$c_{vh}[m/s]$
	3152	476	1,74E-09	8,52E-09	1,70E-08

Preloading

Height of preload [m]	Unit weight [kN/m3]	q [kPa]	B (Width of trough) [m]	L (Length of trough) [m]
3.25	18	58.5	40	60

4.2.1 Settlement calculation TK Geo 13

- **Geotechnical class**

The geotechnical category and safety class is determined based on the criteria specified in Eurocode 7. For the project selected for the case study, the design of the deep mixing of the clay using LCC was done in geotechnical category 2 (GK2) and safety class 3 (SK3). In the ultimate limit state design, the stability analysis was performed on selected sections of the road before and after improvement of the soil and required safety factor was obtained for the improved clay soil. However, stability analysis was not included in this study.

- **Stiffness of the column**

The stiffness of the LCC was calculated using the empirical formula described in Eq. 2.27. The stiffness of the column is dependent on the $c_{uk,col}$ value which was obtained from field column penetration test. As already discussed in the review section the stiffness of the column is variable through depth, and this corresponds to the variability in $c_{uk,col}$ value. So, to take the stiffness variation into consideration two different column stiffness values were calculated for the upper and lower half of the column. According to TK Geo 13 (2013) the characteristic undrained shear strength of the column τ_{fuk} determined as $\tau_{fuk} = c_{crit}$. In this analytical calculation, the average $c_{uk,col}$ values were taken 120 and 135 kPa for the upper and lower half of the column based on the results of a column penetration test performed on the project site.

- **Load distribution and stress increment**

The preloading applied on the improved soil block is a soil with a unit weight of 18 kN/m^3 and a height of 3.25 meters. The load distribution was done using a distribution factor which is obtained from Eq. 2.31. The $\Delta\sigma_{LC}$ is a function of the depth of the improved soil block and the influence factor I. The equation for calculation $\Delta\sigma_{LC}$ in Alen et al. (2006) considered the 3D effects, and the depth reduction factors were calculated for both directions along and across the embankment. But in this calculation, considered only one-dimensional effect and the depth reduction factor was calculated only in one direction.

Based on the actual geometry of the improved area and the preloading Eq.2.33 was modified to Eq.4.1 to calculate the I. The depth reduction factor was calculated using Eq. 2.34 and combined with Eq.2.35 together with I to determine the $\Delta\sigma_{LC}$ through the depth of the improved soil block.

$$I = \left(\frac{2}{\pi}\right)\left[\frac{20z}{z^2+1600} + \text{atan}\left(\frac{20}{z}\right)\right] \tag{4.1}$$

- **Settlement calculation**

The calculation of the settlements of the improved soil is based on the performance of three different zones illustrated in Figure 2.11. However, the LCC installed in the case study project was fully penetrated to a firm layer, and there is no zone C in this case. As the geological model in Figure 3.2 shows the soil under the clay is a friction soil and the settlement in this layer was not considered in the analysis even though a certain settlement was expected during the construction period. The depth of zone A is a limiting depth between the plastic and elastic zones and the calculation was performed using an iterative procedure as described in section 2.3.1 and presented in Appendix A. Although it is difficult to calculate the limiting depth. The depth resulted from the calculation showed as insufficient bridging effect was designed between the preload and the LCC. Hence the settlement in zone A was not treated separately. As earlier described in Chapter 3 a preloading was applied after the installation of the columns. The primary purpose of the preloading is to reduce the time for consolidation. According Larsson (2006) due to the preloading most of the settlements in zone A could appear during the construction time and doesn't have a long-term effect.

The settlement calculation of the improved clay soil was performed by dividing the whole depth into sublayers to capture the deformation in each layer. Three different sections were selected at 27/180, 27/200 and 27/220 to calculate the consolidation settlements due to the preloading. The main reason for this is to consider the effect of the variation of the clay thickness as well as the spacing between column on the settlement of improved soil.

- **Compression of improved soil**

The ε developed due to $\Delta\sigma_{LC}$ was assumed to be equal in the soil and the column based on the assumption discussed in the review section and it is expressed in Eq. 2.38. The M_{block} is a function of a and calculated by using E_{col} and M_{soil}. Accordingly, $\Delta\sigma'_{v,col}$ and $\Delta\sigma'_{v,soil}$ were obtained from Eq. 2.39 and 2.40 in order to determine the ε both in soil and in the column. The column can't carry load above the critical shear stress hence it is necessary to calculate the maximum compressive strength of the column at failure. The σ'_{LCC} was calculated using Eq. 2.41 which is derived based on MC rupture hypothesis. By using the value of σ'_{LCC} the $\Delta\sigma_{col,max}$ was determined to compare with $\Delta\sigma'_{v,col}$. All the calculations were performed in an excel template which is prepared for this purpose.

- **Degree of consolidation and time dependent settlement**

As already discussed in Chapter 2 the U was estimated based on the principle which considered the LCC as a vertical drain. The flow in the radial direction is dominant in the process of consolidation and in this analysis k_h assumed three times k_v. The drainage in the improved soil block was considered on one side and the drainage length is equal to the length of the column. As per TK Geo 13 (2013) recommendation the k_{col} was estimated 500 times k_{soil}.

By using the values of k_{col} and k_{soil} as an input the k_{block} was obtained from Eq. 2.28. The c_{vh} is one of the main factor that influence the U and assumed 2 times c_{vv}. Finally, the U was calculated using Eq. 2.46 and the curve for time-dependent settlement of the improved soil was plotted to determine the rate of consolidation and the time required to reach the final consolidation.

4.2.2 Calculation of settlements as composite ground

The analytical method proposed by Chai & Carter (2011) is originally developed for a soil improvement using soil cement column, and this method is adapted to predict the settlement of a soil improved by LCC. In Chai & Carter (2011) analytical method two approaches were presented for calculation of the settlements of the improved soil. In this case, the calculation of settlements of the improved soil was performed by using only the equilibrium approach.

- **Stress distribution and settlement calculation**

The equilibrium method considered the effects of the stress concentration ratio between the clay soil and the LCC to calculate the settlement of the improved soil as shown in Figure 2.14. The value of m was calculated by taking the ratio of D_c to D_s also possible to calculate from the ratio σ_{col} to σ_{soil} both should give the same value. But σ_{col} and σ_{soil} are depend up on the value of m and it is necessary to calculate the m value first. The value of D_c and D_s were calculated based on Eq. 2.58 and 2.59. the value of v_c and v_s was assumed to 0.3. The main factors that influence the settlement of the improved soil are m_{vs} and μ_s. The μ_s is the ratio σ_{soil} to σ obtained from Eq. 2.53 whereas the m_{vs} was calculated based on the value of D_s. The vertical displacement was considered uniform at any horizontal level which is similar with TK Geo 13 (2013). Finally, the settlement of the improved soil was obtained from Eq. 2.55. In this case the clay soil was divided in two layers corresponding to the upper and lower half of the column length. As described in TK Geo 13 (2013) method different stiffness values were applied for the upper and lower half of the column to consider the variation of stiffness through depth.

Consolidation and time dependent settlement

The rate of consolidation and time-dependent settlement of the improved clay soil were calculated with the same concept and procedure applied in TK Geo 13 (2013). However, the input parameters are not the same and the degree of consolidation was calculated by considering both flow in the radial and vertical direction. The U_r was calculated using Eq. 2.63 and used the stress concentration ratio as an input. The k_c was estimated 500 times k_s which is the same assumption with TK Geo 13 (2013) method and the c_r was assumed 2 times c_v. The U_v was calculated using the conventional method and combined with U_r to get U_{vr} as expressed in Eq. 2.64. Then time-dependent settlement curve was plotted using the U_{vr} obtained from the calculation.

4.3 Settlement prediction - numerical

According to Baker (2000) the mechanism that the load distribution within the LC block is the most significant issue in regard with estimation of settlements. The distribution of the load can be influenced by the geometry, the magnitude of the load and the stiffness of the column and the surrounding soil.

The geometry in this regard means the spacing between columns, diameter, and length of the column. To determine the analysis as linear or nonlinear the magnitude of the load is the influencing factor. A finite element program, Plaxis 2D commercial software was used to model and analyze the consolidation settlement of the LCC. Plaxis is a program developed based on the finite element method which is intended to apply to a 2D and 3D engineering design of soil and rock deformation and stability analysis.

4.3.1 Model conversion

Since the aim is to perform a 2D numerical analysis, it is very vital to convert the axisymmetric model into its' equivalent plane strain model. Even though there is no well-studied and published conversion method for LCC in particular, well-established methods are available in relation with vertical drains. So, the analysis was performed based on the idea that considered the column as a vertical drain. As studies in Tan et al. (2008) and Tuan & Toshiyuki (2008) indicated several methods have been proposed for vertical drains to convert axisymmetric to plane strain numerical models.

In this numerical analysis, the method developed by Tan et al. (2008) was selected to do the conversion of the axisymmetric to plane strain model. The conversion method was done based on the analytical solution for consolidation, and the matching includes the derivation of the equivalent plane strain parameter and geometry. The matching scheme categorized into two parts, the geometry-matching scheme, and the parameter-matching scheme. In this study, a complete analysis was performed using a combined and geometry matching model. A trial analysis has been done using the parametric matching model but not included in this report since the model resulted an erroneous settlement according to Tan e al. (2008) conclusion.

In the geometry matching model, the $k_{h,pl}$ and $E_{c,pl}$ were kept the same with $k_{h,ax}$ and $E_{c,ax}$ but b_c and R were calculated based on Eq. 2.77 and 2.78 respectively. In the combined matching model both the parameters and the geometry were converted. The geometry matching was performed using the same equation applied in the case of geometry matching model. Whereas the matching of the permeability was performed using Eq. 4.2 which is obtained from the revision of Tan et al. (2008) studies by Castro & Sagaseta (2010).

$$\frac{k_{h.pl}}{k_{h.ax}} = \frac{2.B^2}{3.R^2.\left(\frac{N^2}{N^2-1}.\ln(N)-\frac{3.N^2-1}{4.N^2}\right)} \tag{4.2}$$

Where: $N = \frac{r_c}{R}$, r_c is radius of the column and R is radius of influence area of drainage in axisymmetric and B half of the width of influence zone of drainage in plane strain model.

4.3.2 Input parameters

The necessary input parameters used in Plaxis analysis are derived from the geotechnical investigation reports as well as from field test results of the project selected for this study. The stiffness and permeability of the soil and the column are the two critical parameters which will have significant effects on the result of consolidation settlements. Those parameters were calculated based on the conversion scheme corresponding to each model. The Poisson's ratio υ of the clay and the column was assumed to 0.3. The permeability of the LCC was taken as ten times the permeability of the clay soil.

The undrained secant modulus of the LCC was obtained using Eq. 3.3, which is based on its undrained cohesion. According to Åhnberg (2006) the effective cohesion of the LCC was estimated using Eq. 4.3

$$c'_{col} = 0.46\, c_{u,col} \tag{4.3}$$

The void ratio of the clay and the LCC depends on the water content, and it will change during the consolidation process. For this analysis, the initial void ratio of the dry crust, the clay soil, and the LCC was estimated by the empirical formula described in Eq. 4.4.

$$e_i = w\left(\frac{\rho_s}{\rho_w}\right) \tag{4.4}$$

Where w is the water content, the bulk density of unimproved soil and ρ_w is the unit weight of the water. The water content of the column (ω_{LCC}) is different from the water content of the clay soil due to the addition of the binders, according to Åhnberg (2003) the ω_{LCC} was determined using Eq. 4.5.

$$\omega_{LCC} = \frac{\rho_s \cdot \left(\frac{\omega_N}{\omega_N+1}\right) - ax}{\rho_s\left(\frac{1}{\omega_N+1}\right) + (1+a)x} \tag{4.5}$$

Where ω_N is the natural water content of unimproved soil (as decimal number); x is the amount of dry binder added to the soil (t/m^3); and a is the content of non-evaporable water of the hydration product (as decimal).

The lateral earth pressure coefficient K_o for the clay soil was estimated by using an empirical formula, which is recommended in TK Geo 13 (2013).

$$K_o = 0.31 + 0.71(\omega_L - 0.2) \tag{4.6}$$

Accordingly, the $K_{o,OCR}$ for the LCC obtained from Eq. 4.7 using the liquid limit obtained from Eq. 4.49.

$$K_{o,OCR} = K_o . OCR^{0.55} \tag{4.7}$$

A summary of input data used for numerical analysis are presented in Appendix C.

4.3.3 Plaxis Simulation

- **Modeling**

The preloading applied on the LCC foundation was simulated by using a linear elastic 2D plane strain FEA. A total of 6 cases were analyzed as shown in Table 4.2. In this study, Plaxis 2D V 2017 was used to run the simulations of the analysis.

- **2D Modeling**

The LCC was modeled as a continuous plane strain walls, and two stiffness values were considered in each length as well as for all columns along the calculation section. The center to center spacing between two walls and the thickness of the walls used in plane strain geometry matching is the same in the case of the combined matching. The calculation was performed using Eq. 2.77 and 2.78 to match the geometry for the conversion of axisymmetric to plane strain model as the input data presented in Appendix C.

Due to symmetry half of the geometry of the preloaded area was modeled and the model area had a total width of 60 m with a vertical thickness of 15,15 and 10 meters from the ground surface for sections 27/180, 27/200 and 27/220 respectively. The boundary condition and the finite element mesh adopted are as shown in Figure 4.1.

Table 4.2 Cases analyzed in Plaxis simulation

Section	Case	Type	Method	Spacing	Secant Modulus	Permeability
27/180	Case_1	Single Column	Geomtery Matching	0.71 (0.88) m	E_{50}	k_c
	Case_2	Single Column	Combined Matching	0.71 (0.88) m	$E_{50,pl}$	$k_{c,pl}$
27/200	Case_3	Single Column	Geomtery Matching	0.88 m	E_{50}	k_c
	Case_4	Single Column	Combined Matching	0.88 m	$E_{50,pl}$	$k_{c,pl}$
27/220	Case_5	Single Column	Geomtery Matching	0.88 m	E_{50}	k_c
	Case_6	Single Column	Combined Matching	0.88 m	$E_{50,pl}$	$k_{c,pl}$

E_{50}: is the secant modulus of the column $E_{50,pl}$: the secant modulus of column in plane strain model k_c: permeability of column $k_{c,pl}$: permeability of column in plane strain model k_s: permeability of soil $k_c = 10k_s$. The numbers in parentheses are optional spacing between walls used for comparison.

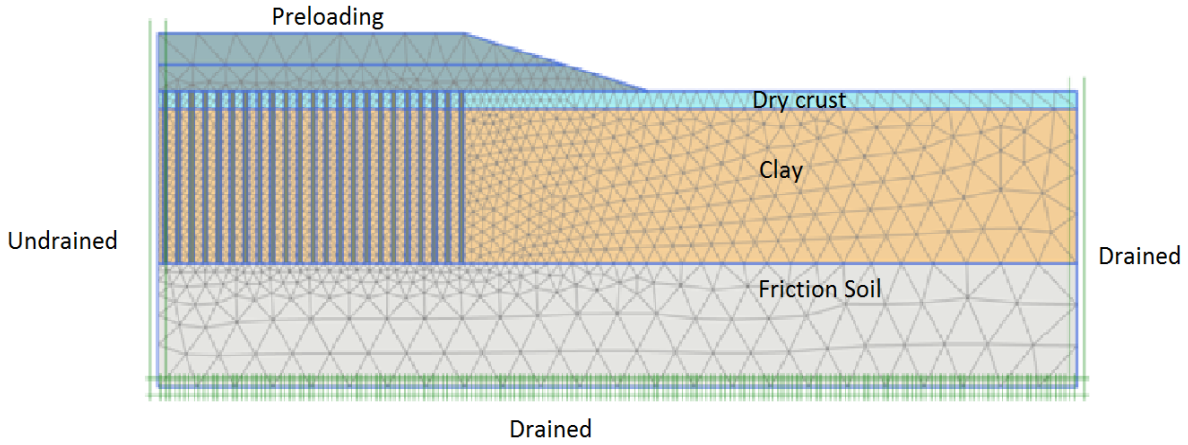

Figure 4.1 2D Finite element mesh and boundary conditions of drainage and deformation

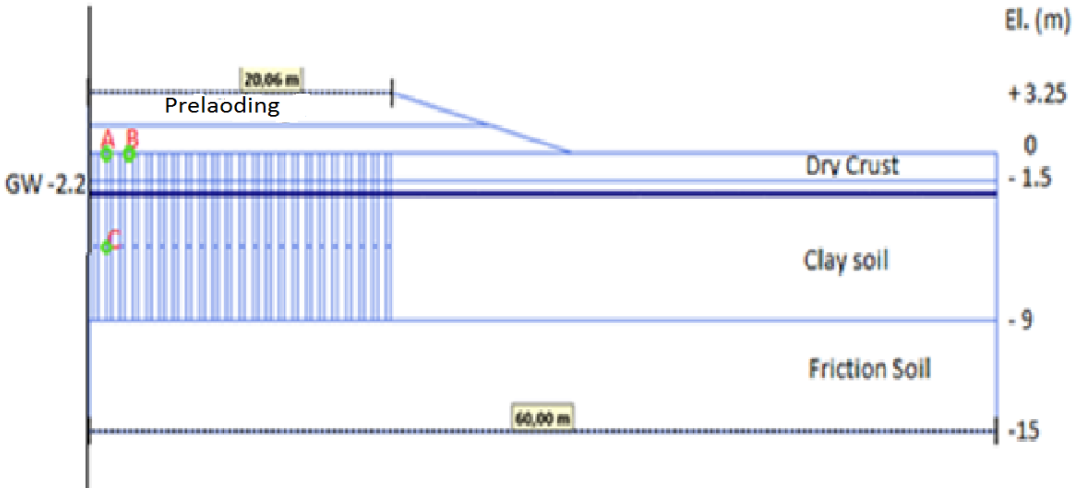

Figure 4.2 Geometry of the preloading and installed LCC at the center of the improved area.

As the model in Figure 4.1 shows the left and right side of the model the horizontal displacements (x-direction) were restricted which is normally fixed but it is free to move vertically (y-direction), the main purpose of these boundaries is to make rigid and smooth (Chai et al. 2015). In the bottom boundary, it is fully fixed; both the horizontal and vertical displacements were restricted. The clay soil, as well as the friction soil below the clay, was considered as completely permeable. The drainage boundary on the right side is considered to be open whereas the left side considered to be closed. In this 2D model, the foundation soil and the LCC were represented by 15 nodded triangular elements with excess pore water pressure with degrees of freedom at all nodes. Fifteen-nodded triangular elements without excess pore water pressure were used to represent the soil used as a preloading.

The geometry of the preloading with LCC is as shown in Figure 4.2 has a line of symmetry on the left of the boundary. A selected soil material was placed on top of the LCC with a height of 3.25 m. The LCC are placed in square grids that cover the width, in which the concrete trough will be placed. The dry crust is 1.5 meter deep in which the top 0.5 meter was removed and replaced by a selected material to have a good working platform. The groundwater is 2.2 meters below the ground surface. Two points are marked as point A and B as shown in Figure 4.2 for calculation of settlements of the LCC and the clay soil. Point C is marked in the middle of the column depth for calculation of excess pore water pressure that will develop due to the preloading.

- **Material models**

Since our goal is to do settlement calculations through consolidation process, so the development of excess pore water pressure in the clay u_s and the column u_c are important for the analysis. Hence the undrained material models were selected for both the clay soil and the LCC. The type of drainage can be selected based on the effective stress path. Both the undrained A and B drainage type will result in effective stress path and pore water pressure development. But the undrained B may not give a fully correct effective stress path and pore water pressure since the friction angle is set to zero and the cohesion is equal to the undrained shear strength. In this case, undrained A drainage type was selected for both materials.

The clay was represented by a soft soil model by considering its high degree of compressibility and its saturation. The LCC and the preloading were represented by a linear elastic-perfectly plastic model which obeys the MC failure criteria. The friction soil was represented by an isotropic hardening soil model, which uses hyperbolic stress-strain curve. It has an advantage over the MC model, which controls stress level dependency. In the soft soil, the model parameters modified swelling index K^* and the modified compression index λ^* were estimated by a curve fitting using a CRS test result obtained from Plaxis and using data from the field test. The results from the curve fitting are presented in Appendix C. The secant modulus of the column used as in put in the MC model was estimated from Eq. 3.3 and stiffness in the hardening soil model for the friction soil were obtained from TK Geo 13 (2013). The k_v was taken from the CRS test results and the k_h was assumed three times k_v.

- **Simulation Steps**

The length of the columns was considered uniform along the calculation section, which is the same as the width of the improved area. As mentioned earlier, the stiffness of the column considered the same in each column, but different values were used for the upper and lower half length of the column. The simulation of the preloading was performed in two distinct steps.

Table 4.3 Simulation steps in Plaxis finite element analysis.

ID	Start from phase	Calculation type	Loading type	Time interval [day]	Estimated end time [day]
Initial phase	N/A	K0 procedure	Staged construction	0	0
Phase 1 (No LCC installed 1st stage load application)	Initial phase	Consolidation	Staged construction	2	2
Phase 2 (Consolidation analysis)	Phase 1	Consolidation	Staged construction	25	27
Phase 3 (2nd stage load application)	Phase 2	Consolidation	Staged construction	2	29
Phase 4 (Consolidation analysis)	Phase 3	Consolidation	Staged construction Minimum excess pore pressure	0	29
Phase 5 (LCC installed 1st stage load application)	Initial phase	Consolidation	Staged construction	2	2
Phase 6 (Consolidation analysis)	Phase 5	Consolidation	Staged construction	25	27
Phase 7 (2nd stage load application)	Phase 6	Consolidation	Staged construction	2	29
Phase 8	Phase 7	Consolidation	Staged construction Minimum excess pore pressure	0	29

In the first step consolidation calculation was performed without activating the LCC and similar calculation was performed in the second step but the LCC was activated in this case. Each step has four different phases depending on the loading stage and the time given for consolidation and loading. The calculation was performed in the order as presented in Table 4.3. The loading was applied in two different stages; a 1-meter height of selected soil preload was placed at the first stage and the remaining 2.25 meters on the second stage.

4.3.4 Sensitivity analysis

The sensitivity analysis was performed to evaluate the influence of the model parameters on the results of settlement calculation. This analysis is helpful if the parameters are not determined correctly. The analysis will give a value of sensitivity score against the given criteria. The scores obtained from the analysis will be used to evaluate which parameter has a major and which have a minor influence.

In this case, the model used for calculation section 180 was selected for the analysis. Some of the parameters which are assumed to influence the settlement of the improved soil, the permeability, the modulus, effective cohesion, the modified swelling index and the modified compression index were used in the analysis. The deformation in the vertical direction was set as a criterion since the objective of the numerical analysis is to calculate the consolidation settlement. The maximum and minimum values of the parameters were given independent of the reference values specified in the material database. The sensitivity analysis was performed for the minimum and maximum values and the variation from the reference value were calculated, and a score given for each parameter as results presented in Appendix C.

Sensitivity analysis was also done to check either the permeability of the clay or the lime cement column has a significant influence on the settlement of the improved soil. This analysis includes evaluation of the most influencing flow direction corresponding to the permeability. So, both the vertical and horizontal permeability of the clay and the LCC were used in this analysis with a criterion of vertical settlement.

5 Results

5.1 Analytical results

5.1.1 Using TK Geo 13 (2013)

The analytical calculation begins with the assumption of equal deformation in the soil and the LCC hence the same result was obtained from the calculation. The settlement calculations were performed on three different sections of the improved area as described in section 3.2.4 to see the effect of the variation in the thickness of the clay layer on settlements. The results from each section were plotted as shown in Figure 5.1 to make a comparison between them.

The difference between settlements at each section is not significant as the results presented in Figure 5.1. Almost the same result was obtained at sections 200 and 220 even though the length of columns at section 200 was slightly higher. A marginally lower settlement was achieved at section 180 compared to the two others which is the expected result since smaller column spacing was applied in this case. A maximum difference of 1 cm settlement was achieved between section 180 and 200. This indicates that the column spacing is more influential than the thickness of the clay. In the first 100 days, the rate of consolidation is the same at all sections, and the settlement increases gradually until it reaches its maximum value. The final consolidation was achieved in 100 days at section 180 whereas 200 days were required for sections 200 and 220. The curve became a horizontal line once the settlement reached its maximum value.

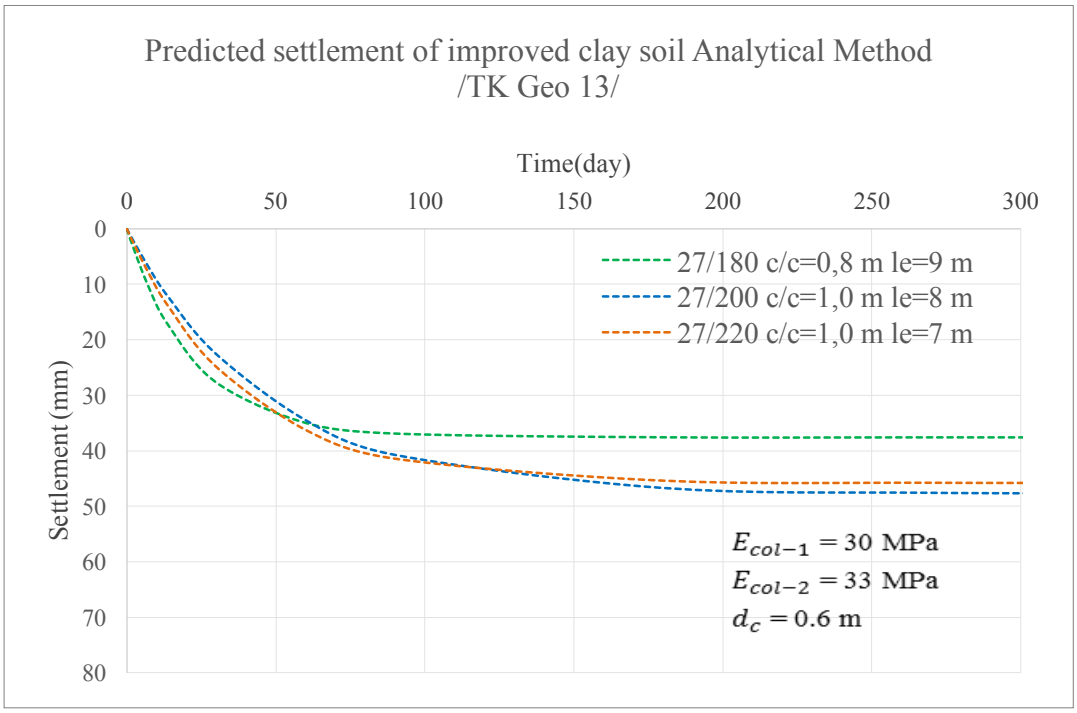

Figure 5.1 Settlement of the improved clay soil calculated at three different sections using analytical method based on (TK Geo 13 2013) and other guides.

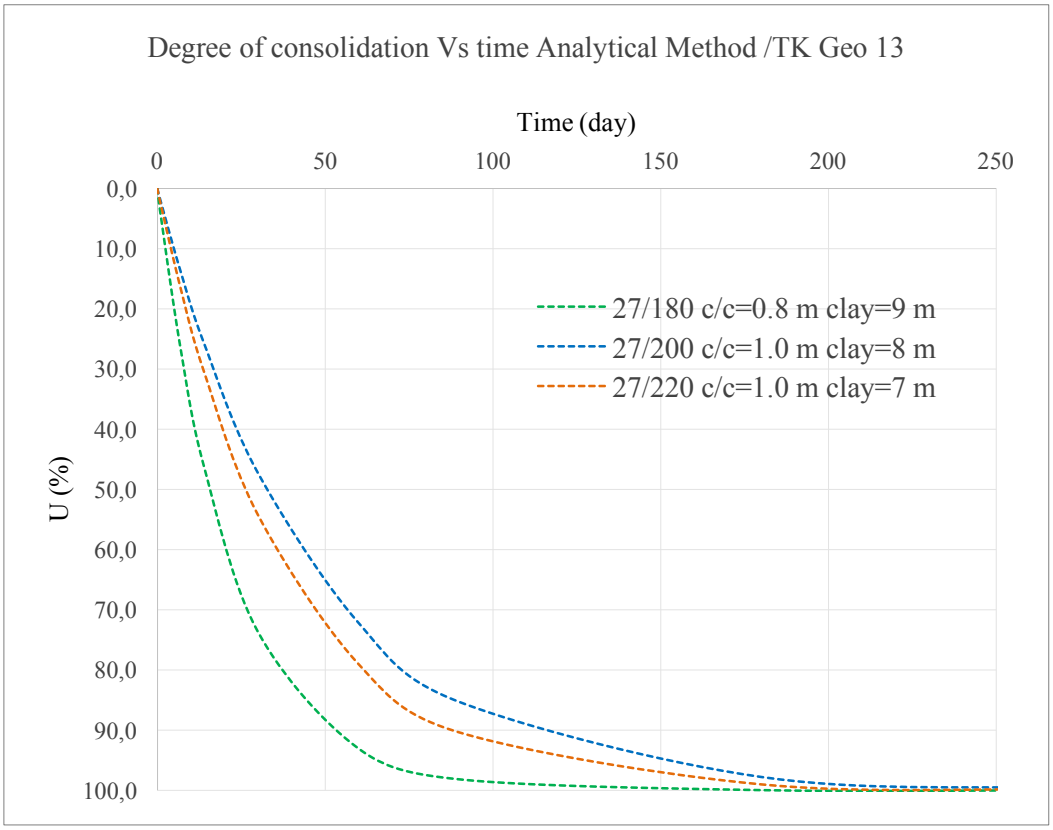

Figure 5.2 Degree of consolidation calculated corresponding to settlement of each section.

The degree of consolidation for long-term settlements of the improved clay soil also calculated at each section. The calculation was done based on the effect of flow in the radial direction since it has a significant impact on the rate consolidation. As the plot in Figure 5.2 shows that 90% of consolidation was achieved in 50 days at section 180 whereas at sections 200 and 220 it took around 100 days to reach the same degree of consolidation. This indicates that the rate of consolidation is slightly higher at section 180 compared to the two others which are with smaller column length and larger spacing.

5.1.2 Equilibrium method (Chai & Carter 2010)

Two different approaches have been proposed by Chai & Carter (2010), but only the equilibrium approach was used for settlement calculation of the improved clay soil. The composite modulus method is using the area weighted average value of the constrained moduli and volume compressibility of the column and the soil. Due to the higher constrained modulus of the column, this method produced a very small settlement and not considered for further analysis. The equilibrium method gave a reasonable result compared to the composite modulus. Similar calculation sections described in section 5.1.1 also used for this method.

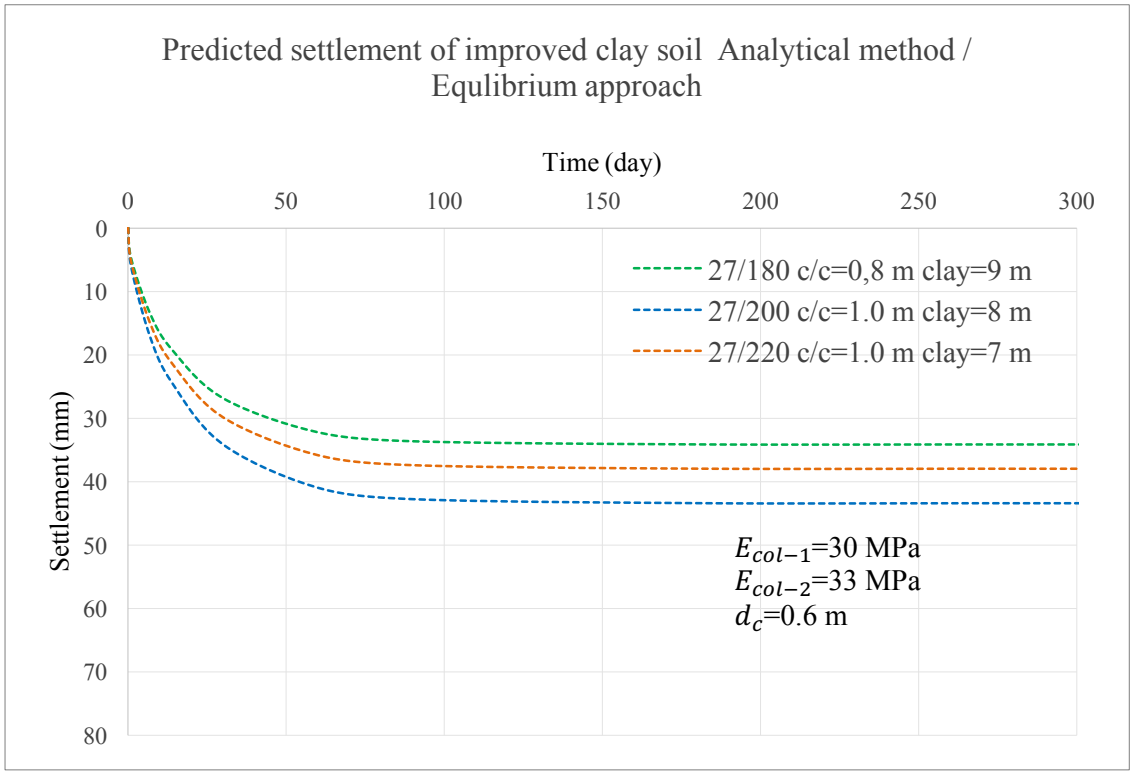

Figure 5.3 Settlement of improved clay soil calculated at different section using composite ground method (Equilibrium approach)

As the results in Figure 5.3 shows almost the same settlement was obtained at all sections and a lower settlement was obtained at section 180. The effect of the column spacing is not significant in here, a difference of less than 1 cm observed between settlement at section 180 with column spacing 0.8m and section 200 with column spacing 1.0 m. All curves have similar nature showed a gradual increment of settlement in the first 50 days and eventually reached its maximum and then to the final settlement. In all the three sections the final settlement was obtained in consolidation time of 100 days.

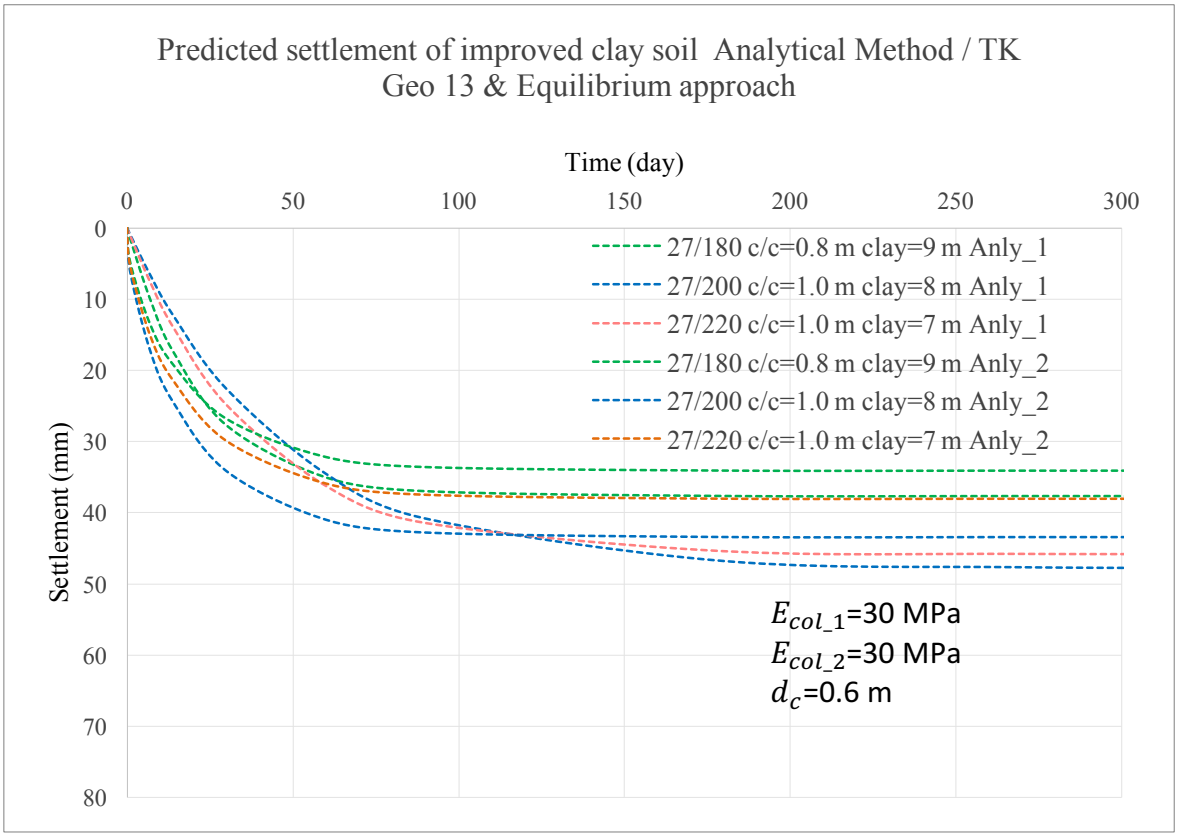

Figure 5.4 Settlements of LCC improved clay soil calculated with two analytical approaches.

The curves in Figure 5.4 show the long-term settlements of the improved clay soil obtained from both analytical method 1 and 2. The two analytical methods gave almost the same result at all sections. At section 200 both methods produced slightly higher settlement compared to the other sections. But the analytical method 1 gave a bit higher settlement with the same column length and spacing. The same settlement was obtained at section 180 of analytical method 1 and section 220 of analytical method 2.

5.2 Numerical Results

In the numerical analysis, the axisymmetric model was converted into its equivalent 2D plane strain model by using the geometrical and combined matching methods. Accordingly, Plaxis simulation was performed for temporarily applied preload as described in section 4.3. To select the most compatible material model and to check the correctness of the output results a different combination of material models were used for the LCC and the clay soil. Overall three-different combination of material models were used in the trials as the input data presented in Appendix C, but no significant difference had observed regarding the output results. Based on similar studies done on this area and by considering the effectiveness of the model corresponding to the behavior of the column and the clay soil MC and Soft Soil material models were used for the LCC and the clay soil respectively.

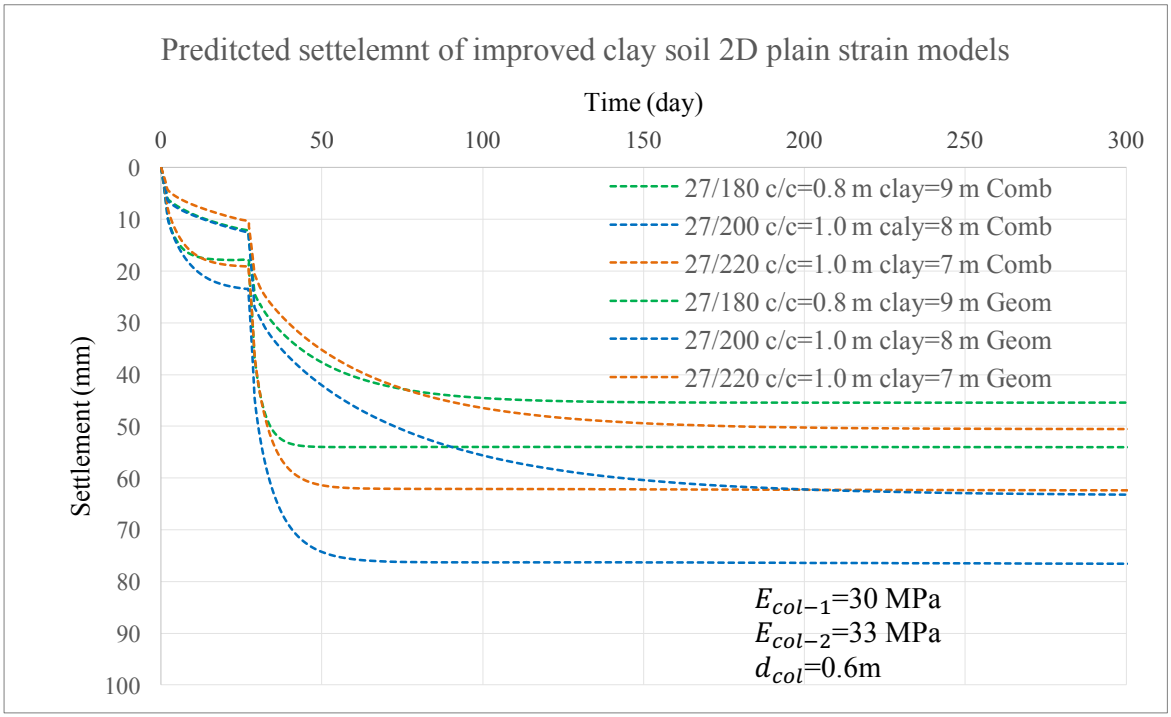

Figure 5.5 Settlement of the improved clay soil calculated at different section using 2D plane strain geometry and combined matching models.

Table 5.1 Deviation of results between numerical methods

Section	Geomtery Matching S(mm)	Combined Matching S(mm)	Diff (mm)	Devation (%)
180 (0.8m)	45	54	9	20
200 (1.0m)	63	76	13	21
220 (1.0m)	52	63	11	21

Note: - Numbers in parenthesis are the column spacing.

Figure 5.5 presents that the time-dependent settlement curves obtained from the simulation using both the geometry and combined matching methods. The combined matching method gave a higher settlement at all calculation sections compared with the geometrical matching. A maximum deviation of 1.3 cm which means 21% was obtained between the two methods as presented in Table 5.1. The geometry matching model gave almost the same consolidation settlement at section 180 and 200 even though the spacing between plane strain walls was different for each section. A smaller settlement was achieved at section 220 compared with section 200 due to the difference in length of a column. The combined matching model resulted in the same consolidation settlement at section 200 and 220 at the same time it is also observed that the difference in column length doesn't have any effect on the result between these two sections. Although a bit higher settlement was obtained at section 180.

The curves presented in Figure 5.5 are not smooth throughout the consolidation process; this is due to the different loading stage. The curves were plotted for settlement of a point located at the top of the LCC. The combined matching method shows a rapid consolidation. The settlement curves of all sections have the same nature, in the beginning, they showed a sudden increase and reached a maximum value with the first ten days and then eventually reached the final settlement in around 50 days. In the case of geometry matching model, a slower rate of consolidation was observed compared to the combined matching model. It took 180 days to reach the final settlement, which is a realistic length of consolidation time.

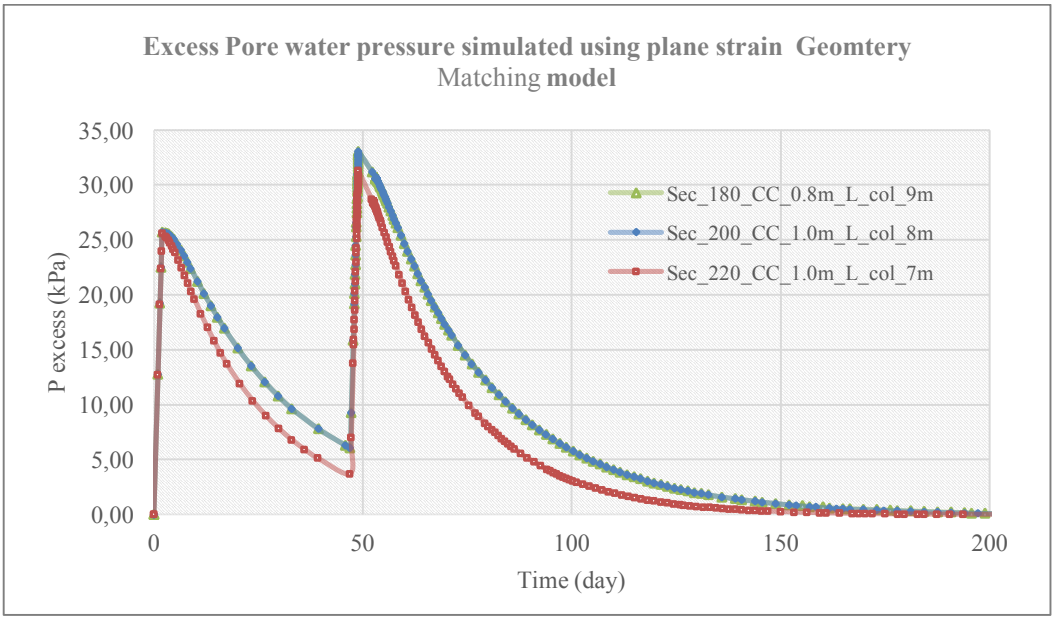

Figure 5.6 Excess pore water pressure simulated at each section using plane strain model geometry matching

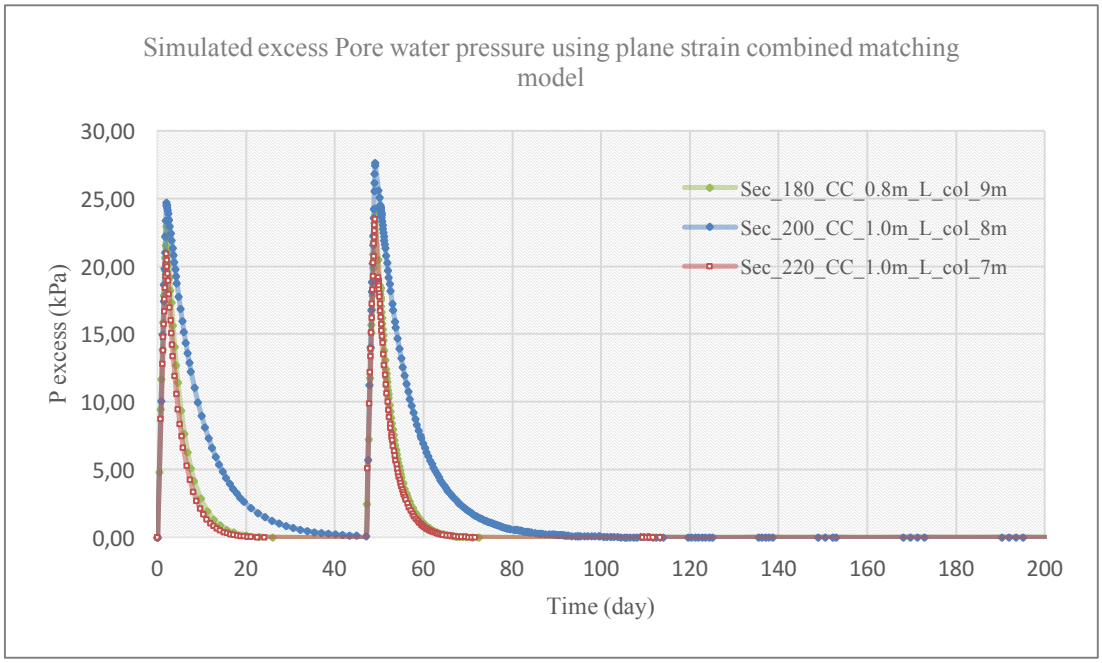

Figure 5.7 Excess pore water pressure simulated at each section using plane strain model combined matching.

The excess pore water pressure developed at the mid-depth of the LCC was simulated in both matching models. The geometry matching model shows a bit higher excess pore water pressure compared with the combined matching. Figure 5.6 and 5.7 show the simulated excess pore water pressure at the designated sections of the improved clay soil using the geometry and the combined matching models respectively. The rate of drainage is quicker in the combined matching model than geometry matching model. As presented in Figure 5.7 of section 200 excess pore water pressure of 24 kPa was developed in the first two days due to the first stage loading and suddenly drop down to less than one kPa in 30 days.

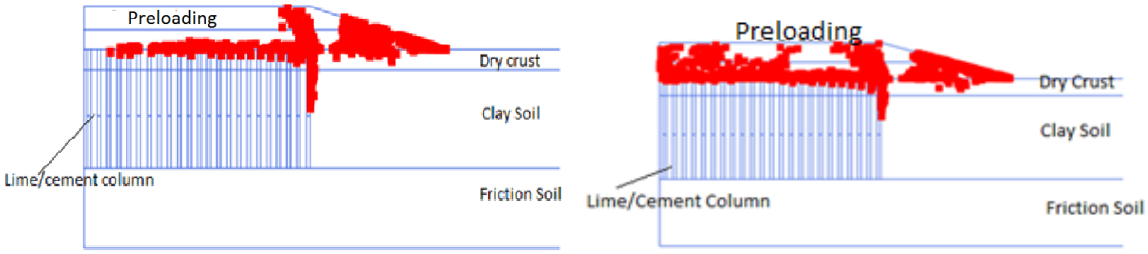

(a) Geometry Matching (b) Combined Matching

Figure 5.8 Simulated plastic stress points for both the geometry and combined matching models at the end of consolidation.

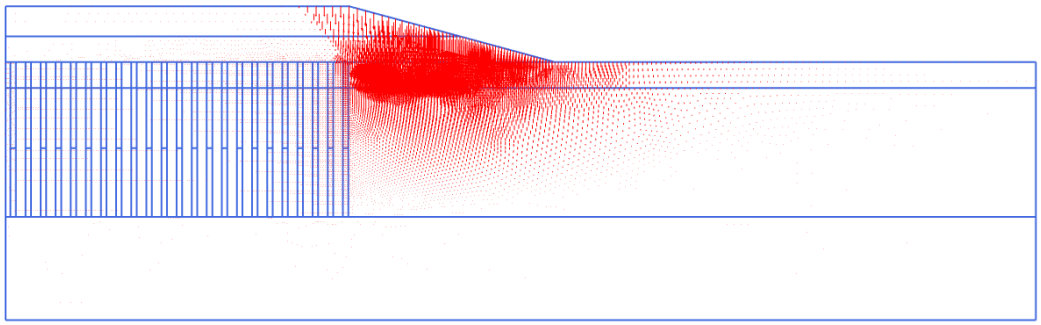

Figure 5.9 Simulated vertical displacements in Geometry matching method.

But in the case of geometry matching model of the same section and loading stage, an excess pore water pressure of 25 kPa was developed in the first two days and took 50 days to dissipate and reach to the minimum value which was set as a criterion in the final phase of the simulation. Equal excess pore water pressure was developed at sections 180 and 220 in both the geometry and combined matching model even though different plain strain wall spacing and column length have been used in the two sections. The marginally higher excess pore water pressure was developed at section 200 in the case of both models.

Simulation results are presented in Figure 5.8 to investigate the stress state of the material models at the end of the consolidation process. Slightly more plastic points were observed in the combined matching model mostly on the upper parts of the column periphery and the center part of the preload. Almost the same numbers of plastic stress points observed on the upper parts of the column edge in the case of both simulation models, but more points are observed on the outer column of the geometry-matching model than the combined. This indicates that plastic yielding occurred in the column material. The presence of more plastic points near to the edge of the preload indicates more deformation on the outer columns than the inner as shown in Figure 5.9.

5.3 Field measurements

As described in section 3.2.4 the settlement of the LCC improved clay soil was monitored by using a controlling units (markpeglars) which were installed before the application of the preloading. A total of 23 deep settlement plates were installed for this purpose. Among these, some of the deep settlement plates did not provide representative measurements, and those are excluded.

Measurements from deep settlement plates closer to the calculation sections were selected for comparison. Two approaches were used in this case. In the first approach, measurements of deep settlement plates P_11, P_12 and P_14 which are placed at the center line of the road section were taken corresponding to section 180, 200 and 220 respectively. In the second approach, the average of measurements from the three deep settlement plates along the calculation section was taken to get the most representative measurement values. Almost the same measurement results were obtained in both cases. According to the design of the project, it was planned to put the preloading for six months. But the measurements presented in Figure 5.10 were done for a time span of around four months. As shown in Figure 5.10 there was no settlement at the beginning and slightly increases in the first 15 days then almost the same settlement was measured in the continuing ten days. This part corresponds to the first loading stage. The settlement of the improved clay suddenly increased after the second stage load application and reached to its maximum value in 50 to 60 days of consolidation time. Nearly the same settlement was measured at all the three deep settlement plates in the last 40 to 45 days.

There is no significant difference between settlements measured at each point. An equal measurement was achieved at P_11 and P_14 which is slightly smaller compared with measurement at P_12. A marginally higher settlement was measured at P_12 since higher column spacing, and column length was applied. The field measurement was started before the application of the preloading, a measurement of zero settlement was recorded. Though there might be some initial settlement due to different impacts like the movement of machines during production, traffic movements during the loading and unloading process and others. Settlements due such impacts are not considered in the measurement since it is difficult to capture it.

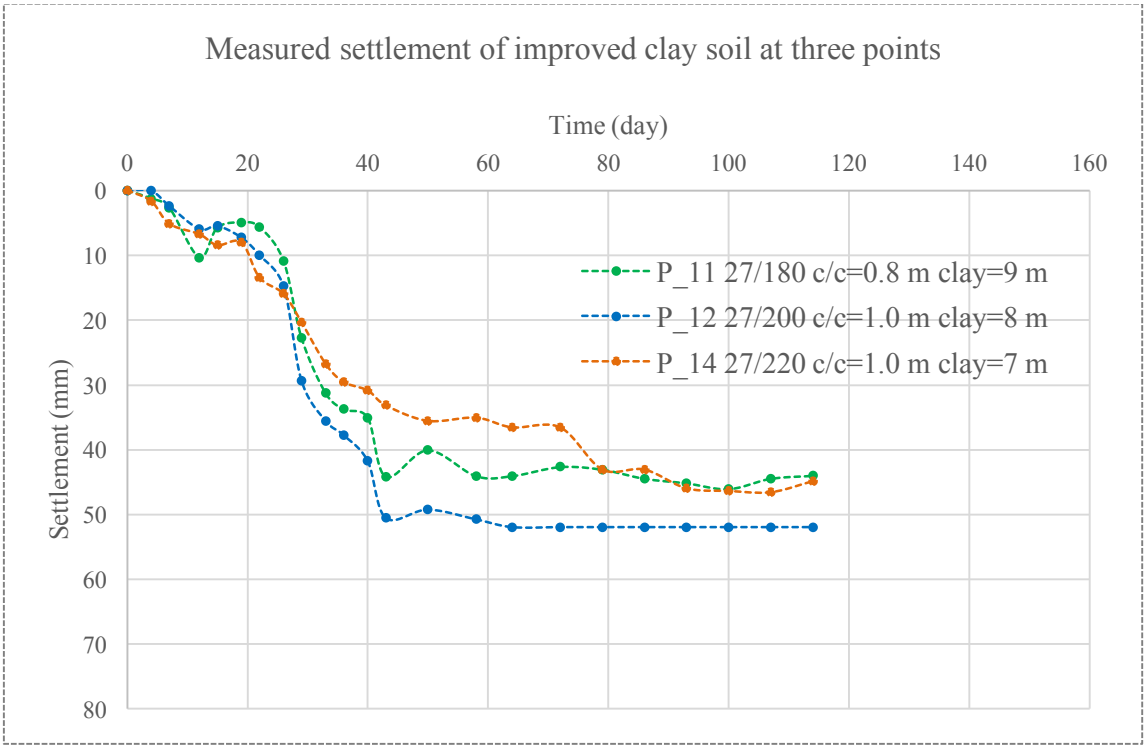

Figure 5.10 Settlements of improved clay soil measured from field at three designated control points corresponding to each calculation sections.

5.4 Result comparison

The same assumption was considered in both analytical calculations. However, the settlement in analytical method 2 (Equilibrium approach) mainly depends on the stress ratio and the coefficient of volume compressibility. So, the settlement of the improved clay was significantly influenced by the change in the stress ratio. In the case of the analytical method 1 (TK Geo 13 2013), the settlement of the improved soil was enormously influenced by the change in additional stress and stiffness of the column. The change in stress addition results in a change in compression of the improved soil which is the deformation of the LCC.

The results obtained from the two analytical methods were compared as presented in Table 5.2. Both methods showed a good agreement between them at all sections regarding long-term settlements with a difference of less than 1 cm, with a maximum deviation of 21% at section 220.

In the numerical analysis, both the 2D plane strain models produced a closer result. Although the combined matching model showed a higher settlement at all sections with a maximum difference of 1.3 cm which is deviated by 21%. In addition to this, the combined matching method generated a higher settlement in a short duration, which means the rate of consolidation was rapid. This effect comes due to the matching of the permeability and geometry of the column at the same time. Hence the combined matching model couldn't produce the correct rate of consolidation of the improved soil.

A comparison was made between settlements predicted by analytical and numerical methods with field measurements corresponding to each calculation section. Both the field measurements and the calculated settlements are listed in Table 5.3. The field-measured settlements are plotted together with the calculated results as presented in Figure 5.11, 5.12 and 5.13 consequently to the calculation sections 180, 200 and 220 respectively.

Table 5.2 Deviation of results between analytical methods

Section	Analytical_1 S(mm)	Analytical_2 S(mm)	Diff (mm)	Devation (%)
180 (0.8m)	38	34	4	12
200 (1.0m)	48	43	5	12
220 (1.0m)	46	38	8	21

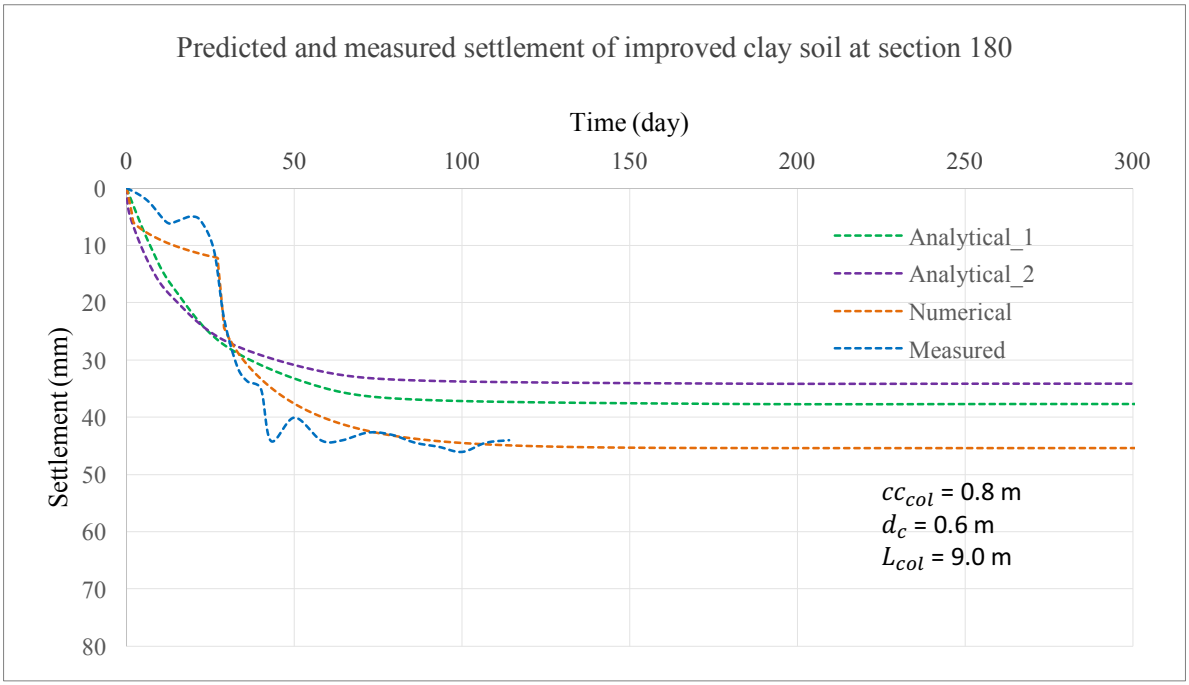

Figure 5.11 Settlement of improved clay soil comparison of numerical, analytical and field measurements at calculation section 180.

Table 5.3 Measured and calculated settlements of improved clay soil

		Calculated Settlements							
		Analytical_1		Analytical_2		Numerical			
	Measuered					Geomtery matching		Combined matching	
Section	Settlement S (mm)	S(mm)	RE (%)	S(mm)	RE (%)	S(mm)	RE (%)	S(mm)	RE (%)
180 (0.8m)	45	38	-16	34	-24	45	0	54	20
200 (1.0m)	52	48	-8	43	-17	63	21	76	46
220 (1.0m)	46	46	0	38	-17	52	13	63	37

Table 5.3 contains a relative error (RE) between the measured and the calculated values which is defined as:

$$RE = \frac{S_{cal} - S_{mea}}{S_{mea}} . 100(\%) \quad (5.1)$$

Where S_{cal} and S_{mea} are calculated and measured settlements of the improved clay soil. As the results presented in Table 5.3, the combined matching model overestimate the settlements at all calculation sections. Regarding long-term consolidation settlements, the geometrical matching model made a good agreement with a maximum relative error of 21% positive.

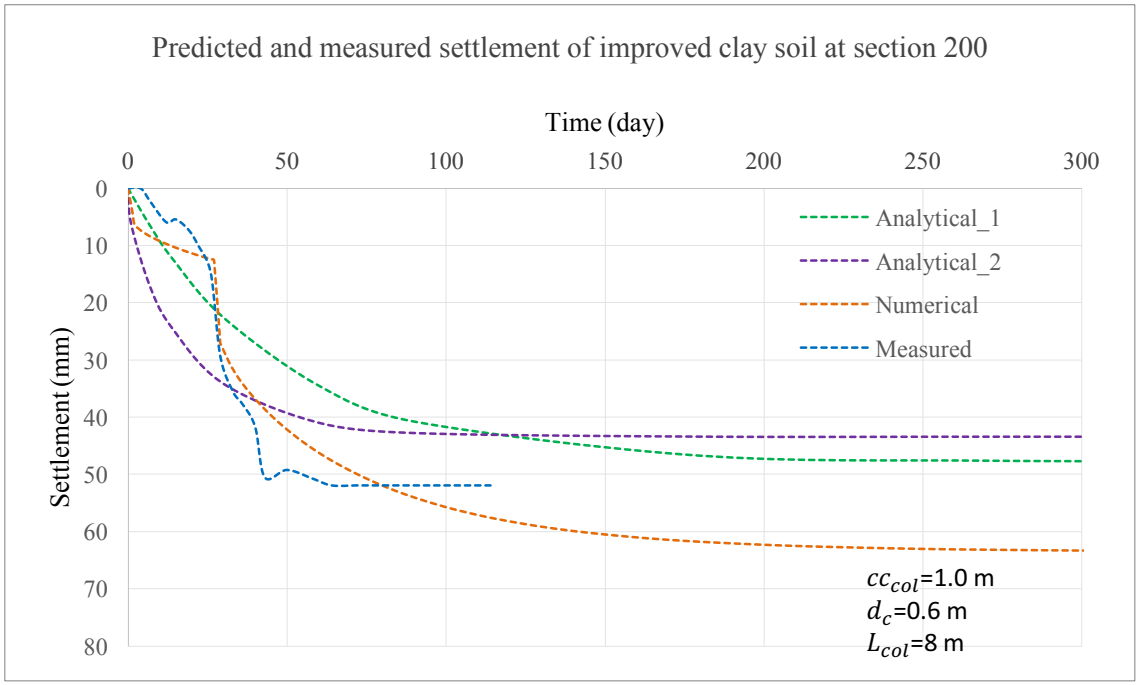

Figure 5.12 Settlement of improved clay soil comparison of numerical, analytical and field measurements at calculation section 200.

Results from both analytical methods made a good agreement with the field measurement at all sections. At section 180 slightly significant difference was achieved with a maximum relative error of 24 % negative from results of analytical method 2. As the results presented in Table 5.3, both analytical methods predicted somewhat smaller settlement than the field measurements at all sections while the numerical method produced almost equal consolidation settlement with the field measurement.

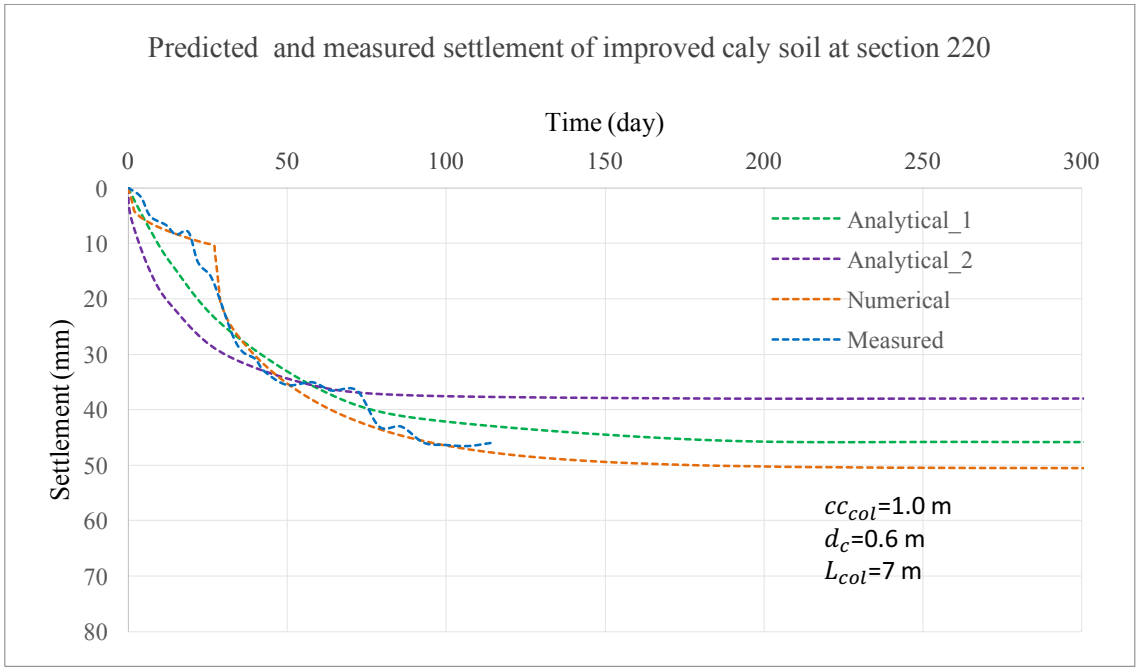

Figure 5.13 Settlement of improved clay soil comparison of numerical, analytical and field measurements at calculation section 220.

The consolidation settlements presented in Figures 5.11-13 contain numerical results of the geometrical matching model. So, only results from the geometrical matching model was plotted for comparison since it produced more reliable results. A settlement curve also plotted using results from the combined matching model which is presented in Appendix C. The combined matching model didn't predict the correct consolidation behavior of the improved clay soil and not presented in this section.

As shown in Figure 5.11-13 both analytical and numerical predictions are made a good agreement with the filed measurement at all sections regarding the long-term settlement of the improved clay soil except analytical method 2. This method slightly underestimates the settlement at section 180 with a maximum relative error of -24 %. Concerning the rate of consolidation, a reasonable agreement was achieved at all sections. The numerical method showed a good agreement with the field measurement compared to the analytical methods. Both analytical methods resulted in a moderately higher rate of consolidation in the first 50 days.

6 Discussion

In this study, both the prediction and field measurement of time-dependent settlements were performed for a load (selected soil material) placed on LCC improved clay soil for a time span of six months. The assumptions on the material behavior of the clay and LCC are the same in both analytical and numerical calculations. The clay soil, as well as the LCC, were considered as linear elastic-perfectly plastic material during the application of load in both calculation models. Whereas different assumptions were considered regarding the input parameters used for analytical and numerical analyses.

Calculation models

In the analytical approach, a model which is developed for deep mixing soil improvement was applied. The calculation model used in Alen et al. (2006) is the same as the model in TK Geo 13 (2013). But Alen et al. (2006) considered Boussinesq's solution for homogenous infinite half space in the load distribution. In this model, the soil layer was divided into three different zones to calculate the settlements depending on the behavior of the soil and the column in each zone. However, according to the studies in Sällförs & Alen (2012) it is difficult to calculate settlement in zone A and often it is estimated using experience from similar cases. The LCC and the clay are considered as a composite material and only the settlement of the soil layer until the firm strata were calculated. The LCC has a full interaction with the surrounding soil since they were considered as a composite material. In this case, the soil and the column will deform equally at any depth.

Stiffness and permeability

As explained in the review section the stiffness and permeability are the two critical parameters that can influence the settlement of the improved clay soil both in the numerical and analytical calculations. The elastic modulus of the column was determined from an empirical formula, which uses the undrained shear strength of the column as an input. The laboratory and field test results showed a good strength of the LCC in strength development period of 7 and 28 days. The shear strength of the clay soil is much smaller than the shear strength of the column. So, in the calculation using the maximum strength of the column from individual test result might underestimate the real settlement of the improved soil. The size of the column, as well as the spacing between them, also had a significant influence on the settlement. The settlement calculations were performed by using the average undrained shear strength from the column probing tests. This is a good approach as proved by the better agreement between the calculations and filed measurement results.

The consolidation of the LCC was significantly affected by its rate of permeability which is estimated based on the permeability of the clay soil. The coefficient of consolidation of the column is much higher than the clay soil, due to this a radial flow will occur towards the column then the column partially serves as a vertical drain. So, the rate of consolidation was determined by considering the column as a vertical drain. The permeability of the clay soil was multiplied by a factor to get a fair match between the calculated and the real permeability of the column on the field. The factors assumed to match the permeability of the column produced a good result both in the analytical and numerical analyses regarding the time-dependent consolidation settlements.

Comparative analysis

From the comparison of results presented in chapter 5, the two analytical methods had a good agreement between them concerning time-dependent long-term settlements as well as the rate of consolidation. A reasonable agreement was achieved between analytically calculated, and field measured consolidation settlements at all sections. As presented in Figure 5.11 and 5.12 both analytical methods produced a better agreement regarding the rate of consolidation in the first 50 days. After that the field measurement showed a sudden diversion. At all calculation sections, consolidation increases gradually in the first 100 days then changed to a constant rate. In Figure 5.13 both methods produced a good agreement with the field measurement.

As the numerical results presented in Table 5.1, shows that the combined matching model gave a higher value which overestimates the long-term settlements of the improved clay soil compared to the measured settlements. The rate of consolidation is also faster compared with the results of the geometry matching model, as shown in Figure 5.5. Simulation of excess pore water pressure was performed to use as an additional comparison between the two conversion models. In the case of the combined matching model the excess pore water pressure was dissipated very quickly. Besides the model had not produced the same rate of consolidation with the filed measurements. The geometry matching model produced almost the same rate of consolidation with the field measurements at all calculation sections. So, it is a recommended method to convert the axisymmetric to plane strain model.

Material performance

The performance of the material of the LCC was investigated as results presented in Figure 5.8. The presence of numerous plastic stress points at the top part of the column showed as it comes to plastic yielding while the column below the dry crust is intact and deform elastically with the surrounding soil. This result indicates that the lower parts of the column, as well as the soil, are stiffer than the upper portion.

Column spacing and depth of clay

The results from both analytical and numerical predictions revealed that the spacing between the columns had a significant effect on the size of the settlement. The spacing between columns included in the calculation regarding area improvement ratio. Hence the settlement and area improvement ratio have a direct relation independent of the thickness of the clay soil. This has proven by using different column spacing 0.8 and 1 meters at section 180. The settlement in the case of 1.0-meter column spacing was increased by 1.5 cm. The thickness of the clay soil also affected the size of the settlement as results at section 200 and 220 indicated. In both prediction methods, the depth of the clay soil was different at sections 200 and 220 while the column diameter and spacing were the same. Hence an increase in the settlement was achieved with a higher clay thickness.

Influence of parameters

As expected, the results of the sensitivity analysis gave a higher score for the stiffness of the LCC compared to other parameters. The effect of the stiffness was also verified by using higher and lower stiffness values, and a significant difference was observed. This analysis tells us that it is essential to give a strict attention for the stiffness of the column. In reality, the strength of the column is variable through depth as well as column to column. This variability depends on the distribution of the binder during mixing, amount of binder, the type of soil and other similar factors. So, performing field production control tests can help to assess the variability as well as the strength of the column. In similar way sensitivity analysis was performed to check the influence of the permeability of the column and clay soil on the vertical deformation and excess pore water pressure development. As expected, the vertical permeability of the LCC had a significant influence on the rate consolidation and excess pore water pressure development. So, an emphasis is required on estimating permeability of the column since it has a significant impact on the final time of consolidation.

7 Conclusion

In this study, it was targeted to perform a comparative analysis between theoretical analyses and field measurements of a consolidation settlements of clay soil improved by LCC. Settlement predictions were performed using analytical as well as numerical methods. The field measurement was used as a reference to compare with results obtained from the analytical and numerical analyses. Two different analytical methods and two numerical models were used in the analysis and then the following conclusions were drawn.

- Both analytical methods produced a better agreement with field measurements regarding long-term consolidation settlements at all calculation sections. However, the analytical method 2 (equilibrium approach) underestimated the consolidation settlement at section 180 with a relative error of -24%. Concerning the rate of consolidation both methods made a reasonable agreement with the field measurement.

- The numerical analysis made a good agreement with the field measurements concerning both the long-term consolidation settlement as well as the rate of consolidation at all sections. Regarding the correctness, the predicted settlements and rate of consolidation the geometry matching model gave a good result, and it is a recommended method to convert the axisymmetric to a 2D plane strain model.

- As expected, the settlements of the improved clay soil was significantly affected by the stiffness of the LCC. The settlement of the LCC decrease when its stiffness increases this depends on many factors but the amount of binder used in column production probably is the most significant.

- As expected, the spacing between columns and the length of the column influenced the size of the settlement of the improved soil. The smaller spacing and short length of column both resulted in a lower settlement independent to each other.

The assumptions regarding input parameters, the selection of material model's and the procedures applied in both the analytical and numerical calculations were different. There might be some uncertainties which need further research regarding the analysis as well the field measurements. However, in this study, the numerical method produced a better agreement with the field measurement than the analytical methods. Therefore, it is concluded that the numerical analysis can deliver more reliable result if the proper material model and input parameters are applied.

8 Suggestions to further work

- It would be useful to examine the effect of the lateral deformation. As the analysis in Jiang et al. (2013) indicates that both the column and the surrounding soil deform not only in the vertical direction but also in the lateral direction.

- In the practical design, the long-term creep settlement often considered as negligible. However, Brian (2014) studied that the creep settlement will take the majority of the total long-term settlement depending on the type of clay soil. So, it would be beneficial to investigate the creep settlement regarding the ground performance and the design lifespan of the structure to build.

- It would also be useful to perform a numerical analysis for deformation of LCC improved clay soil using 3D FE program since it has an advantage over the 2D to apply the actual geometry of the structure.

- As described in Chapter 4, the permeability of the LCC was determined based on the assumed factor in the case of both numerical and analytical calculations. The factors were set based on the principle to make a reasonable match of permeability of the LCC with its field performance. It would be useful to investigate the permeability of the LCC based on its actual performance in the field.

References

Abosh, H., Ichmoto, E., Enoki, M. & Harada, K. 1979. "The composer-A method to improve characterstics of soft clay by inclusion of large diameter of sand column." *Proceeding of International conference on soil reinforcement: Reinforced earth and other techniques.* Paris. 221-216.

Alen, C., Sällfors, G., Bengtsson, P., and Baker, S. 2006. *Test embankments highway 45/North link – Embankments on lime cement column stabilized soil – Calculation model for settlements.* Report 15, Linköping: Swedish deep stabilization research center.

Almagir, M., Miura, N., Poorooshasb, B. , and Madhav, M.R. 1996. "Deformation analysis of soft ground reinforced by columnar Inclusions,." *Computer and Geotechnics* (Elsevier Science Ltd) 18 No. 4: 267-290.

Axelsson, M., and S. Larsson. 2004. "Column penetration tests for lime-cement columns in deep mixing-experiences in Sweden." *Grouting and Ground treatment* . American Socitiy of Civil Engineers.

Baker, S. 2000. *Deformation behavior of LCcolumn Stabilized Clay, Report 7.* Linköping: Swedish deep stabilization research center.

Bergman, N. 2015. "Aspects of probabilistic serviceability limit state design of dry deep mixing." Civil and Architectural Engineering Division of Soil and Rock mechanics, KTH royal institute of technology, Stockholm.

Brian, S. 2014. ”The infleunce of creep on the settlement of foundations supported by stone columns.” NUI Galway, Galway, Ireland.

Broms, Bengt. 1984. *Stabilization of soil with lime columns design hand book* . Singapore.

Castro, J. & Sagaseta, C. 2010. Disscussion of "Simplified Plane-Strain Modeling of Stone- Column Reinforced ground." by Tan, S.A., Tjahyono, S., and Oo, K.K. *Journal of geotechnical and geoenviromental engineering* Vol 136, pp. 892-894.

Chai, J., and Pongsivasathit, S. 2010. "A method for predicting consolidation settlements of floating column improved clayey subsoil."

Chow, Y.K. 1996. "Settlement analysis of sand compaction pile." *Soils and foundation:* 36: 111-113.

Ähnberg, H. 2006. *Strength of stabilized soils- A laboratory study on clays and organic soils stablized with diffrent types of binder.* Lund: Swedish Deep stabilization Research Center.

Gong, X., Tian, X., and Hu, W. 2015. "Simplified method for predicating consolidation settlement of soft ground improved by floating soil-cement column." (Central South University press and Springer-Verlag).

Jiang, Y., J. Han, & G. Zheng. 2013. "Numerical Analysis of Consolidation of soft soils fully – penetrated by deep mixed columns,." *Journal of Civil Engineering* (Korean society of civil engineers) 17: 96-105.

Kivelö, M. and Broms, B.B. 1999. "Mechanical behaviour and shear resistance of lime/cement columns ."

Lambe, H., and Whitma, R. 1979. "Soil mechanics." 157. New York.

Larsson, .R. 2007a. *Deep stabilization with binder stablized column and mass stabilization - A guide.* Linköping: Swedish Deep Stabilization.

Larsson, R. 2006. *Deep Mixing with binders stabilized column and mass stabilization – Guidance.* Report 17, Linköping: Swedish deep stabilization research center.

Larsson, S. 2003. *Mixing Processes for Ground Improvement by Deep Mixing.* Report 6 , Linköping: Swedish Deep Stabilization Research center.

Larsson, S. 2005a. "State of Practice report session 6: Execution, monitoring and quality control." *International conference on deep mixing* . Stockholm .

Quang, N.D., and J. Chai. 2016. "Permeability of lime - and cement - treated clayey soils." (Department of Civil Engineering and Architecture, Saga university).

Sällfors, G., and Alen, C. 2012. "Geotechnics – BOM 045 Lime cement columns."

Salem, M, och R El-Shrebiny. 2013. ”Comparison of measured and calculated consolidation settlements of thick underconsolidated clay.” *Alexandria Engineering Journal* (Cairo University).

Steensen-Bach, J.O, P.E Bengtsson, and Y Rocgbeck. 1996. "Large Scale Triaxial tests on samples from lime-cement columns." *Proceedings 12th Nordic Geotechnical Conference, NGM* 135-146.

Tan, S.A., Tjahyono, S., and Oo, K.K. 2008. "Simplified Plane-Strain Modeling of Stone- Column Reinforced ground." *Geotechnical and Geoenviromental Engineering* (ASCE) 134(2): 185-194.

TK Geo 13 2013. " Swedish Transporation Adminstration Technical Criteria for geo construction." Börlange: Swedish Transporation Adminstration.

TK Geo 13. 2013. "Swedish Transportation Adminstartion Technical Advice for geoconstruction." Börlange: Swedish Transportation Adminstartion.

Appendix A

Laboratory and Field test results

A_1 Laboratory test results for compressive strength

Stabilisering av jord

Projekt **FSK05 - Tpl Hjulsta FSE502**

Uppdragsnummer	*Uppdragsgivare*	*Gransk./Tabell*	
244166	Tyréns AB, Stockholm	*Löp-nr*	25801
Provtagningsdatum	*Provtagningsredskap*	*Datum/Sign*	2014-02-03
2013-05-24	Kv St I ø 50mm	*Undersökningsdatum*	
		2013-10-18 -	2013-11-15

Inblandningsdatum 2013-10-18 *Lagringstemperatur* 7 °C

Bland-ning	Ostabiliserad jord: Den-sitet ρ [t/m³]	Vatten kvot w [%]	Kon-flyt-gräns w_L [%]	Skjuv-hållf.h. τ_{fu} [kPa]	Stabiliserad jord: Tillsatsmedel Enligt b nedan	Cement Kalk [%]	Tid för tryck-försöket [dygn]	Den-sitet ρ [t/m³]	Vatten kvot w [%]	Skjuvhållfasthet Tryck-försök [kPa]	Kon-försök [kPa]	Anmärkning
1	1.62	68	60		110	50/50	7	1,68	53	95		
							7	1,68	53	95		
							28	1,68	53	138		
							28	1,67	54	154		
2	1.70	57	47	14,0	90	50/50	7	1,72	48	88		
							7	1,71	48	81		
							28	1,72	49	136		
							28	1,72	48	185		

a) kg per löpmeter pelare med pelar Ø 0 mm
b) kg/m² jord
c) % på naturfuktig jord

Bl.	Borrhål	Djup [m]
1	131682	3.0
2	131682	7.0

Cement: Byggcement, Standard PK Slite
Kalk: Nordkalk TERRA TM 100 (osläckt kalk 0,0-0,1 mm)

SWECO

SWECO GEOLAB

Enaxligt tryckförsök
enl SIS-CEN ISO/TS 178-7:2005

Projekt **Hjulsta Tpl**			
Uppdragsnummer	*Uppdragsgivare*	*Gransk./Tabell*	
244166	Tyréns AB, Stockholm	*Löp-nr*	25801
Provtagningsdatum	*Provtagningsredskap*	*Datum/Sign*	2013-11-18
2013-05-24	Kv St I ø 50mm	*Undersökningsdatum*	2013-10-18 - 2013-11-15

Borrpunkts ID:	131682	*Koncentration:* Cement/Kalk	50/50 %	
Djup:	3.0 m	*Inblandningsmängd:*	110 *kg/m³*	*Bland.nr* 1

Antal dygn	c_u, kPa	q_u, kPa vid	ε,%	Provhöjd, cm/ prov Ø,		w, %	ρ, t/m³	Tid till brott, min	Def-hast. mm/min	E50 - modul, kPa	Anm.	Brottyp enl.
7	95	190	3,00	10,0	5,0	53	1,68	1,56667	1,914563	8650		a
7	95	190	2,63	11,0	5,0	53	1,68	1,53333	1,886625	14334		a
28	138	277	2,63	10,0	5,0	53	1,68	1,4	1,877723	23501		a
28	154	307	1,89	10,0	5,0	54	1,67	1,06667	1,770934	26308		a

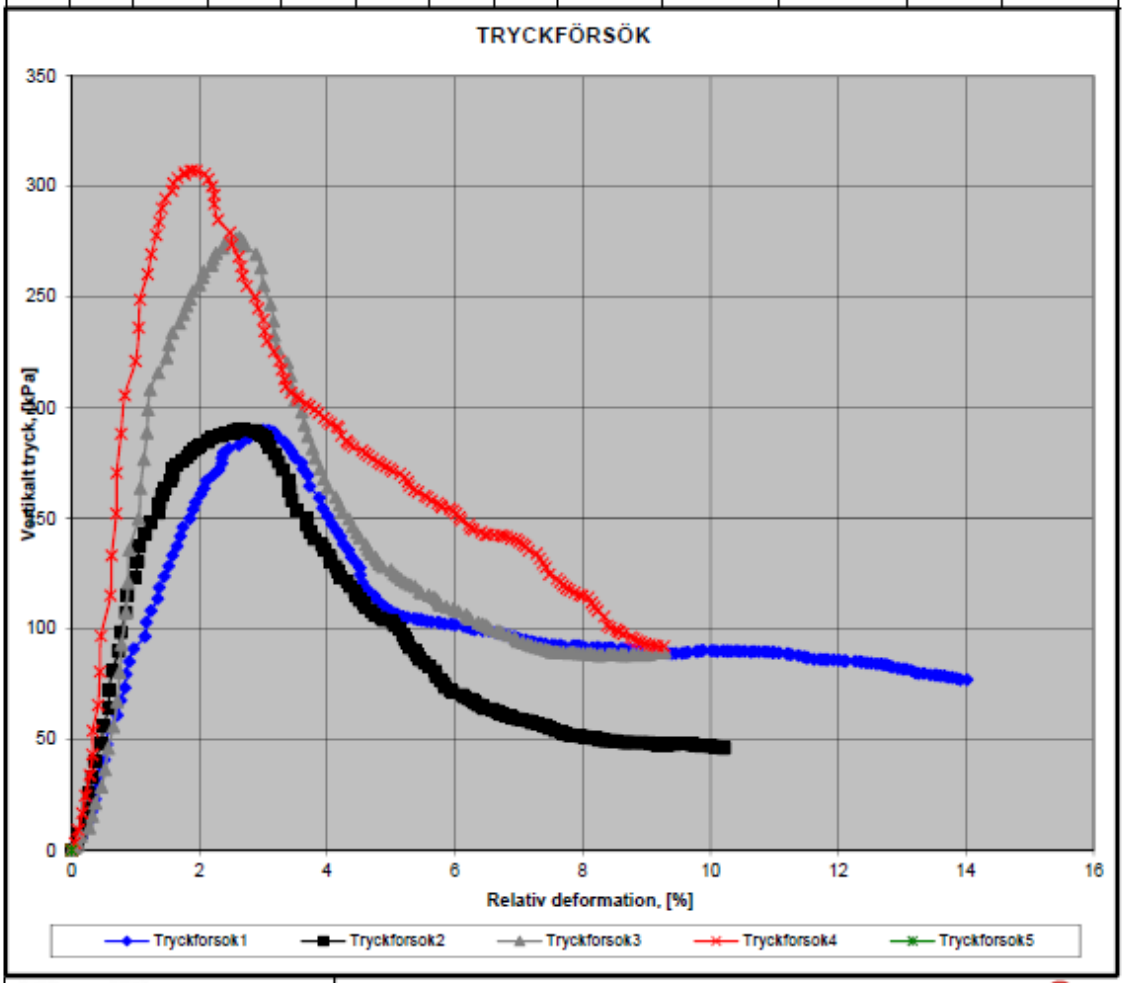

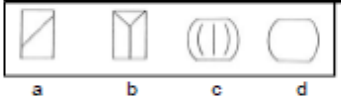

SWECO GEOLAB, Gjörwellsgatan 22, Box 34044,
100 26 STOCKHOLM, Tel: 08-695 60 00, Fax: 08-695 63 60,
geolab@sweco.se, www.sweco.se/geolab, Ingår i SWECO VBB AB

P:\2172\Uppdrag 2014\25801\KC\[Sida 4 140203.xlsx]

SWECO
1(1)

SWECO GEOLAB

Enaxligt tryckförsök
enl SIS-CEN ISO/TS 178-7:2005

Projekt **Hjulsta Tpl**			
Uppdragsnummer	*Uppdragsgivare*	*Gransk./Tabell*	
244166	Tyréns AB, Stockholm	*Löp-nr*	25801
Provtagningsdatum	*Provtagningsredskap*	*Datum/Sign*	2013-11-18
2013-05-24	Kv St I ø 50mm	*Undersökningsdatum*	2013-10-18 - 2013-11-15

Borrpunkts ID: 131682		*Koncentration:* Cement/Kalk 50/50 %		
Djup: 7.0 m		*Inblandningsmängd:* 90 *kg/m³*	*Bland.nr* 2	

Antal dygn	*c_u, kPa*	*q_u, kPa vid ε,%*		*Provhöjd, cm/ prov Ø,*		*w, %*	*ρ, t/m³*	*Tid till brott, min*	*Def-hast. mm/min*	*E50 - modul, kPa*	*Anm.*	*Brottyp enl.*
7	88,2	176	3,39	10,0	5,0	48	1,72	1,8	1,884948	12774		a
7	80,6	161	3,36	10,0	5,0	48	1,71	1,7	1,97452	8072		a
28	136	272	2,53	10,0	5,0	49	1,72	1,36667	1,850622	17462		a
28	185	371	2,79	10,0	5,0	48	1,72	1,46667	1,904016	24230		a

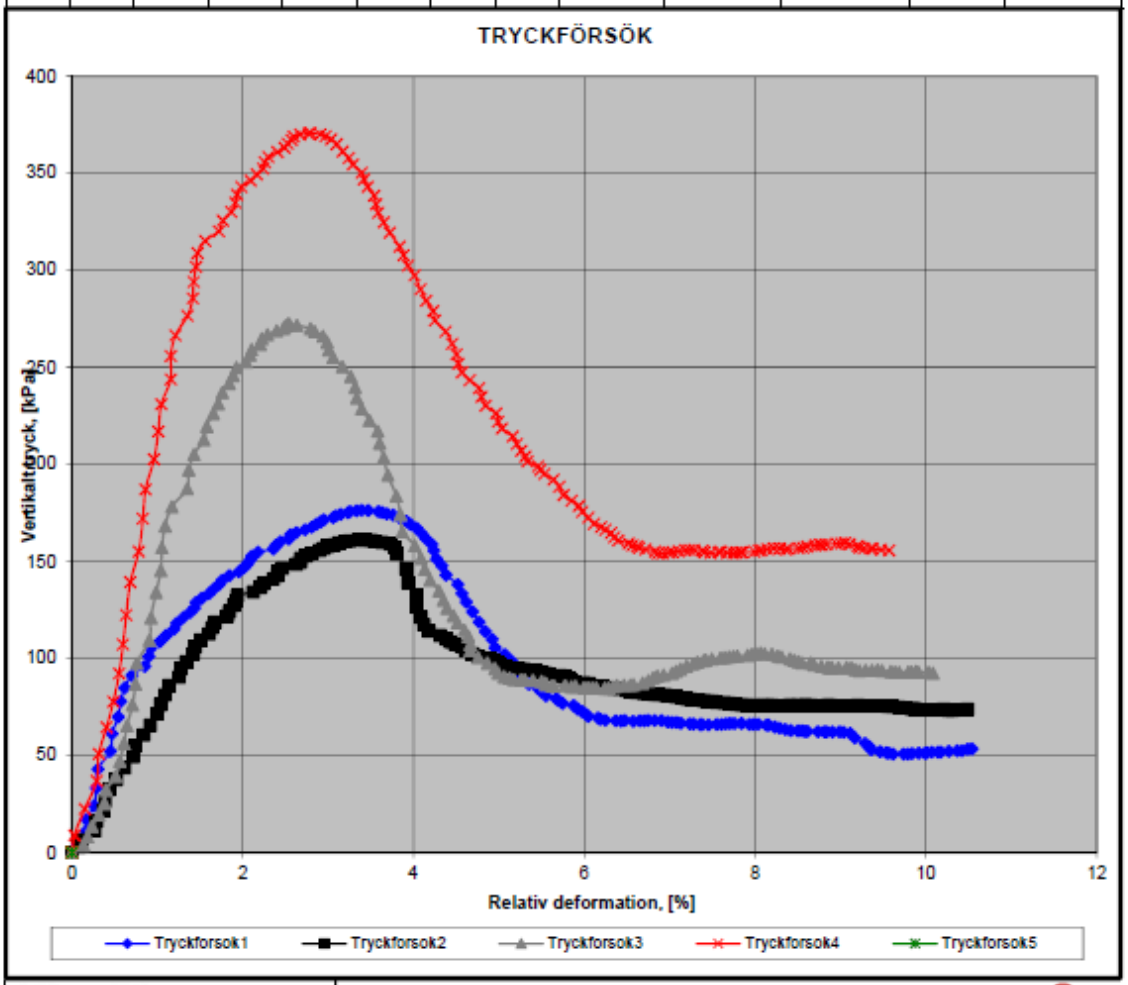

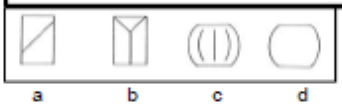

SWECO GEOLAB, Gjörwellsgatan 22, Box 34044,
100 26 STOCKHOLM, Tel: 08-695 60 00, Fax: 08-695 63 60,
geolab@sweco.se, www.sweco.se/geolab, Ingår i SWECO VBB AB

P:\2172\Uppdrag 2014\25801\KC\[Sida 5 140203.xlsx]

SWECO
1(1)

Location of sample columns for quality control test

A column penetration test had been performed for control of the quality of the installed lime column as well as its continuity. The test had been carried out continuously during the construction period and 25 pcs of columns tested for the whole installation area. The test result is attached here with.

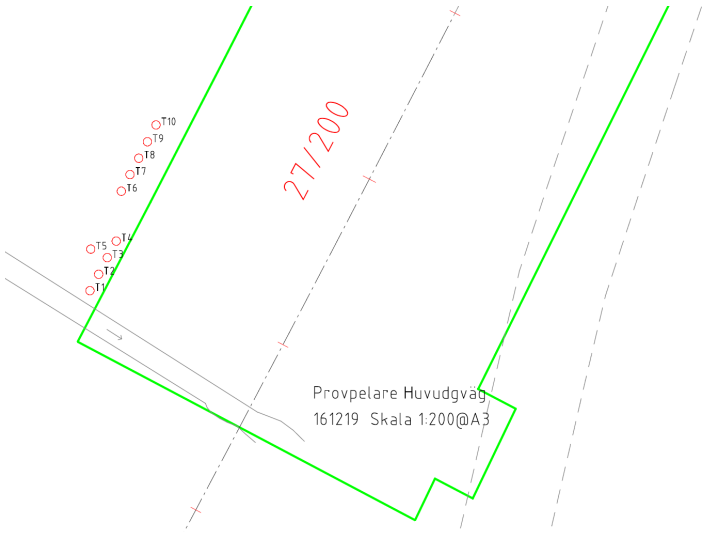

Figure C1. Location of column selected for sample tests

A_2 Field production control test results (Column penetration test)

NCC
Akallalänken

Produktionskontrol

NCC, Akallalänken, produktionskontroll 5, 28-32 dygn.

FKPS-sondering utfördes 2017-04-24 i 10 st pelare.

Resultaten av sonderingarna redovisas enligt följande:

Utmatningsdiagram	sid. 4-22
Skjuvhållfasthet, spetsmotstånd vid förborrning, FKPS-sondering, vinkeländring samt sjunkhastighet för enskild pelare med inblandningen 25/31kg/m och stigning 20mm/varv.	sid. 5-23
Sammanfattande analys för samtliga 10 KC- pelare, med inblandningen 25/31kg/m och stigning 20mm/varv, utförda med sond 500x15 mm.	sid. 24

Sammanfattning:
Vid förborrning har en krona med 58 mm i diameter använts.
Vid FKPS-sondering har sond med dimensionen 500x15mm använts.
Vid utvärderingen av skjuvhållfasthet har omräkningsfaktorn 12,5 använts.

Borås 2017-05-02

Omräkningsfaktor för FTPS-sondering

Dmixab använder omräkningsfaktorn 12,5 för KPS-vinge 500x15mm.
Omräkningsfaktorn baseras på förborrningskronans diameter som är 58mm
Beräkning av omräkningsfaktorn redovisas nedan:

Förborrningskrona	58 mm	A_{FB}=	2642	mm^2
Vinge 500x15	500 mm			
	15 mm			
Spets sonderingsvinge	50 mm	$A_{Stång}$=	1963	mm^2
Tvärsnittsarea vinge	(500-50)*15+$A_{stång}$	A_{sond}=	8713	mm^2
Skillnad A_{FB} och $A_{stång}$		$\Delta A_{stång}=(A_{FB}-A_{stång})$=	679	mm^2
Korrigerad tvärsnittsarea på sonden		$A_{sond,korr}=A_{sond}-\Delta A_{stång}$=	8035	mm^2
Utvärdering av $c_{u,pel}=(0,1/A_{sond,korr})*Q_{spets}$		$0,1/A_{sond,korr}$=	12,45	≈12,5

Utvärdering av $c_{u,pel}=12,5*Q_{spets}$

Generell utvärdering för olika FKPS-sonderingar

Pelarsondering och förborrning 50mm krona

Pelardiameter (mm)	Bredd B (mm)	Tvärmått d (mm)	Tvärsnitts-area (mm^2)	Omräknings-faktor	Rek. Omräkn. faktor
500	400	20	8 963	11,16	**11**
600	500	15	8 713	11,48	**11,5**
800	600	15	10 213	9,79	**9,5**
	250	15	4 963	20,15	**18**

Pelarsondering och förborrning 58mm krona

Pelardiameter (mm)	Bredd B (mm)	Tvärmått d (mm)	Tvärsnitts-area (mm^2)	Omräknings-faktor	Rek. Omräkn. faktor
500	400	20	8 285	12,07	**12**
600	500	15	8 035	12,45	**12,5**
800	600	15	9 535	10,49	**10**
	250	15	4 284	23,34	**18**

Omräkningsfaktorn 12,5 för KPS 500x15 användes i BViV projektet på 45:an, som komplement vid hård pelare användes 250x15 vinge. Omräkningsfaktorn var då försiktigt vald till 16 (teoretiskt 21-23)

dmixab
dry soil mixing

Katrinebergsgatan 23
504 39 Borås
Tel: 031-189990, Fax 031-72 69 991

Mikael Birgersson
Tel:031-189990
E-post:mikael@dmixab.se

dmixab
dry soil mixing

B110

Detaljer

Tid	**Förare**	**LB**	**Totalt**
3/28/2017 7:02	Johnny Rundqvist	9.8 m	259 kg
Kund	**Maskin**	**LS**	**Snitt**
NCC	M4	9.3 m	27.9 kg/m
Objekt	**Verktyg**	**Blandning**	**Marknivå**
AKALLALÄNKEN	PB600	KC50/50	0 m
Kilo i Botten	**Lutning X**	**Lutning Y**	**Tanktryck**
8	0.2°	0.4°	5.5 bar

Diagram

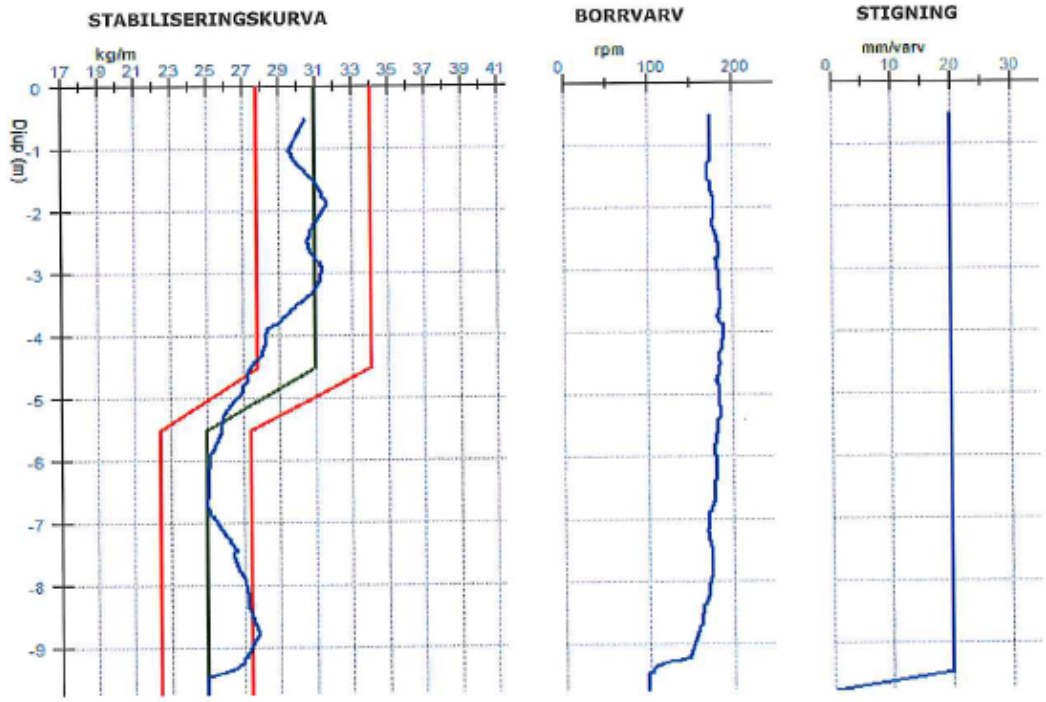

venska dmixab AB Katrinebergsgatan 23A 504 39 Borås
l: 031-72 69 990 fax: 031-72 69 991
ww.dmixab.se
fo@dmixab.se
bankgiro: 5807-6373
orgnr: 556630-0314

NCC

Produktionskontroll 5 28-32 dygn
Akallalänken Huvudväg

Pelar nr: B110
Koordinater X: 6587751,014 Y: 143652,084

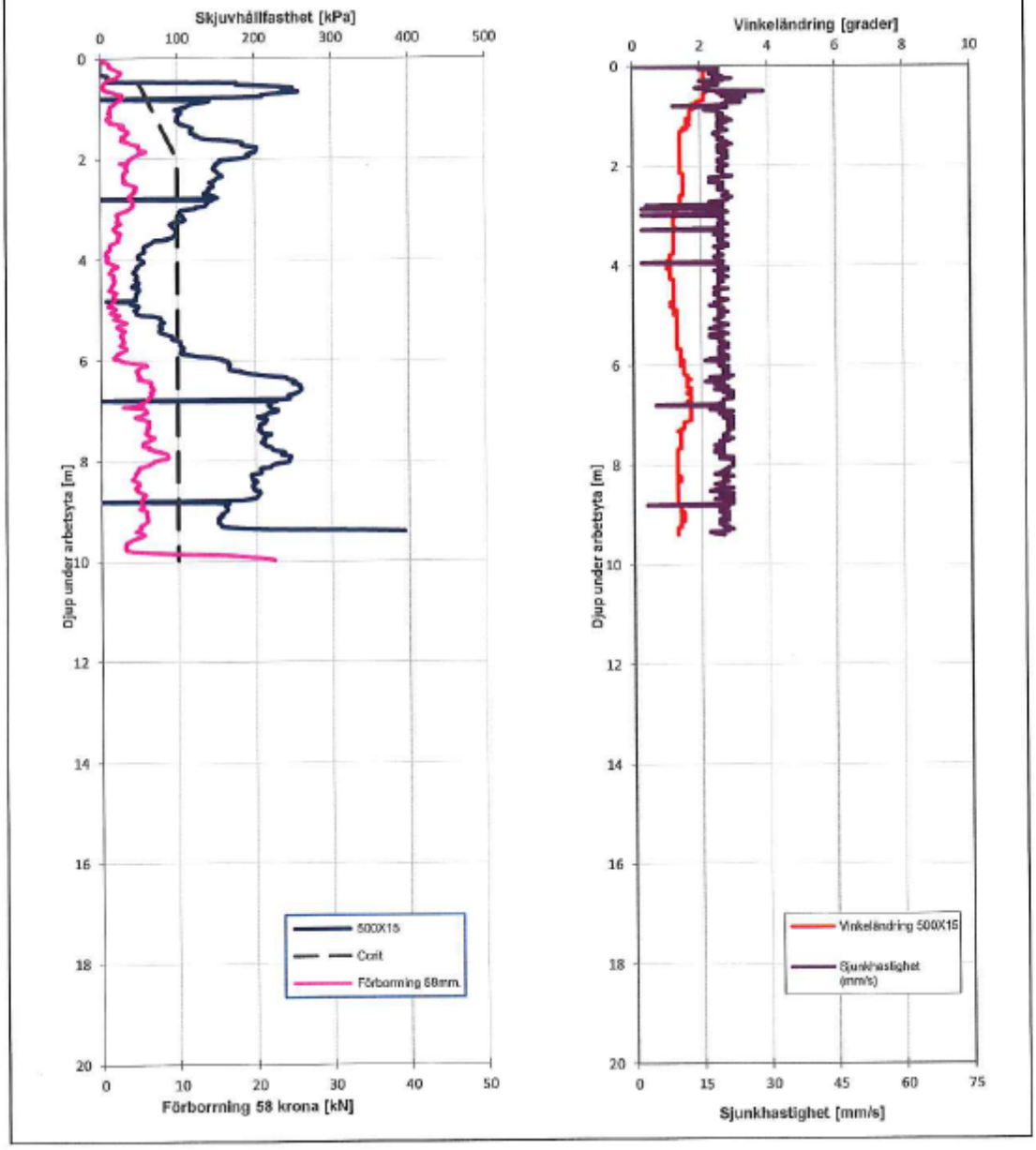

Pelar nr: B110	Verktyg: PB600	Stigning: 20mm/r
Tillverkningsdatum: 2017-03-28	Faktor: 12,5	Diameter: 600mm
Provdatum: 2017-04-24	KC 50/50: 25/31kg/	Pelarlängd: 9,8m
Projekt nr: 2015-4	Sond: 500X15mm	Utförd Längd: 9,4m

dmixab
dry soil mixing

B113

Detaljer

Tid	Förare	LB	Totalt
3/28/2017 4:46	Johnny Rundqvist	9.5 m	247 kg
Kund	**Maskin**	**LS**	**Snitt**
NCC	M4	9.0 m	27.6 kg/m
Objekt	**Verktyg**	**Blandning**	**Marknivå**
AKALLALÄNKEN	PB600	KC50/50	0 m
Kilo i Botten	**Lutning X**	**Lutning Y**	**Tanktryck**
8	0.5°	0.0°	5.5 bar

Diagram

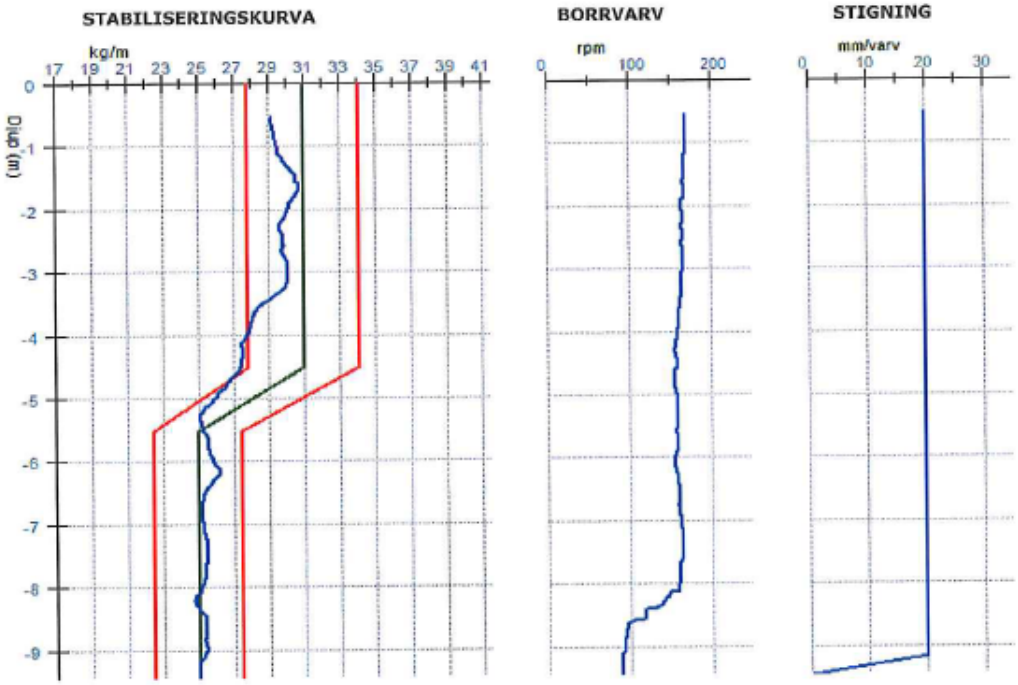

Svenska dmixab AB Katrinebergsgatan 23A 504 39 Borås
tel: 031-72 69 990 fax: 031-72 69 991
www.dmixab.se
info@dmixab.se
bankgiro: 5807-6373
orgnr: 556630-0314

NCC

Produktionskontroll 5 28-32 dygn
Akallalänken Huvudväg

Pelar nr: B113
Koordinater X: 6587748,344 Y: 143650,717

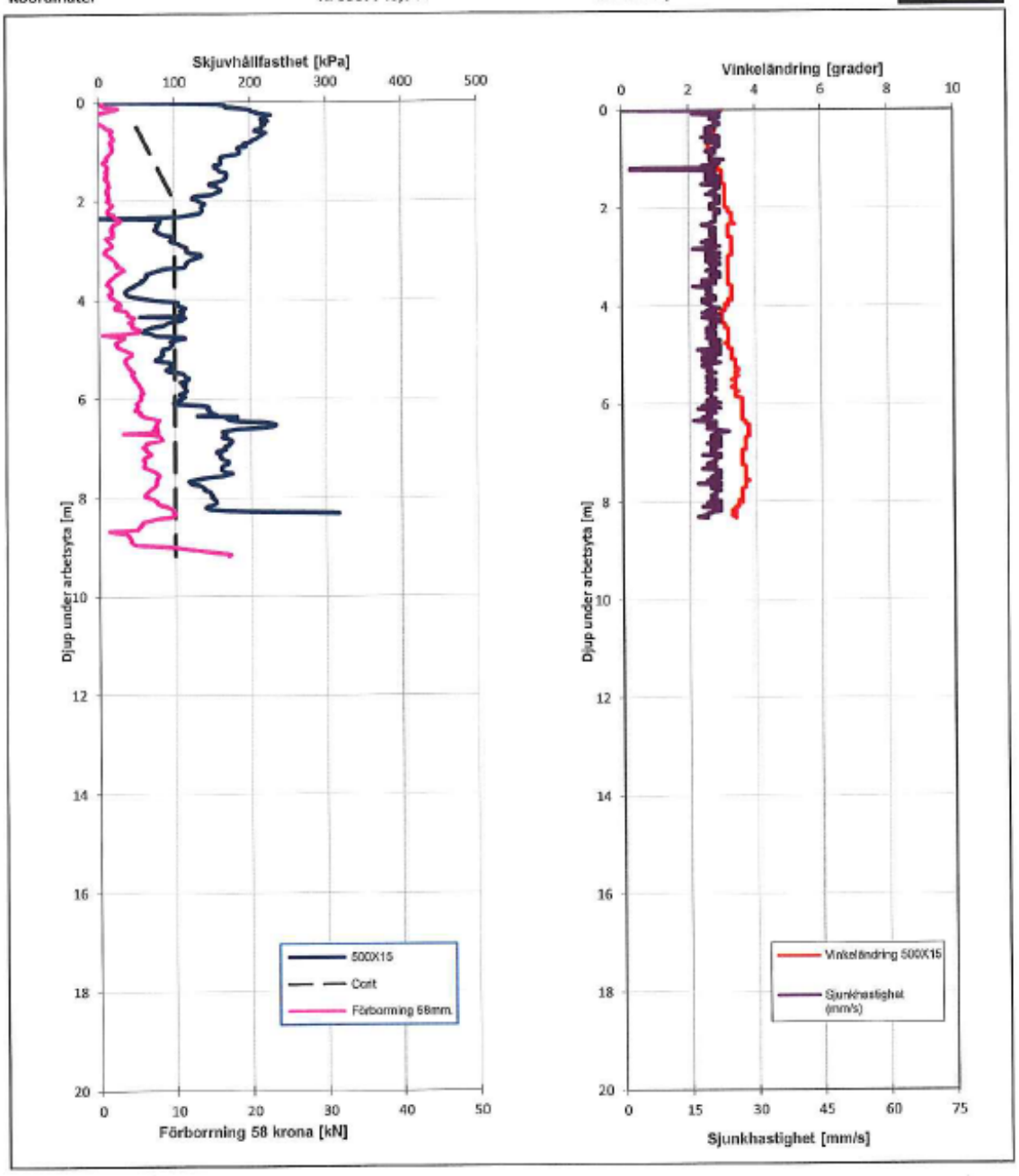

Pelar nr: B113	Verktyg: PB600	Stigning: 20mm/r
Tillverkningsdatum: 2017-03-28	Faktor: 12,5	Diameter: 600mm
Provdatum: 2017-04-24	KC 50/50: 25/31kg/	Pelarlängd: 9,5m
Projekt nr: 2015-4	Sond: 500X15mm	Utförd Längd: 8,3m

dmixab
dry soil mixing

B115

Detaljer

Tid	**Förare**	**LB**	**Totalt**
3/28/2017 4:00	Johnny Rundqvist	9.3 m	250 kg
Kund	**Maskin**	**LS**	**Snitt**
NCC	M4	8.8 m	28.4 kg/m
Objekt	**Verktyg**	**Blandning**	**Marknivå**
AKALLALÄNKEN	PB600	KC50/50	0 m
Kilo i Botten	**Lutning X**	**Lutning Y**	**Tanktryck**
8	0.2°	0.1°	5.5 bar

Diagram

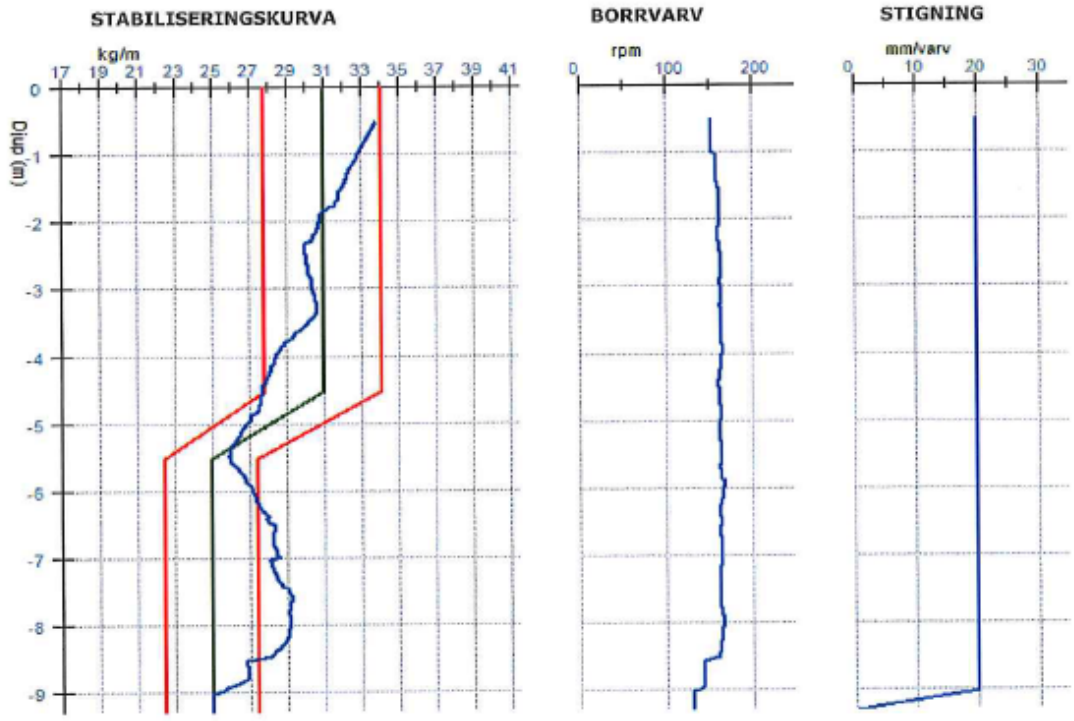

venska dmixab AB Katrinebergsgatan 23A 504 39 Borås
l: 031-72 69 990 fax: 031-72 69 991
ww.dmixab.se
fo@dmixab.se
bankgiro: 5807-6373
orgnr: 556630-0314

NCC

Produktionskontroll 5 28-32 dygn
Akallalänken Huvudväg

Pelar nr: B115
Koordinater **X: 6587746,564** **Y: 143649,806**

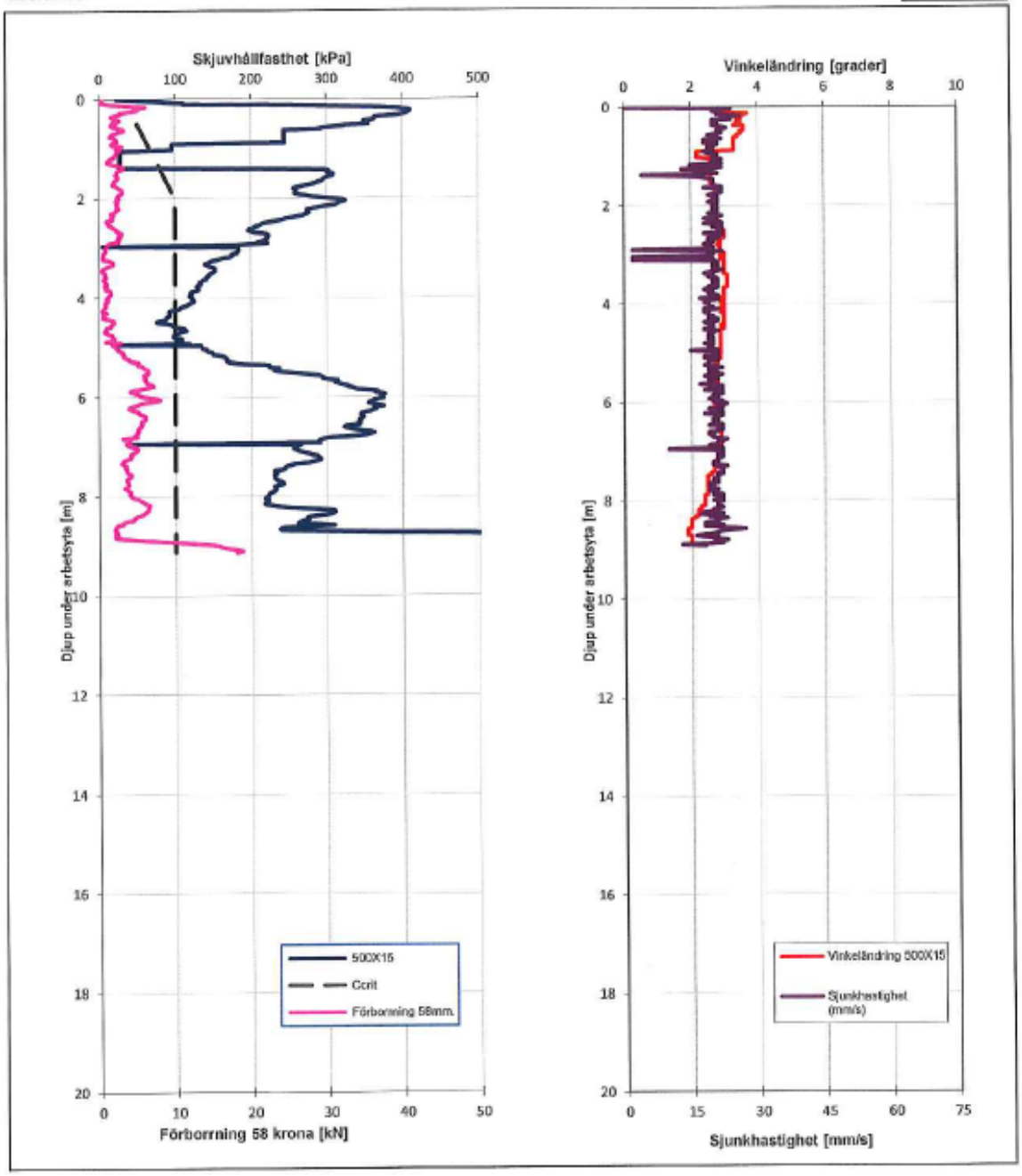

Pelar nr: B115	**Verktyg: PB600**	**Stigning: 20mm/r**
Tillverkningsdatum: 2017-03-28	**Faktor: 12,5**	**Diameter: 600mm**
Provdatum: 2017-04-24	**KC 50/50: 25/31kg/**	**Pelarlängd: 9,3m**
Projekt nr: 2015-4	**Sond: 500X15mm**	**Utförd Längd: 8,9m**

dmixab
dry soil mixing

B1807

Detaljer

Tid	Förare	LB	Totalt
3/28/2017 8:27	Johnny Rundqvist	9.2 m	242 kg
Kund	**Maskin**	**LS**	**Snitt**
NCC	M4	8.7 m	27.8 kg/m
Objekt	**Verktyg**	**Blandning**	**Marknivå**
AKALLALÄNKEN	PB600	KC50/50	0 m
Kilo i Botten	**Lutning X**	**Lutning Y**	**Tanktryck**
8	-0.1°	0.2°	5.5 bar

Diagram

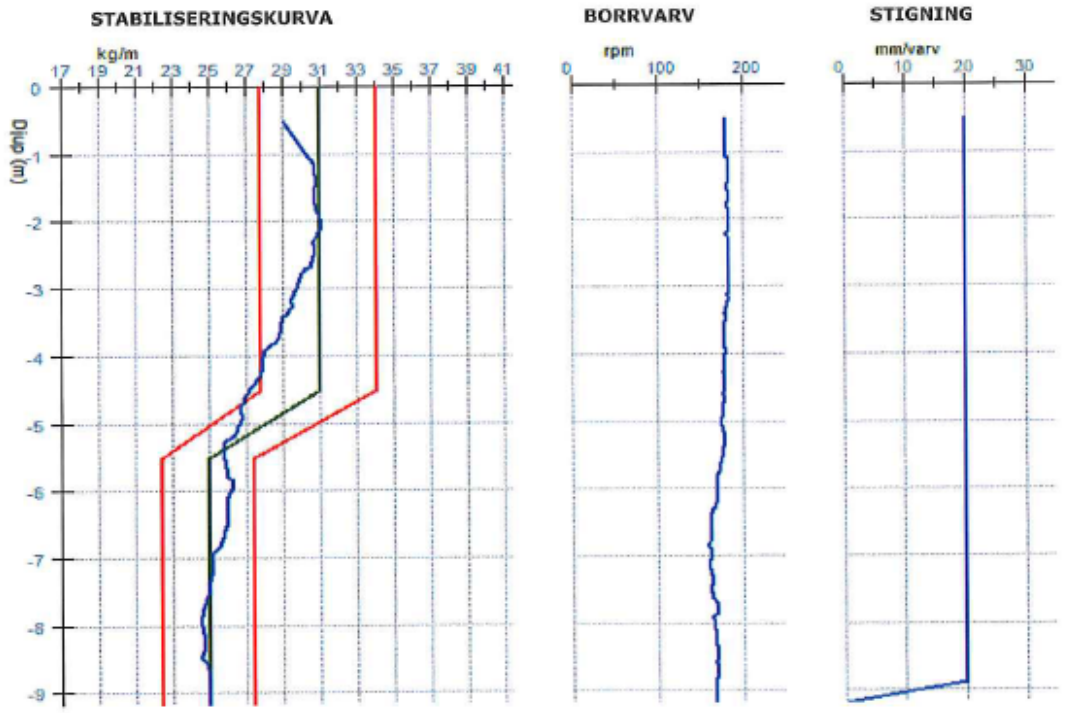

enska dmixab AB Katrinebergsgatan 23A 504 39 Borås
: 031-72 69 990 fax: 031-72 69 991
ww.dmixab.se
fo@dmixab.se
bankgiro: 5807-6373
orgnr: 556630-0314

NCC

Produktionskontroll 5 28-32 dygn
Akallalänken Huvudväg

Pelar nr: B1807
Koordinater **X: 6587749,160** **Y: 143655,927**

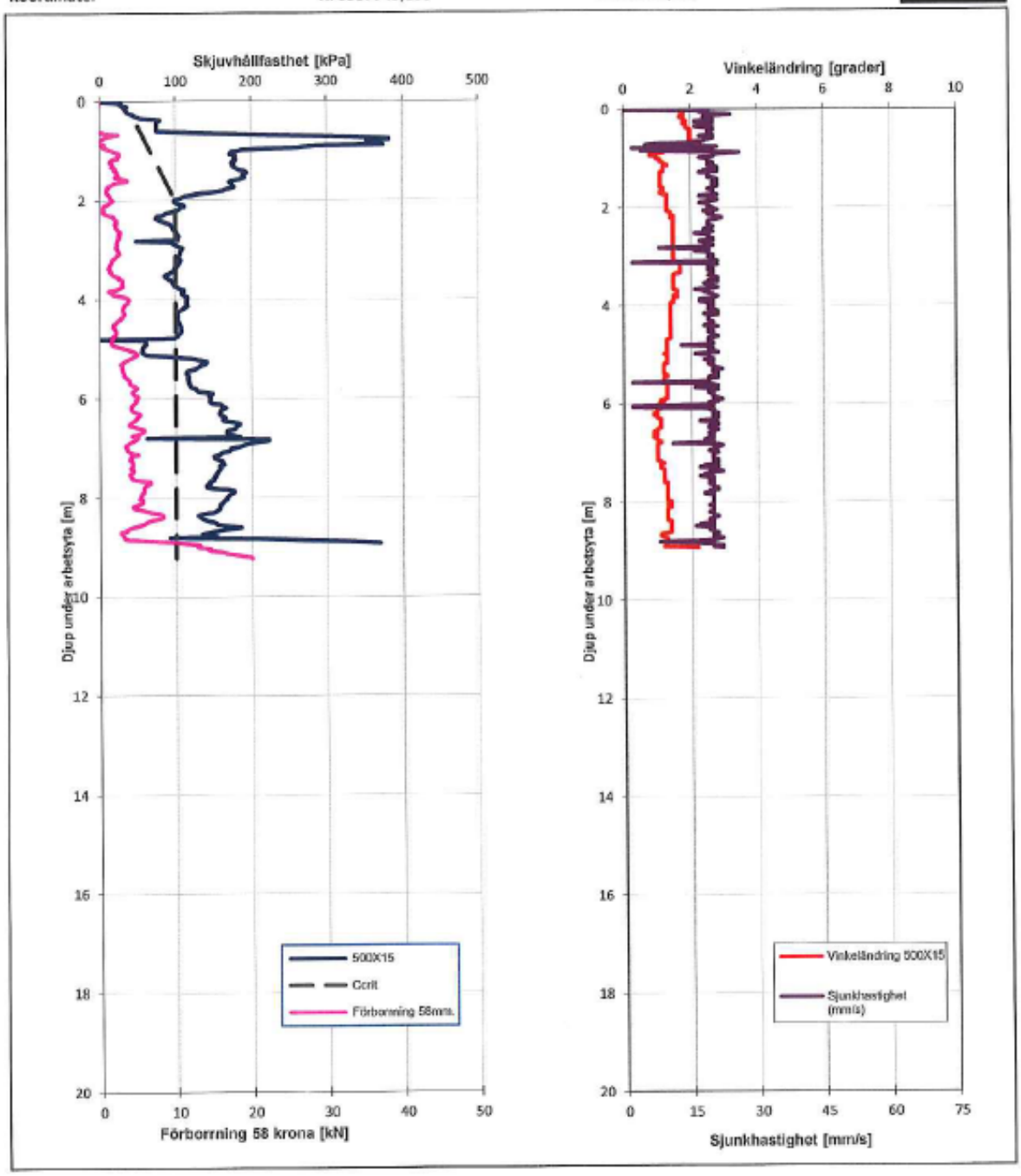

Pelar nr: B1807	**Verktyg: PB600**	**Stigning: 20mm/r**
Tillverkningsdatum: 2017-03-28	**Faktor: 12,5**	**Diameter: 600mm**
Provdatum: 2017-04-24	**KC 50/50: 25/31kg/**	**Pelarlängd: 9,2m**
Projekt nr: 2015-4	**Sond: 500X15mm**	**Utförd Längd: 8,9m**

dmixab
dry soil mixing

B1809

Detaljer

Tid	**Förare**	**LB**	**Totalt**
3/28/2017 8:20	Johnny Rundqvist	9.1 m	245 kg
Kund	**Maskin**	**LS**	**Snitt**
NCC	M4	8.6 m	28.4 kg/m
Objekt	**Verktyg**	**Blandning**	**Marknivå**
AKALLALÄNKEN	PB600	KC50/50	0 m
Kilo i Botten	**Lutning X**	**Lutning Y**	**Tanktryck**
8	-0.1°	0.0°	5.5 bar

Diagram

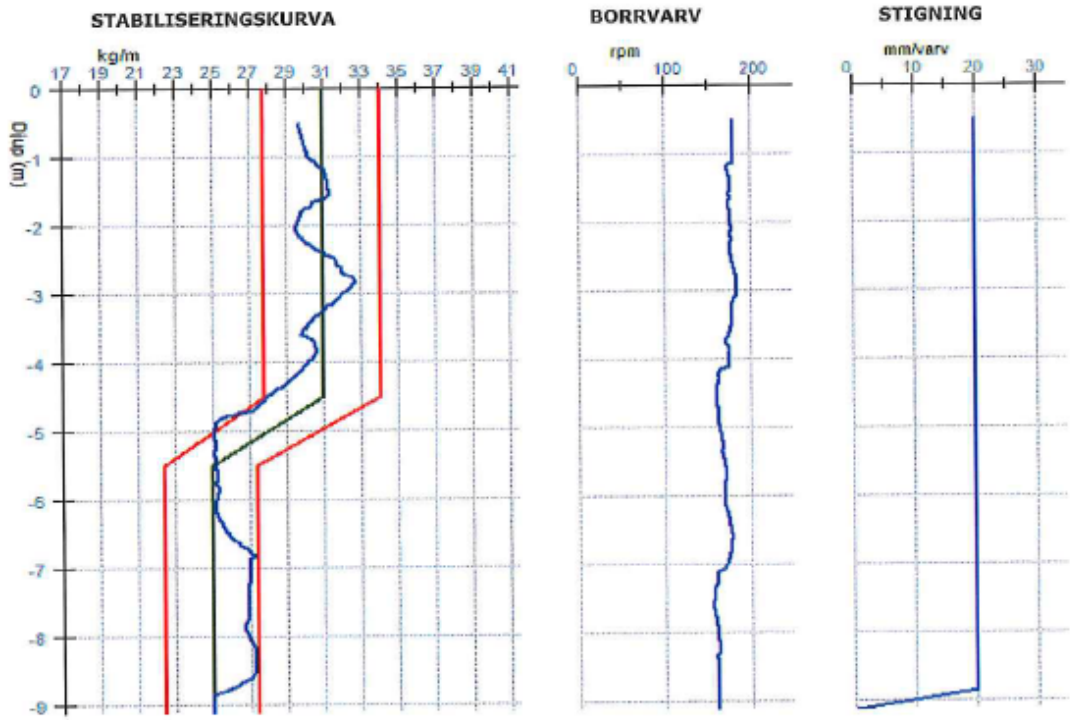

nska dmixab AB Katrinebergsgatan 23A 504 39 Borås
: 031-72 69 990 fax: 031-72 69 991
w.dmixab.se
o@dmixab.se
bankgiro: 5807-6373
orgnr: 556630-0314

NCC

Produktionskontroll 5 28-32 dygn
Akallalänken Huvudväg

Pelar nr: B1809
Koordinater X: 6587748,229 Y: 143657,698

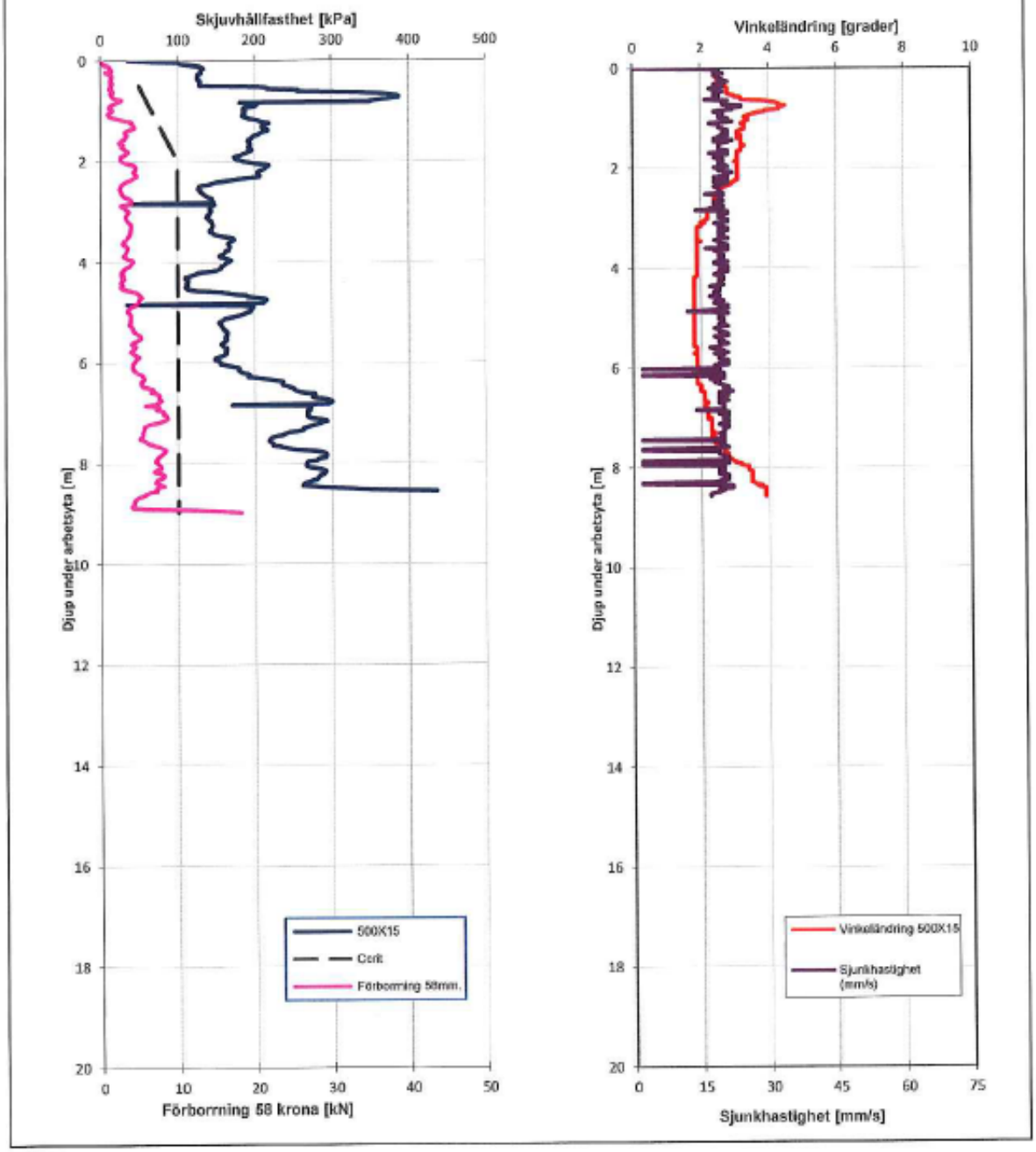

Pelar nr: B1809	Verktyg: PB600	Stigning: 20mm/r
Tillverkningsdatum: 2017-03-28	Faktor: 12,5	Diameter: 600mm
Provdatum: 2017-04-24	KC 50/50: 25/31kg/	Pelarlängd: 9,1m
Projekt nr: 2015-4	Sond: 500X15mm	Utförd Längd: 8,5m

NCC

Produktionskontroll 5 28-32 dygn
Akallalänken Huvudväg

Sammanfattande diagram 25/31 kg/m, 20mm/r

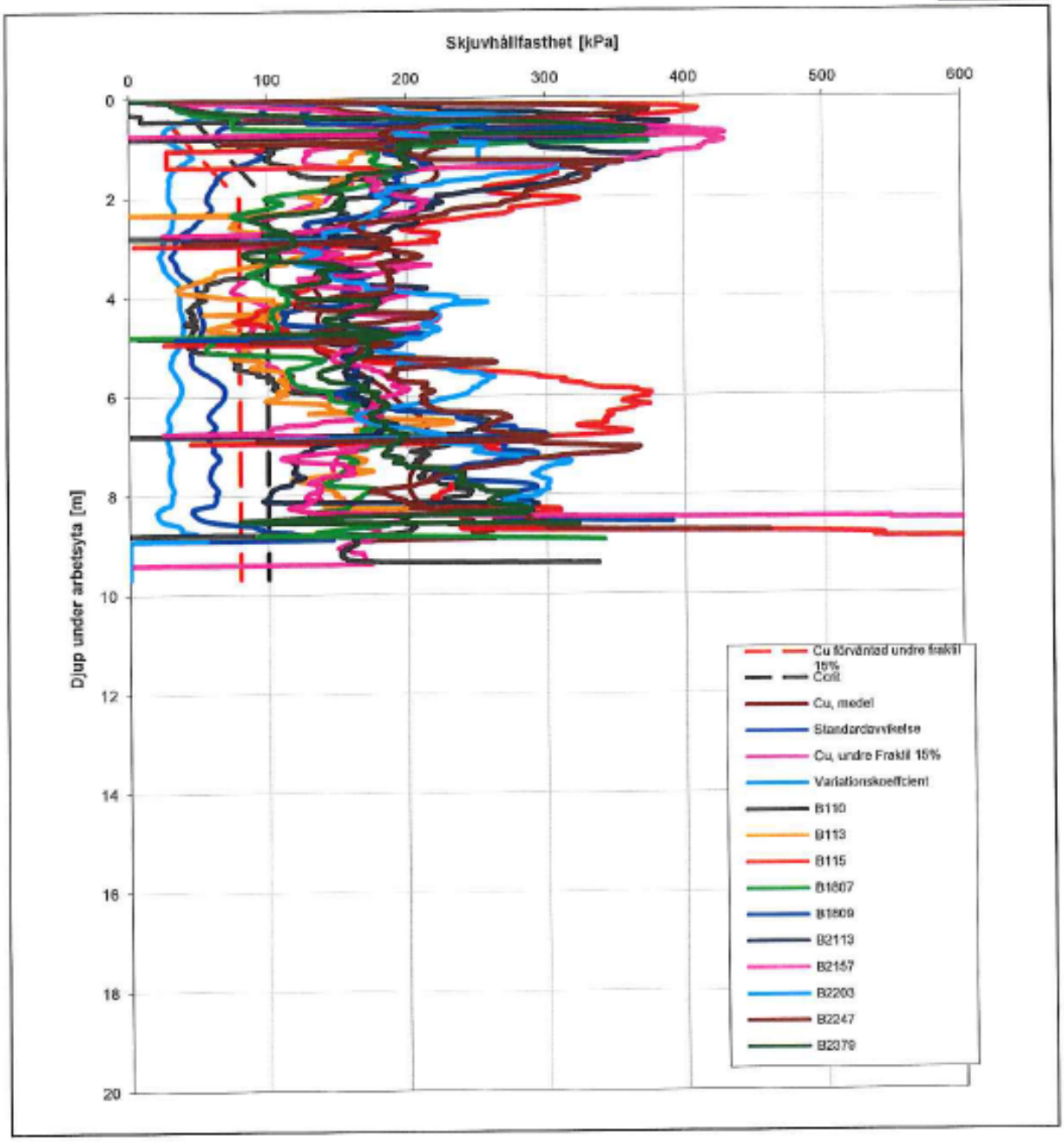

Tillverkningsdatum: 2017-03-28
Provdatum: 2017-04-24
Projekt nr: 2015-4
Pelarlängd: 8,7-9,8m

Verktyg: PB600
Faktor: 12,5
KC 50/50: 25/31kg/
Sond: 500X15mm

Stigning: 20mm/r
Diameter: 600mm

NCC

Produktionskontroll 0 28-32 dygn
Akallalänken Huvudväg

Sammanfattande diagram 25/31 kg/m, 20mm/r

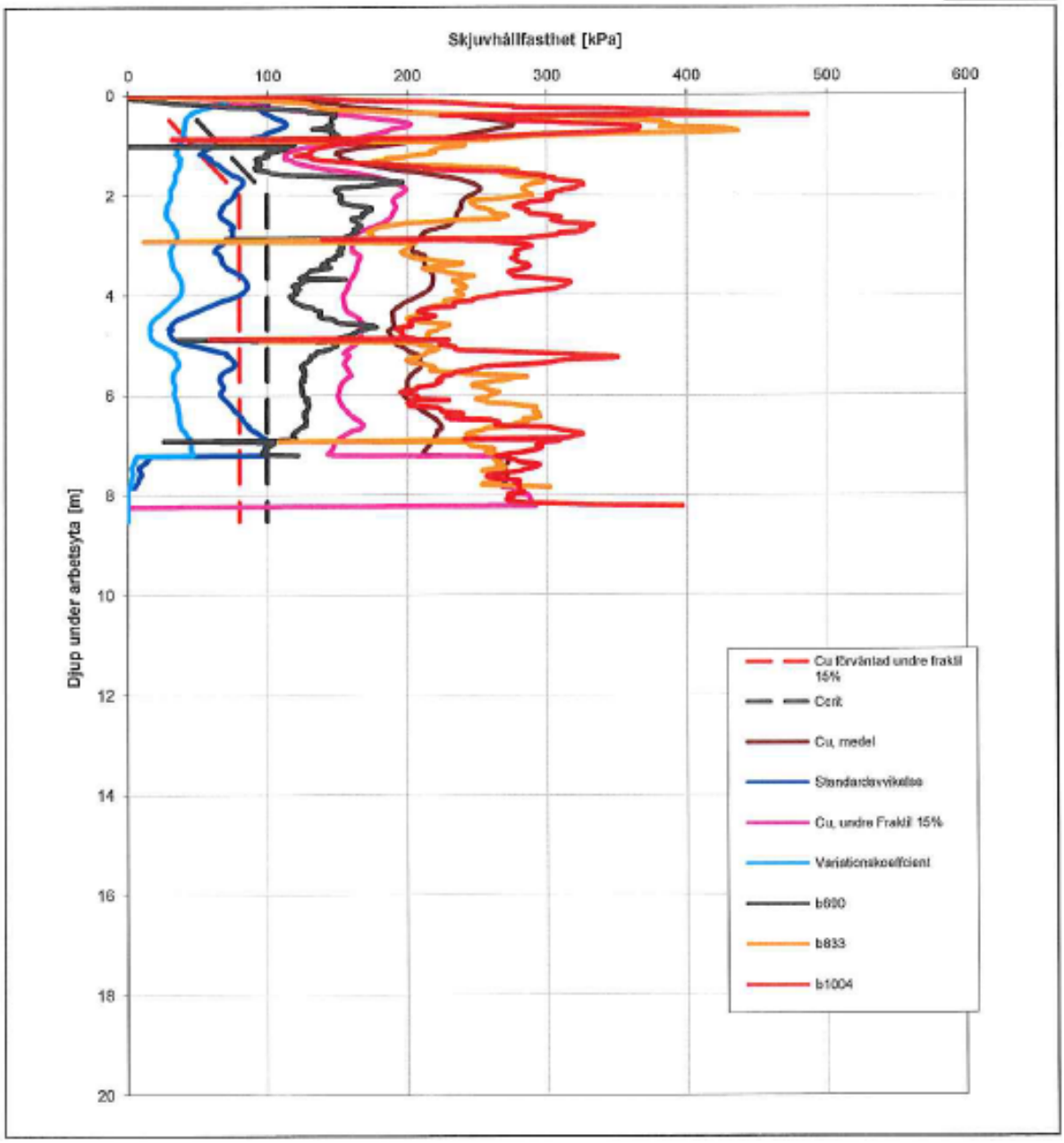

Tillverkningsdatum: 2017-04-03	Verktyg: PB600	Stigning: 20mm/r
Provdatum: 2017-05-02	Faktor: 12,5	Diameter: 600mm
Projekt nr: 2015-4	KC 50/50: 25/31kg/	
Pelarlängd: 7,7-8,1m	Sond: 500x15mm	

Appendix B

Analytical calculations and input parameters

B_1 Calculation of additional stress in Analytical Method_1

The additional stress of the block $\Delta\boldsymbol{\sigma_{LC}(z)}$ is calculated according to the principle described in Eq. 4.12, but in this case, it is considered in one-dimensional effects.

$$\Delta\sigma_{LC}(z) = (1-\eta_{LC}).\sigma(q,\mu_z.z) + \eta_{LC}.q \quad for\ z < L_{col} \quad and\ x < B/2$$

The depth reduction factor μ_z across the concrete trough calculated as: -

$$\mu_z = 1 - 0{,}4\left(\frac{B}{H}\right) = 1 - 0{,}4\left(\frac{20}{17}\right) = 0{,}53$$

Where B- half of the width of the improved area since it is symmetric H- depth of the soil layer.

The load distribution factor η_{LC} is depends on the stiffness of the LCC and the stiffness of the soil as expressed in Eq. 4.9:

$$\eta_{LC} = \left(\frac{L_{col}}{d}\right)^{\beta} with\ \beta = \frac{1}{\left(\frac{M_{block}}{M_{soil}}\right)^{0.1} - \left(\frac{M_{soil}}{M_{block}}\right)^{0.1}}$$

The stiffness of the soil and the column will vary with stress level, in principle the load distribution is calculated iteratively.

$$\beta = \frac{1}{\left(\frac{13945}{3152}\right)^{0.1} - \left(\frac{3152}{13945}\right)^{0.1}} = 3{,}3 \qquad \eta_{LC} = \left(\frac{10}{15}\right)^{3.3} = 0{,}2$$

The surface load at the bottom of the back fill under the trough is 56,5 kPa additional stress.

$$\Delta\sigma_{LC}(z) = 0.8 * 58.5 * I(0.53.z) + 0{,}2 * 58.5$$

To calculate the influence factor Eq. 2.33 is simplified according to the dimension of the area to be improved with B=40 m and x=20 m:

$$I = \left(\frac{2}{\pi}\right)\left[\frac{20z}{z^2+1600} + \operatorname{atan}\left(\frac{20}{z}\right)\right]$$

Calculation of depth of zone A

The depth of zone A can be calculated by using the principle described in section 4.2.1. The force equilibrium between part of the preloaded soil and the friction forced develop along the perimeter of the column will give a formula to find the depth of zone A. A pyramidal shape of the preloaded soil will act on the clay soil and the rest will act on the column. So, the equilibrium equation could be:

$$V_{pyr}.\gamma_{p.load} = \pi.d_c.c_u.d$$

$$d = \frac{\sqrt{3}(cc_{col} - d_c)^3.\gamma_{p.load}}{6.\pi.d_c.c_u}$$

Where: V_{pyr} volume of pyramidal shape of the preloaded soil, d is depth of zone A, cc_{col} is center to center distance of the column, d_c the diameter of the column, $\gamma_{p.load}$ is the unit weight of the preloaded soil and c_u undrained shear strength of the soil. In settlement calculation at section 27/180 kms for the input values $d_c = 0.6\,m$ $cc_{col} = 0.8\,m$ $\gamma_{p.load} = 18\,kN/m^3$ and $c_u = 10\,kN/m^2$ d obtained as 0,0022 m. This indicates that insufficient bridging effect is designed.

B_2 CRS test results extracted from MUR

The input parameters of the clay soil derived from field test results, which is included in the geotechnical investigation report. Some of the data's used for extraction of input parameters are attached in here.

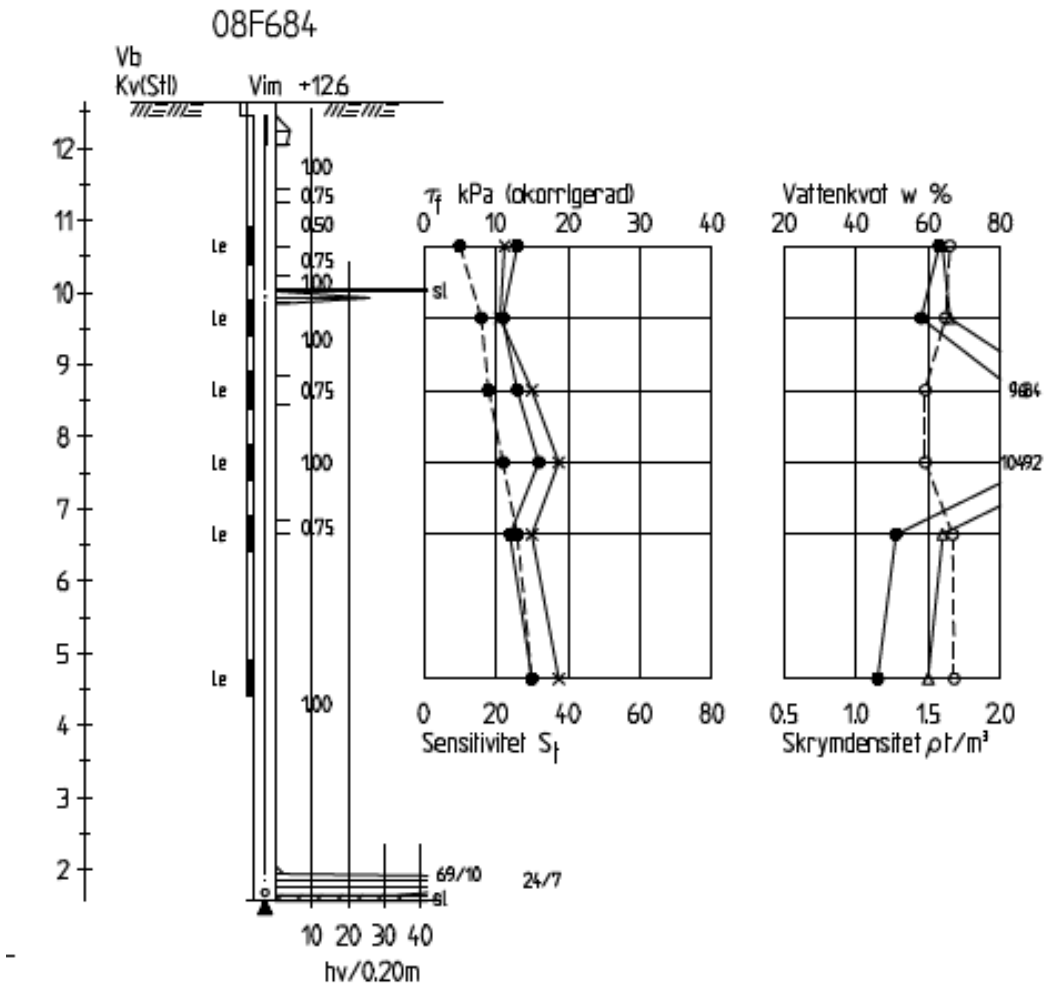
08F684
Vb
Kv(Stl)
Vim +12.6
12
11
10
9
8
7
6
5
4
3
2
1.00
0.75
0.50
0.75
1.00
1.00
0.75
1.00
0.75
1.00
Le
Le
Le
Le
Le
sl
τ_f kPa (okorrigerad)
0 10 20 30 40
Vattenkvot w %
20 40 60 80
9684
10492
0 20 40 60 80
Sensitivitet S_t
0.5 1.0 1.5 2.0
Skrymdensitet ρt/m³
69/10
24/7
sl
10 20 30 40
hv/0.20m

SWECO GEOLAB

Jordprovsanalys

Projekt **E4, Förbifart Stockholm, Del B–km 23/500–28/000**		
Uppdragsnummer	*Uppdragsgivare*	*Gransk./Tabell*
216 670-218	Konsortiet Förbifart Stockholm, Stockholm	*Löp-nr* 18780b
Provtagningsdatum	*Provtagningsredskap / Analysmetod*	*Datum/Sign* 2009-01-16
2009-01-12	Kv St I ø 50mm	*Undersökningsdatum* 2008-07-01 - 2009-01-16

Borrhål/ Sektion	Djup [m]	Benämning / (okulär jordartsklassificering enl. SGF 1981) Jordartsförkortning (enl. SGF/BGS Beteckningssystem 2001:1)	Densitet ρ [t/m³]	Vattenkvot w [%]	Konflytgräns w_L [%]	Sensitivitet S_t	Skjuvhållf.h. τ_{fu} [kPa] 1)	Tjälf. klass/ mtrl typ 2)	Anm
08F684	2.0	Brungrå varvig lera med roströr, vLe	1,65	64	63	10	13	3/4b	
	3.0	Brungrå varvig lera, vLe	1,62	66	58	16	11	3/4b	
	4.0	Brungrå varvig lera, vLe	1,48	96	84	18	13	3/4b	
	5.0	Grå varvig lera, vLe	1,48	104	92	22	16	3/4b	
	6.0	Brungrå varvig lera med enstaka sulfidband, vLe(su)	1,67	64	51	26	12	3/4b	
	8.0	Brungrå varvig lera med enstaka sulfidband, vLe(su) (Referensnivå = My) (Vy = 0.30 m under my 2009-01-12)	1,68	60	46	30	15	3/4b	

1) Okorrigerat värde. Korrigeringen rekommenderas enl. SGF-INFO nr 3
2) Klassning enl. ATB VÄG 2004, VV Publ. 2004:111.

SWECO GEOLAB

Redovisning av ödometerförsök, CRS-försök

Projekt: **E4, Förbifart Stockholm, Del B-km 23/500-28/000**		
Uppdragsnummer: 216670-218	*Uppdragsgivare:* Konsortiet Förbifart Stockholm, Stockholm	*Datum/Sign:* 2009-02-10 *Löp-nr/Gransk.:* 18780b
Sektion/borrhål: 08F684 *Densitet:* 1,65 t/m^3 *Vattenkvot:* 64 % *Benämning:* Varvig lera med rosttrör	*Djup:* 2,0 m *Provningstemp.:* 20 °C	*Ödometer nr:* 4 *Provdiameter:* 50 mm *Provhöjd:* 20 mm *Def.hastighet:* 0,75 %/h

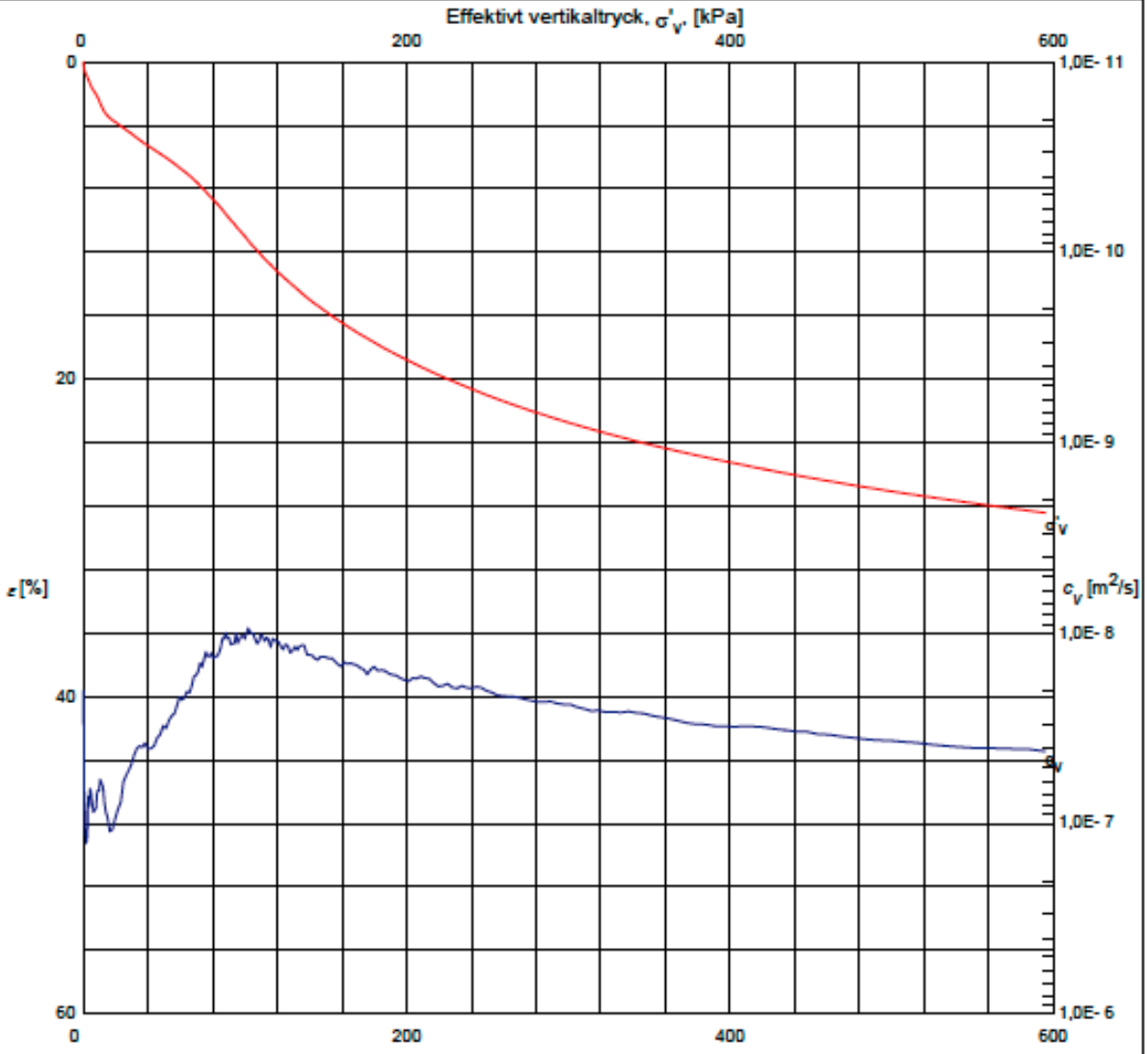

Försöket är utfört och utvärderat enligt Svensk Standard SS 027126. Vid utvärdering av c_v och k har korrektion utförts så att värdena motsvarar en temperatur av 7 °C. Utrustningens egendeformation är beaktad. För utvärdering se bilagda diagram sid 2 - 4.

σ'_c, kPa	M_L, kPa	σ'_L, kPa	M'	$c_{v,\,min}$, m^2/s	k_l, m/s	β_k
66	844	100	13,8	9,6E-9	2,2E-10	2,1

Anm.

SWECO GEOLAB, Gjörwellsgatan 22, Box 34044
100 26 STOCKHOLM, Tel: 08-695 60 00, Fax: 08-695 63 60
geolab@sweco.se, www.sweco.se/geolab, ingår i SWECO VBB AB

P:\2172\Uppdrag 2009\18780b\b09_126.txt 2009-02-13

SWECO

1 (4)

SWECO GEOLAB

Utvärdering av modultal och kontroll av portryck

Projekt: **E4, Förbifart Stockholm, Del B-km 23/500-28/000**		
Uppdragsnummer: 216670-218	*Uppdragsgivare:* Konsortiet Förbifart Stockholm, Stockholm	*Datum/Sign:* 2009-02-10 *Löp-nr/Gransk.:* 18780b
Sektion/borrhål: 08F684 *Densitet:* 1,65 t/m^3 *Vattenkvot:* 64 % *Benämning:* Varvig lera med roströr	*Djup:* 2,0 m *Provningstemp.:* 20 °C	*Odometer nr:* 4 *Provdiameter:* 50 mm *Provhöjd:* 20 mm *Def.hastighet:* 0,75 %/h

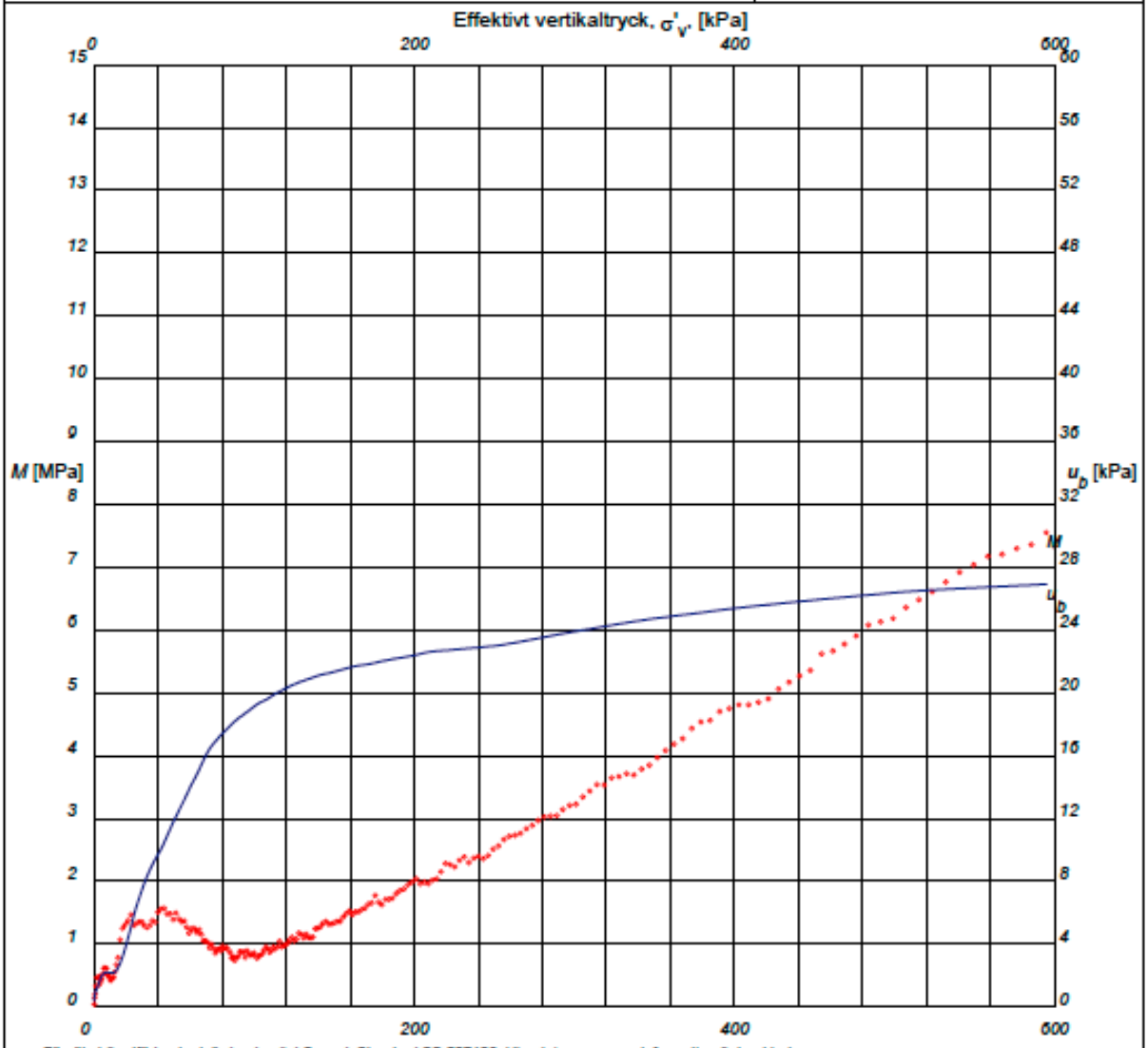

Försöket är utfört och utvärderat enligt Svensk Standard SS 027126. Utrustningens egendeformation är beaktad.

M'	σ'L, kPa
13,8	100

Anm.

SWECO GEOLAB, Gjörwellsgatan 22, Box 34044
100 26 STOCKHOLM, Tel: 08-695 60 00, Fax: 08-695 63 60
geolab@sweco.se, www.sweco.se/geolab, Ingår i SWECO VBB AB

P:\2172\Uppdrag 2009\18780b\b09_126.txt 2009-02-13

SWECO

2 (4)

SWECO GEOLAB

Utvärdering av permeabilitet

Projekt: **E4, Förbifart Stockholm, Del B-km 23/500-28/000**		
Uppdragsnummer: 216670-218	*Uppdragsgivare:* Konsortiet Förbifart Stockholm, Stockholm	*Datum/Sign:* 2009-02-10 *Löp-nr/Gransk.:* 18780b
Sektion/borrhål: 08F684 *Densitet:* 1,65 t/m^3 *Vattenkvot:* 64 % *Benämning:* Varvig lera med roströr	*Djup:* 2,0 m *Provningstemp.:* 20 ^{o}C	*Ödometer nr:* 4 *Provdiameter:* 50 mm *Provhöjd:* 20 mm *Def.hastighet:* 0,75 %/h

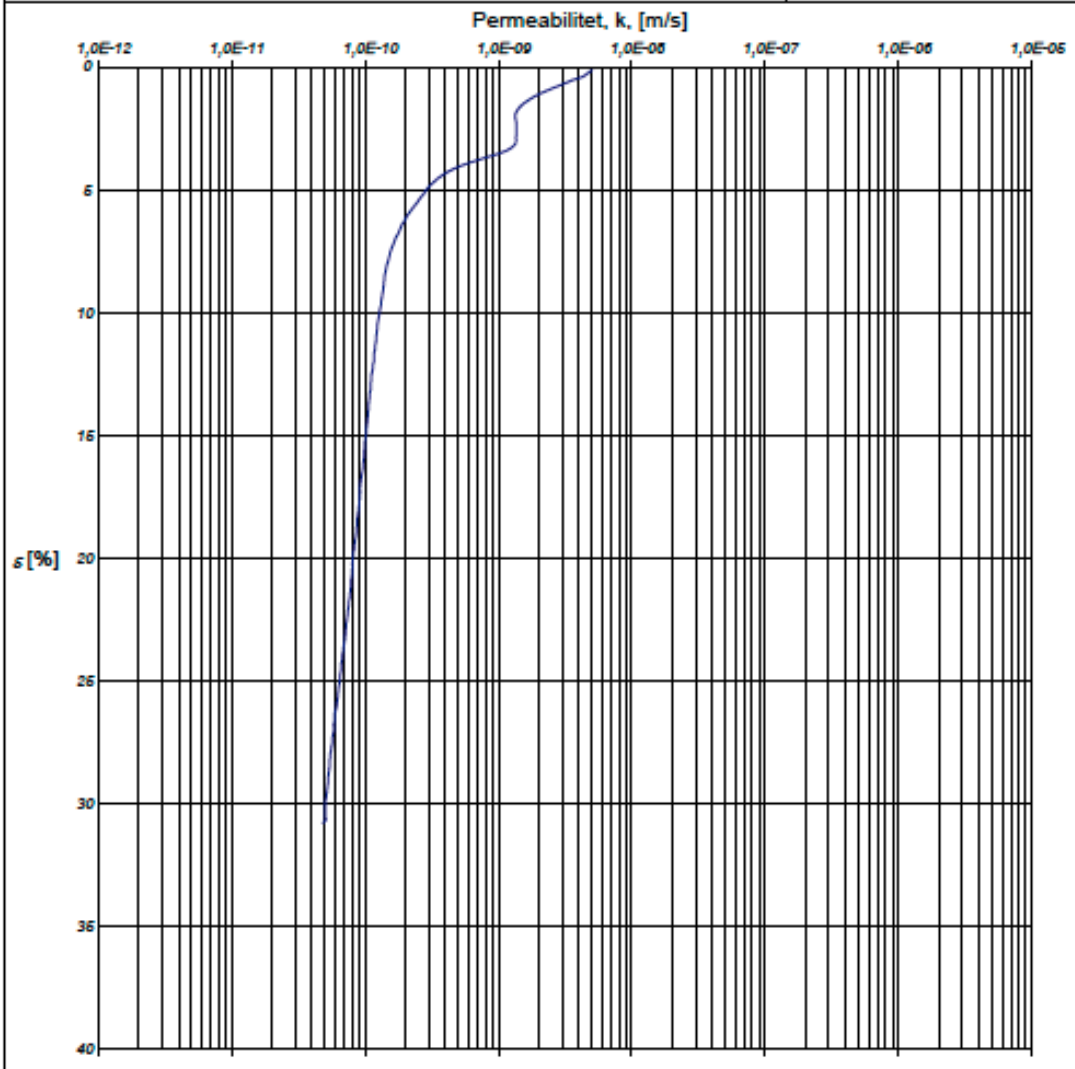

Försöket är utfört och utvärderat enligt Svensk Standard SS 027126. Vid utvärdering av permeabiliteten k har korrektion utförts så att värdena motsvarar en temperatur av 7 ^{o}C.

k_I, m/s	β_k
2,2E-10	2,1

Anm.

SWECO GEOLAB, Gjörwellsgatan 22, Box 34044
100 26 STOCKHOLM, Tel: 08-695 60 00, Fax: 08-695 63 60
geolab@sweco.se, www.sweco.se/geolab, ingår i SWECO VBB AB

P:\2172\Uppdrag 2009\18780b\b09_126.txt 2009-02-13

SWECO

3 (4)

SWECO GEOLAB

Utvärdering av förkonsolideringstryck och linjär modul

Projekt: **E4, Förbifart Stockholm, Del B-km 23/500-28/000**		
Uppdragsnummer: 216670-218	*Uppdragsgivare:* Konsortiet Förbifart Stockholm, Stockholm	*Datum/Sign:* 2009-02-10 *Löp-nr/Gransk.:* 18780b
Sektion/borrhål: 08F684 *Densitet:* 1,65 t/m^3 *Vattenkvot:* 64 % *Benämning:* Varvig lera med roströr	*Djup:* 2,0 m *Provningstemp.:* 20 °C	*Ödometer nr:* 4 *Provdiameter:* 50 mm *Provhöjd:* 20 mm *Def.hastighet:* 0,75 %/h

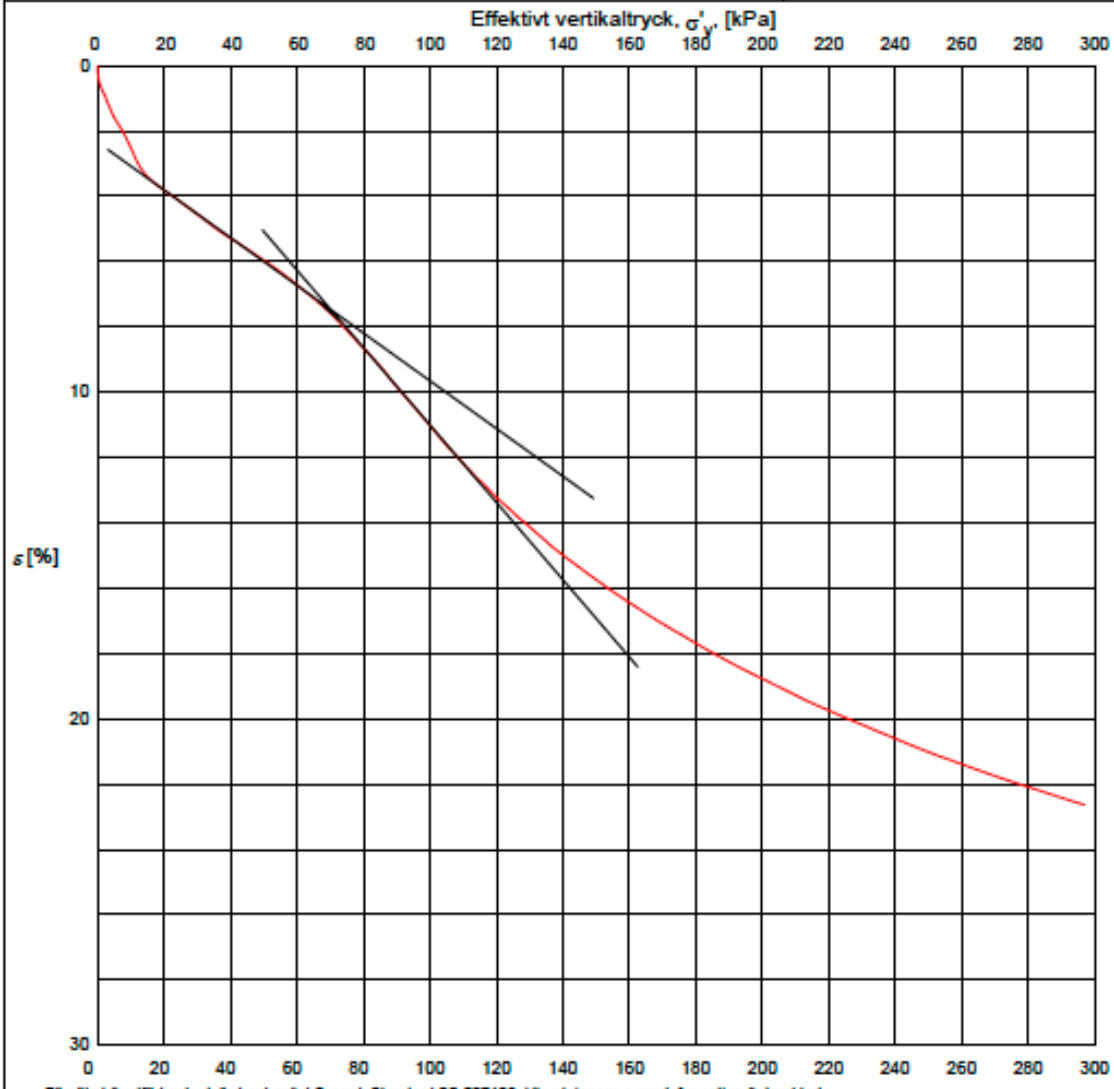

Försöket är utfört och utvärderat enligt Svensk Standard SS 027126. Utrustningens egendeformation är beaktad.

σ'_C, kPa	M_L, kPa	σ'_L, kPa
66	844	100

Anm.

SWECO GEOLAB, Gjörwellsgatan 22, Box 34044
100 26 STOCKHOLM, Tel: 08-695 60 00, Fax: 08-695 63 60
geolab@sweco.se, www.sweco.se/geolab, ingår i SWECO VBB AB

P:\2172\Uppdrag 2009\18780b\b09_126.txt 2009-02-13

SWECO

4 (4)

SWECO GEOLAB

Redovisning av ödometerförsök, CRS-försök

Projekt: **E4, Förbifart Stockholm, Del B-km 23/500-28/000**		
Uppdragsnummer: 216 670-218	*Uppdragsgivare:* Konsortiet Förbifart STockholm, Stockholm	*Datum/Sign:* 2009-02-05 *Löp-nr/Gransk.:* 18780b
Sektion/borrhål: 08F684 *Densitet:* 1,62 t/m^3 *Vattenkvot:* 66 % *Benämning:* Varvig lera	*Djup:* 3,0 m *Provningstemp.:* 20 °C	*Ödometer nr:* 2 *Provdiameter:* 50 mm *Provhöjd:* 20 mm *Def.hastighet:* 0,72 %/h

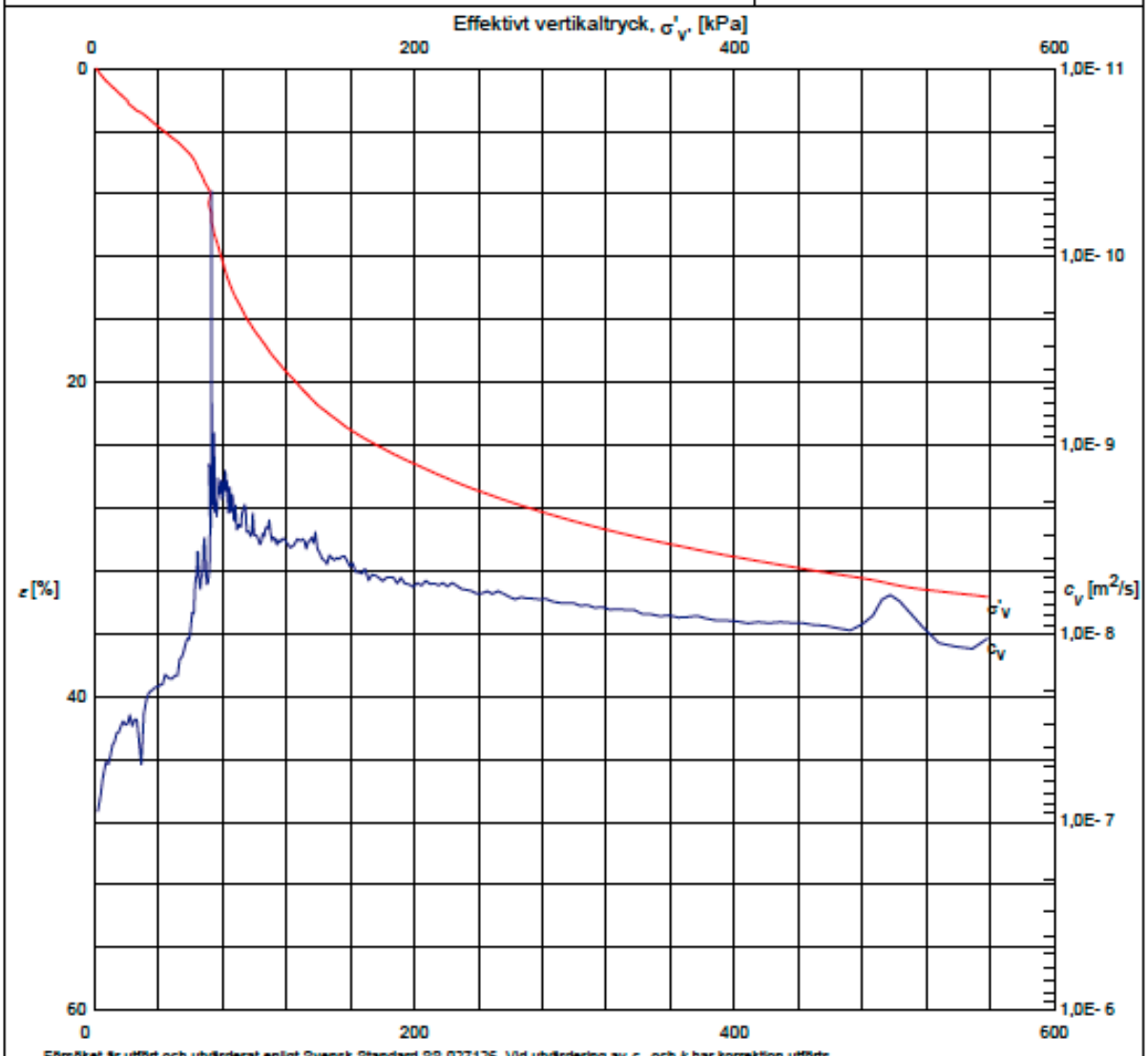

Försöket är utfört och utvärderat enligt Svensk Standard SS 027126. Vid utvärdering av c_v och k har korrektion utförts så att värdena motsvarar en temperatur av 7 °C. Utrustningens egendeformation är beaktad. För utvärdering se bilagda diagram sid 2 - 4.

σ'_C, kPa	M_L, kPa	σ'_L, kPa	M'	$c_{v,\,min}$, m^2/s	k_l, m/s	β_k
60	255	72	15,4	1,7E-9	1,8E-10	3,4

Anm.

SWECO GEOLAB, Gjörwellsgatan 22, Box 34044
100 26 STOCKHOLM, Tel: 08-695 60 00, Fax: 08-695 63 60
geolab@sweco.se, www.sweco.se/geolab, Ingår i SWECO VBB AB

P:\2172\Uppdrag 2006\18780b\b09_113.txt 2009-02-11

SWECO

1 (4)

SWECO GEOLAB

Utvärdering av modultal och kontroll av portryck

Projekt: **E4, Förbifart Stockholm, Del B-km 23/500-28/000**		
Uppdragsnummer: 216 670-218	*Uppdragsgivare:* Konsortiet Förbifart STockholm, Stockholm	*Datum/Sign:* 2009-02-05 *Löp-nr/Gransk.:* 18780b
Sektion/borrhål: 08F684 *Densitet:* 1,62 t/m^3 *Vattenkvot:* 66 % *Benämning:* Varvig lera	*Djup:* 3,0 m *Provningstemp.:* 20 °C	*Ödometer nr:* 2 *Provdiameter:* 50 mm *Provhöjd:* 20 mm *Def.hastighet:* 0,72 %/h

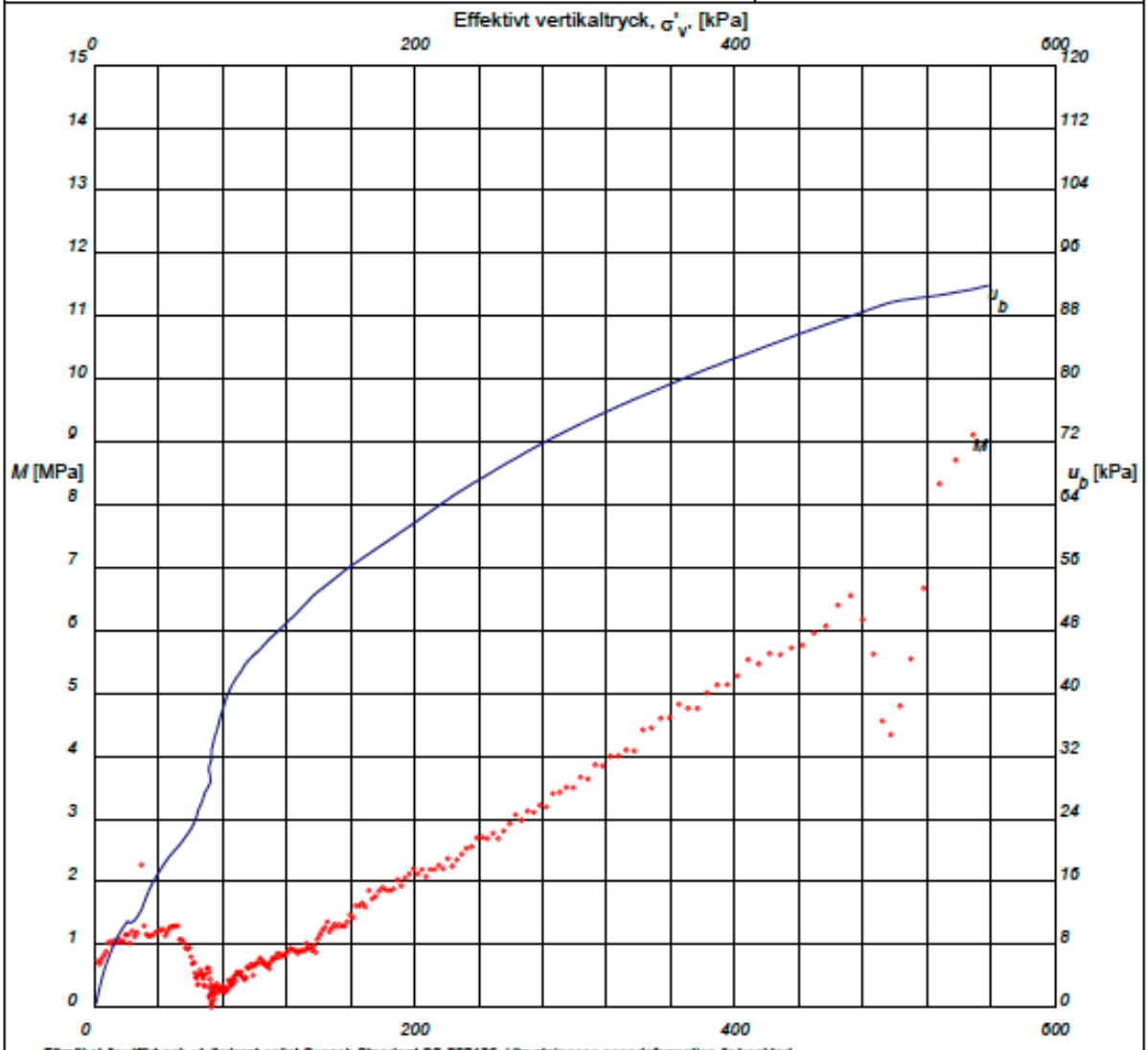

Försöket är utfört och utvärderat enligt Svensk Standard SS 027126. Utrustningens egendeformation är beaktad.

M'	σ'L, kPa
15,4	72

Anm.

SWECO GEOLAB, Globenvägen 22, Box 34044
100 26 STOCKHOLM, Tel: 08-695 60 00, Fax: 08-695 63 60
geolab@sweco.se, www.sweco.se/geolab, Ingår i SWECO VBB AB

P:\2172\Uppdrag 2006\18780b\b09_113.txt 2009-02-11

SWECO

2 (4)

SWECO GEOLAB

Utvärdering av permeabilitet

Projekt: **E4, Förbifart Stockholm, Del B-km 23/500-28/000**		
Uppdragsnummer:	*Uppdragsgivare:*	*Datum/Sign:* 2009-02-05
216 670-218	Konsortiet Förbifart STockholm, Stockholm	*Löp-nr/Gransk.:* 18780b
Sektion/borrhål: 08F684	*Djup:* 3,0 m	*Ödometer nr:* 2
Densitet: 1,62 t/m^3 *Vattenkvot:* 66 %	*Provningstemp.:* 20 ^{o}C	*Provdiameter:* 50 mm
Benämning: Varvig lera		*Provhöjd:* 20 mm
		Def.hastighet: 0,72 %/h

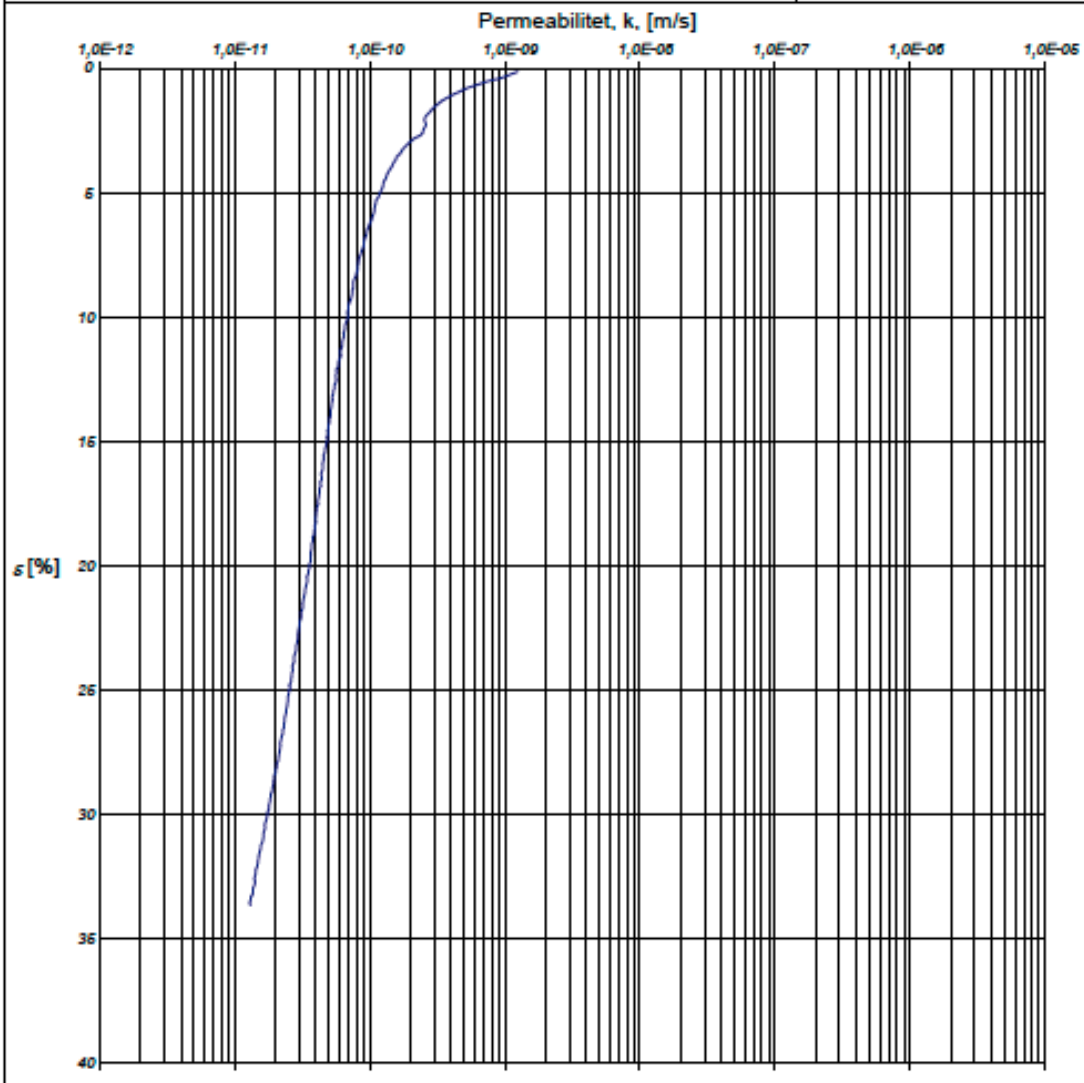

Försöket är utfört och utvärderat enligt Svensk Standard SS 027126. Vid utvärdering av permeabiliteten k har korrektion utförts så att värdena motsvarar en temperatur av 7 ^{o}C.

k_I, m/s	β_k
1,8E-10	3,4

Anm.

SWECO GEOLAB, Gjörwellsgatan 22, Box 34044
100 26 STOCKHOLM, Tel: 08-695 60 00, Fax: 08-695 63 60
geolab@sweco.se, www.sweco.se/geolab, ingår i SWECO VBB AB

P:\2172\Uppdrag 2006\18780b\b09_113.txt 2009-02-11

SWECO

3 (4)

SWECO GEOLAB

Utvärdering av förkonsolideringstryck och linjär modul

Projekt: **E4, Förbifart Stockholm, Del B-km 23/500-28/000**		
Uppdragsnummer: 216 670-218	*Uppdragsgivare:* Konsortiet Förbifart STockholm, Stockholm	*Datum/Sign:* 2009-02-05 *Löp-nr/Gransk.:* 18780b
Sektion/borrhål: 08F684 *Densitet:* 1,62 t/m^3 *Vattenkvot:* 66 % *Benämning:* Varvig lera	*Djup:* 3,0 m *Provningstemp.:* 20 °C	*Ödometer nr:* 2 *Provdiameter:* 50 mm *Provhöjd:* 20 mm *Def.hastighet:* 0,72 %/h

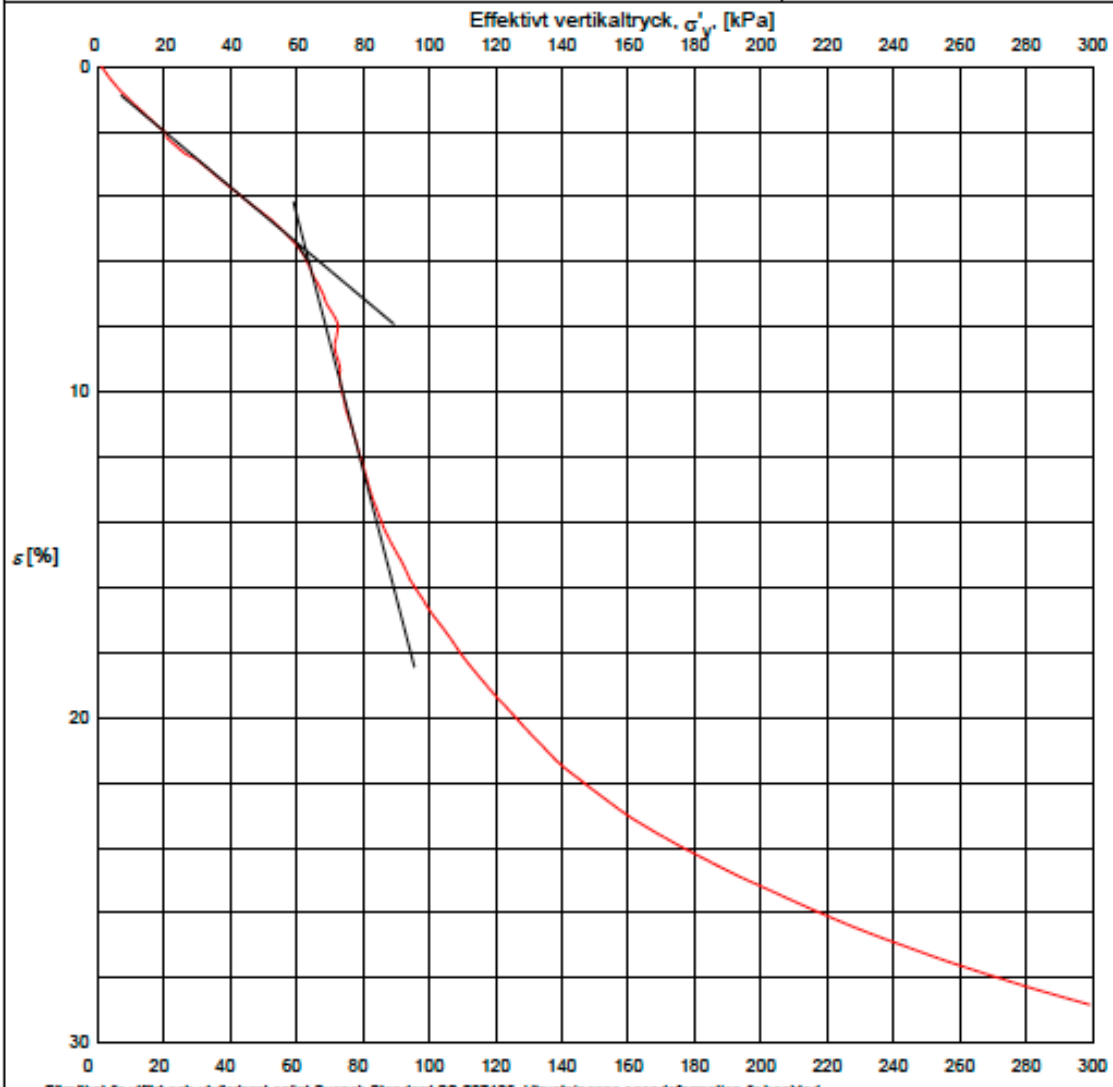

Försöket är utfört och utvärderat enligt Svensk Standard SS 027126. Utrustningens egendeformation är beaktad.

σ'_C, kPa	M_L, kPa	σ'_L, kPa
60	255	72

Anm.

SWECO GEOLAB, Gjörwellsgatan 22, Box 34044
100 26 STOCKHOLM, Tel: 08-695 60 00, Fax: 08-695 63 60
geolab@sweco.se, www.sweco.se/geolab, ingår i SWECO VBB AB

P:\2172\Uppdrag 2006\18780b\b09_113.txt 2009-02-11

SWECO

4 (4)

SWECO GEOLAB

Redovisning av ödometerförsök, CRS-försök

Projekt: **E4 Förbifart Stockholm, Del B-km 23/500-28/000**		
Uppdragsnummer: 216670-218	*Uppdragsgivare:* Konsortiet Förbifart Stockholm, Stockholm	*Datum/Sign:* 2009-02-09 *Löp-nr/Gransk.:* 18780b
Sektion/borrhål: 08F684	*Djup:* 4,0 m	*Ödometer nr:* 1
Densitet: 1,48 t/m^3 *Vattenkvot:* 96 %	*Provningstemp.:* 20 °C	*Provdiameter:* 50 mm
Benämning: Varvig lera		*Provhöjd:* 20 mm *Def.hastighet:* 0,74 %/h

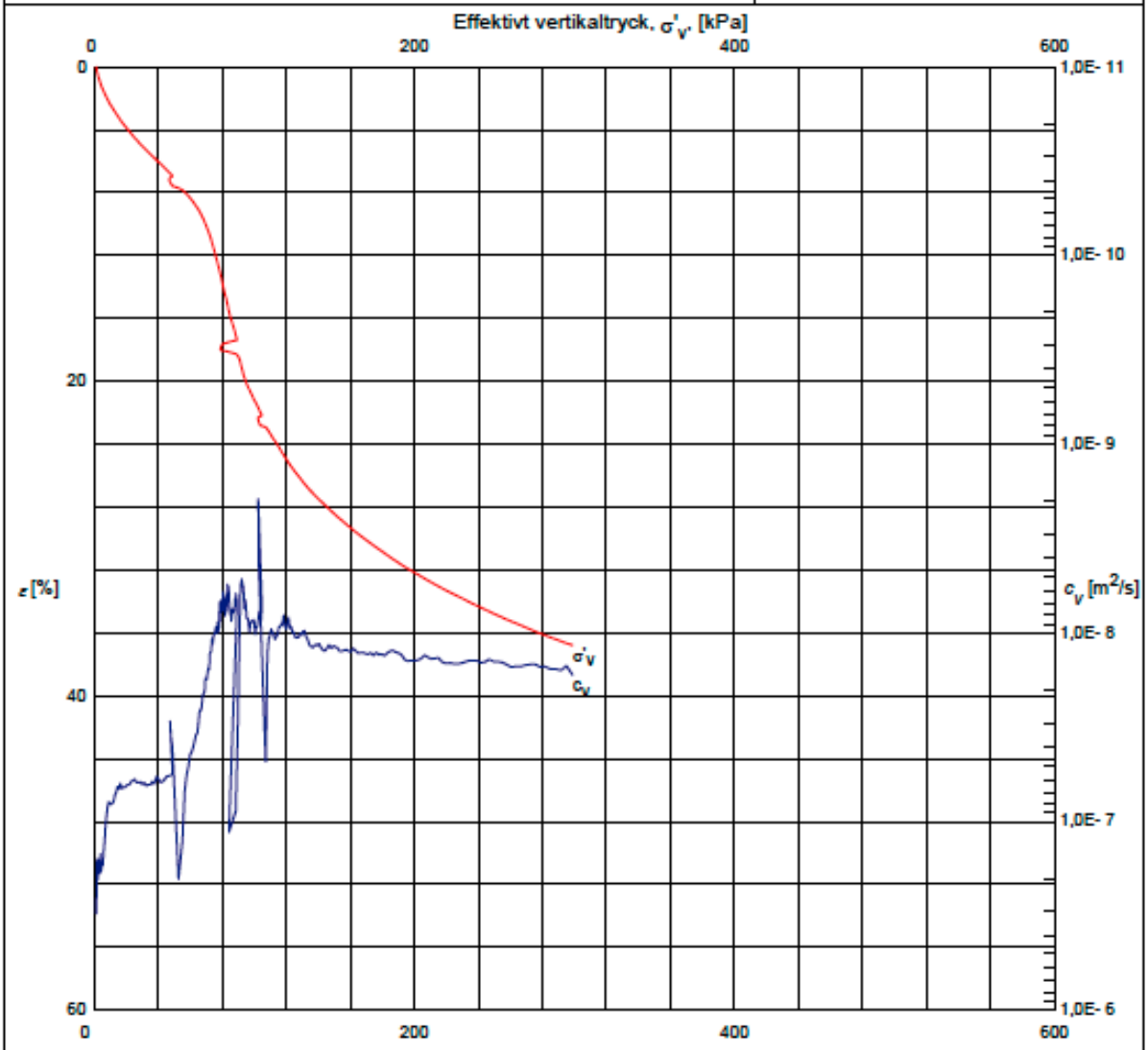

Försöket är utfört och utvärderat enligt Svensk Standard SS 027126. Vid utvärdering av c_v och k har korrektion utförts så att värdena motsvarar en temperatur av 7 °C. Utrustningens egendeformation är beaktad. För utvärdering se bilagda diagram sid 2 - 4.

σ'_C, kPa	M_L, kPa	σ'_L, kPa	M'	$c_{v,\,min}$ m^2/s	k_l, m/s	β_k
63	228	74	11,6	6,7E-9	8,8E-10	3,2

Anm.

SWECO GEOLAB, Gjörwellsgatan 22, Box 34044
100 26 STOCKHOLM, Tel: 08-695 60 00, Fax: 08-695 63 60
geolab@sweco.se, www.sweco.se/geolab, Ingår i SWECO VBB AB

P:\2172\Uppdrag 2006\216760bla09_139.txt 2009-02-11

SWECO

1 (4)

SWECO GEOLAB

Utvärdering av modultal och kontroll av portryck

Projekt: **E4 Förbifart Stockholm, Del B-km 23/500-28/000**		
Uppdragsnummer: 216670-218	*Uppdragsgivare:* Konsortiet Förbifart Stockholm, Stockholm	*Datum/Sign:* 2009-02-09 *Löp-nr/Gransk.:* 18780b
Sektion/borrhål: 08F684 *Densitet:* 1,48 t/m^3 *Vattenkvot:* 96 % *Benämning:* Varvig lera	*Djup:* 4,0 m *Provningstemp.:* 20 °C	*Odometer nr:* 1 *Provdiameter:* 50 mm *Provhöjd:* 20 mm *Def.hastighet:* 0,74 %/h

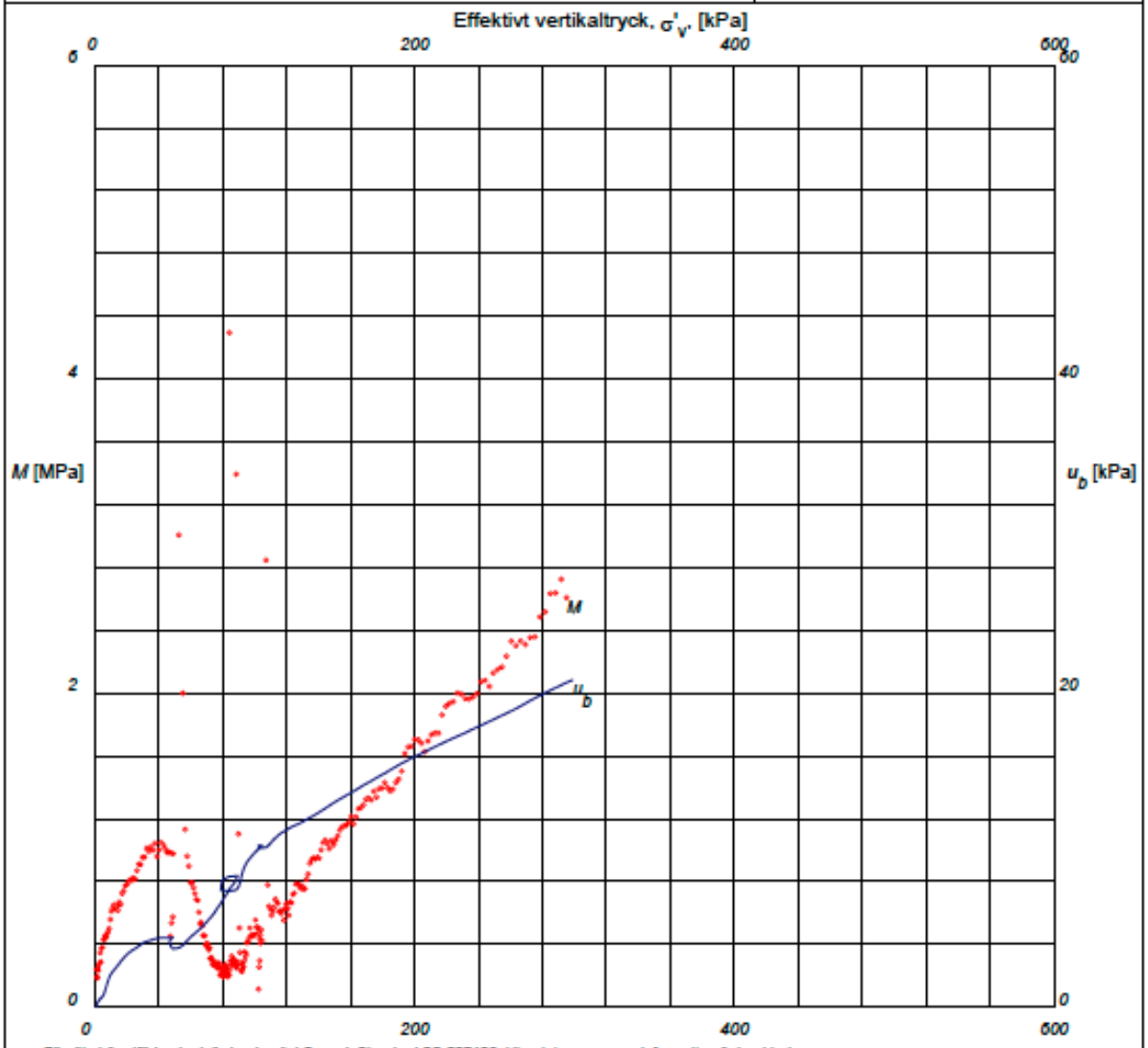

Försöket är utfört och utvärderat enligt Svensk Standard SS 027126. Utrustningens egendeformation är beaktad.

M'	σ'L, kPa
11,6	74

Anm.

SWECO GEOLAB, Gjörwellsgatan 22, Box 34044
100 26 STOCKHOLM, Tel: 08-695 60 00, Fax: 08-695 63 60
geolab@sweco.se, www.sweco.se/geolab, Ingår i SWECO VBB AB

P:\2172\Uppdrag 2006\18780b\a09_139.txt 2009-02-11

SWECO

2 (4)

SWECO GEOLAB

Utvärdering av permeabilitet

Projekt: **E4 Förbifart Stockholm, Del B-km 23/500-28/000**		
Uppdragsnummer: 216670-218	*Uppdragsgivare:* Konsortiet Förbifart Stockholm, Stockholm	*Datum/Sign:* 2009-02-09 *Löp-nr/Gransk.:* 18780b
Sektion/borrhål: 08F684 *Densitet:* 1,48 t/m^3 *Vattenkvot:* 96 % *Benämning:* Varvig lera	*Djup:* 4,0 m *Provningstemp.:* 20 °C	*Ödometer nr:* 1 *Provdiameter:* 50 mm *Provhöjd:* 20 mm *Def.hastighet:* 0,74 %/h

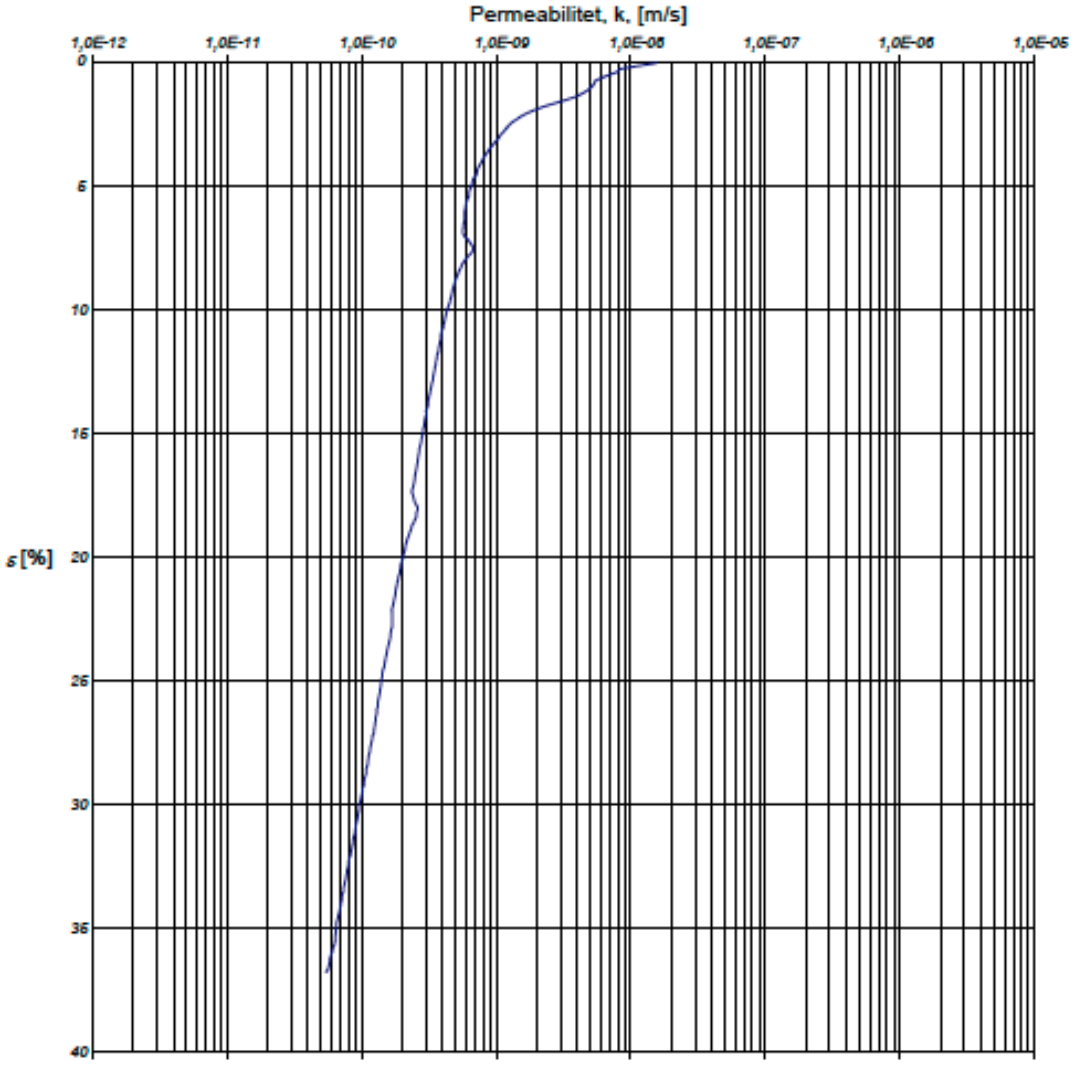

Försöket är utfört och utvärderat enligt Svensk Standard SS 027126. Vid utvärdering av permeabiliteten k har korrektion utförts så att värdena motsvarar en temperatur av 7 °C.

k_I , m/s	β_k
8,8E-10	3,2

Anm.

SWECO GEOLAB, Gjörwellsgatan 22, Box 34044
100 26 STOCKHOLM, Tel: 08-695 60 00, Fax: 08-695 63 60
geolab@sweco.se, www.sweco.se/geolab, Ingår i SWECO VBB AB

P:\2172\Uppdrag 2006\18780b\a09_139.txt 2009-02-11

SWECO

3 (4)

SWECO GEOLAB

Utvärdering av förkonsolideringstryck och linjär modul

Projekt: **E4 Förbifart Stockholm, Del B-km 23/500-28/000**		
Uppdragsnummer: 216670-218	*Uppdragsgivare:* Konsortiet Förbifart Stockholm, Stockholm	*Datum/Sign:* 2009-02-09 *Löp-nr/Gransk.:* 18780b
Sektion/borrhål: 08F684 *Densitet:* 1,48 t/m^3 *Vattenkvot:* 96 % *Benämning:* Varvig lera	*Djup:* 4,0 m *Provningstemp.:* 20 °C	*Ödometer nr:* 1 *Provdiameter:* 50 mm *Provhöjd:* 20 mm *Def.hastighet:* 0,74 %/h

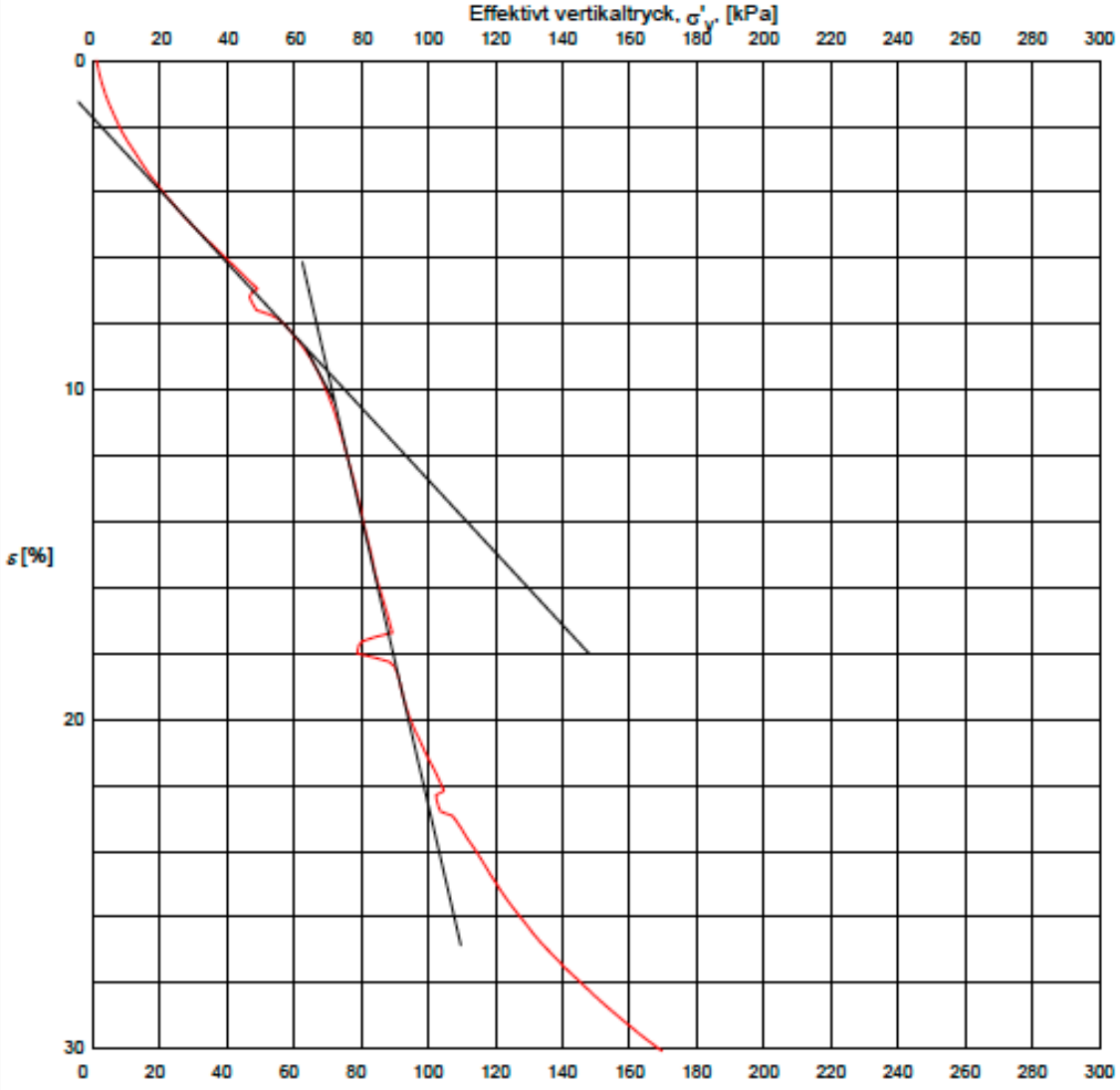

Försöket är utfört och utvärderat enligt Svensk Standard SS 027126. Utrustningens egendeformation är beaktad.

σ'_C, kPa	M_L, kPa	σ'_L, kPa
63	228	74

Anm.

SWECO GEOLAB, Gjörwellsgatan 22, Box 34044
100 26 STOCKHOLM, Tel: 08-695 60 00, Fax: 08-695 63 60
geolab@sweco.se, www.sweco.se/geolab, Ingår i SWECO VBB AB

P:\2172\Uppdrag 2006\18780b\la09_139.txt 2009-02-11

SWECO

4 (4)

SWECO GEOLAB

Redovisning av ödometerförsök, CRS-försök

Projekt: **E4, Förbifart Stockholm, Del B-km 23/500-28/000**

Uppdragsnummer: 216670-218	*Uppdragsgivare:* Konsortiet Förbifart Stockholm, Stockholm	*Datum/Sign:* 2009-02-11 *Löp-nr/Gransk.:* 18780b
Sektion/borrhål: 08F684 *Densitet:* 1,48 t/m^3 *Vattenkvot:* 104 % *Benämning:* Varvig lera	*Djup:* 5,0 m *Provningstemp.:* 20 °C	*Ödometer nr:* 1 *Provdiameter:* 50 mm *Provhöjd:* 20 mm *Def.hastighet:* 0,74 %/h

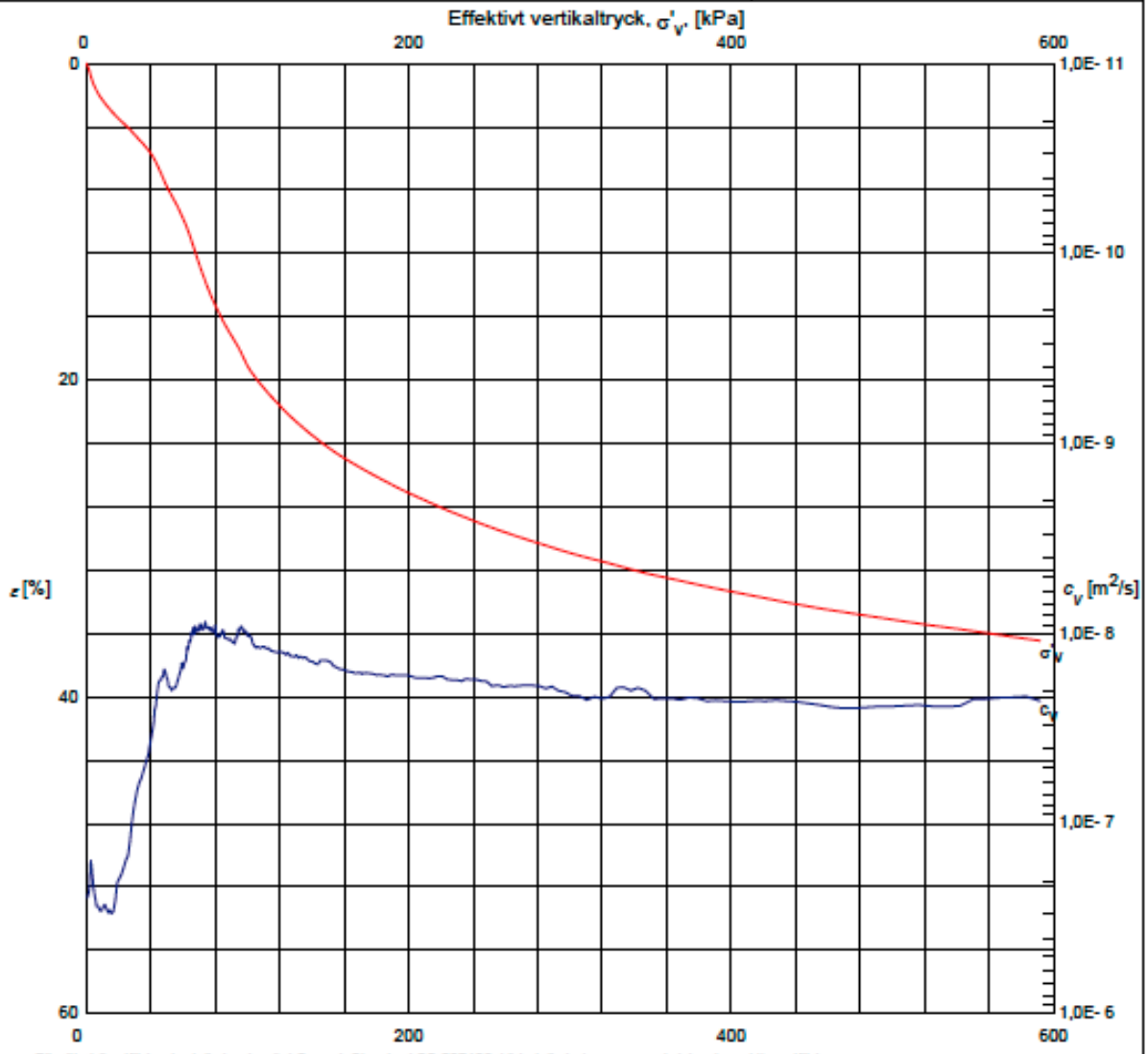

Försöket är utfört och utvärderat enligt Svensk Standard SS 027126. Vid utvärdering av c_v och k har korrektion utförts så att värdena motsvarar en temperatur av 7 °C. Utrustningens egendeformation är beaktad. För utvärdering se bilagda diagram sid 2 - 4.

σ'_C, kPa	M_L, kPa	σ'_L, kPa	M'	$c_{v,\,min}$, m^2/s	k_l, m/s	β_k
39	403	78	14,0	9,3E-9	8,7E-10	3,8

Anm.

SWECO GEOLAB, Gjörwellsgatan 22, Box 34044
100 26 STOCKHOLM, Tel: 08-695 60 00, Fax: 08-695 63 60
geolab@sweco.se, www.sweco.se/geolab, ingår i SWECO VBB AB

P:\2172\Uppdrag 2009\18780bib09_126.txt 2009-02-13

SWECO

1 (4)

Based on the CRS test results presented on the above the necessary input parameters are derived and presented as shown in the table below.

Material	Depth (m)	Δh [m]	Level z (m)	$\gamma\ [\frac{t}{m^3}]$	$\sigma_o'\ [kPa]$	$\sigma_L'\ [kPa]$	$M_0\ [kPa]$	$M_L\ [kPa]$	$M'\ [kPa]$	$c_v[\frac{m^2}{s}]$	$k_L\ [\frac{m}{s}]$
clay	0,0	0,0	13,8	1,760	38,0	81,0	3000	584,0	16,3	1,70E-08	5,50E-10
clay	2,0	2,0	11,8	1,600	33,0	67,0	3000	435,0	10,9	5,20E-09	3,70E-10
clay	3,2	1,2	10,6	1,635	57,5	82,5	3125	573,5	13,6	6,50E-09	2,10E-10
clay	3,8	0,6	10,0	1,610	36,0	70,0	2500	591,0	14,7	1,20E-08	2,30E-10
clay	4,2	0,4	9,6	1,620	36,0	70,0	2500	591,0	14,7	1,20E-08	1,80E-10
clay	4,8	0,6	9,0	1,650	41,0	65,0	2500	355,0	12,7	7,10E-09	8,00E-10
clay	5,2	0,4	8,6	1,550	57,5	77,5	3500	355,0	12,5	8,90E-09	6,40E-10
clay	5,8	0,6	8,0	1,660	38,0	63,0	3000	321,0	14,8	9,40E-09	1,20E-09
clay	6,2	0,4	7,6	1,480	39,0	78,0	4000	403,0	14,0	9,30E-09	8,70E-10
clay	7,2	1,0	6,6	1,670	63,0	102,0	3000	473,0	16,5	1,10E-08	1,50E-09
clay	7,8	0,6	6,0	1,670	67,0	107,0	3000	473,0	16,3	5,60E-09	5,60E-10
clay	8,2	0,4	5,6	1,700	69,0	101,0	3500	502,0	18,0	3,90E-09	2,60E-10
clay	9,2	1,0	4,6	1,680	82,0	107,0	3750	322,0	19,5	3,20E-09	2,50E-10
clay	10,2	0,6	4,0	1,660	71,0	110,0	3750	683,0	14,4	8,20E-09	4,80E-10

B_3 Settlement calculation of improved clay

In the analytical method (based on TK Geo 13) the calculation of the time dependent settlement was performed at three different calculation sections considering different input data's. The calculation sheet presented in here is only for one section, which is at section 180 for column spacing 0.8m, with thickness of clay is 9m.

Geometry of the column and area improvement ratio

d_{col} [m]	cc_{col} [m]	L_{col} [m]	Soil thickness [m]	Area ratio [a]
0,6	0,8	9	15	0,44

Elastic and secant modulus of the LCC were calculated using the empirical formula as per the recommendation of TK Geo 13 (2014).

$E_{col} = 13.C_{crit}^{1.6}\ [kPa]$ $E_{50} = 250.c_u\ [kPa]$ $C_u = C_{crit}$

Column	c_{crit} [kPa]	E_{col} [kPa]	E_{50}^{u} [kPa]
Upper half	120	27582	30000
Lower half	135	33303	33750

Deformation characteristics and strength parameters of the LCC

Upper half of the column (0-5 m)

E_{col} [kPa]	M_{block} [kPa]	$M_{soil(Mo)}$ [kPa]	$M_{soil(ML)}$ [kPa]	$\varphi'[°]$	$\varphi'[rad]$
27582	13945	3152	476	35	0,611

Lower half of the column (5- 10 m)

E_{col} [kPa]	M_{block} [kPa]	$M_{soil(Mo)}$ [kPa]	$M_{soil(ML)}$ [kPa]	$\varphi'[°]$	$\varphi'[rad]$
33303	16472	3152	476	35	0,611

Permeability

k_{soil}	k_{col}	k_{block}
1,7E-09	8,7E-07	3,84E-07

Load distribution in the upper and lower edge of the improved soil block.

β	η_{LC}	$q_{ö} = (1-\eta_{LC}).q$	$q_u = \eta_{LC}.q$
3,0	0,2	45,9	12,1

Temporary load applied on the LCC

Height of surcharge [m]	Unit weight [kN/m3]	q [kPa]	B (Width of trough) [m]	L (Length of trough) [m]
3.25	18	58.5	40	60

$\Delta\sigma = 58.5\ kPa$

Analytical Method _1

Time dependent Consolidation settlement of improved soil at section 27/180 cc_col 0.8m

Column Length		Lcolumn	9	m
Drainage	Single	L	9	m
Total settlement		Δs_{tot}	0,038	m
LCC influence radius		R=0.55*c/c	0,44	m
Radius of the column		r	0,3	
Relationship between influence radius and LCC radius		n=R/r	1,5	
Vertical cofficient of consolidation		Cvv	8,52E-09	m2/s
Horizontal coefficient of consolidation		Cvh	1,70E-08	m2/s
Permability of the clay soil (average)		k_{clay}	1,74E-09	
Permability of the LCC		k_{col}	2,89E-07	
Permability of the LCC soil block (Report 15)		k_{block}	1,29E-07	
Function		f(n)	0,34	

Time (days)	$-2*C_{vh}*t$ t(s)	$R^2*f(n)$	$\exp\left[\frac{-2*C_{vh}*t}{R^2*f(n)}\right]$	U (%)	Settlement (mm)	Remaining Settlement (mm)	Time (month)
0	0,000			0	0	37,6	
1	-0,003	0,07	0,96	4	1,6	36,0	
7	-0,021	0,07	0,73	27	10,1	27,6	
14	-0,041	0,07	0,54	46	17,4	20,2	
30	-0,088	0,07	0,26	74	27,7	9,9	1,0
60	-0,177	0,07	0,07	93	35,0	2,6	2,0
90	-0,265	0,07	0,02	98	37,0	0,7	3,0
180	-0,530	0,07	0,00	100	37,6	0,0	6,0
270	-0,795	0,07	0,00	100	37,6	0,0	9,0
365	-1,075	0,07	0,00	100	37,6	0,0	12,2
720	-2,120	0,07	0,00	100	37,6	0,0	24,0
1080	-3,181	0,07	0,00	100	37,6	0,0	36,0
1260	-3,711	0,07	0,00	100	37,6	0,0	42,0
1800	-5,301	0,07	0,00	100	37,6	0,0	60,0
14600	-42,997	0,07	0,00	100	37,6	0,0	486,7

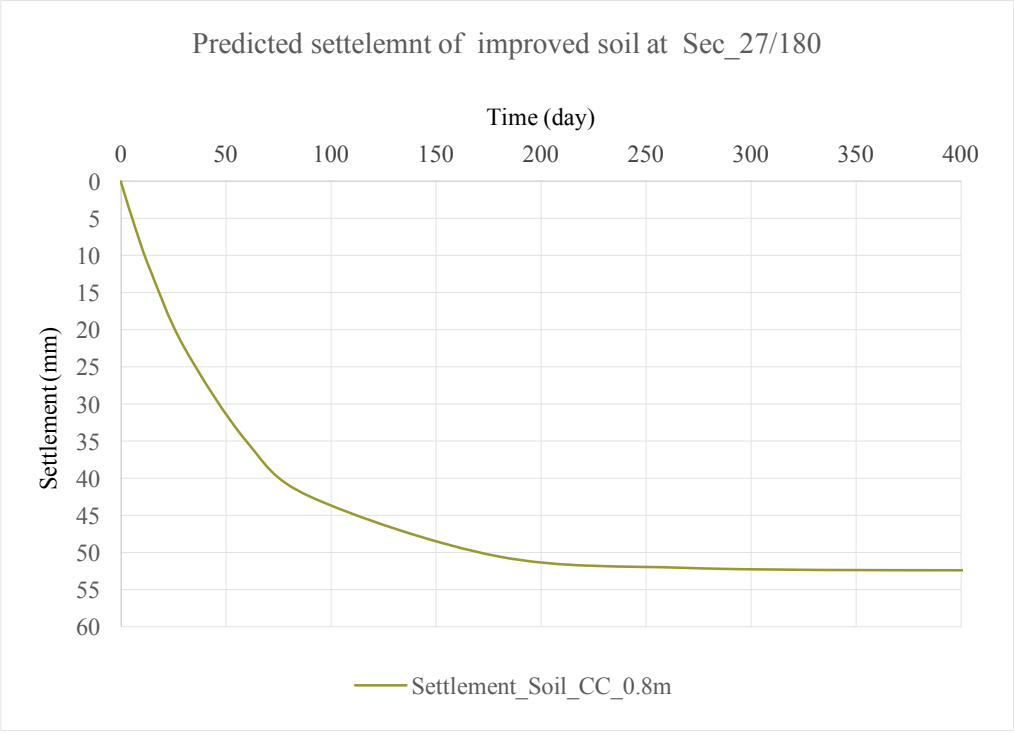

Time dependent Consolidation settlement improved soil at section 27/200

Column Length		Lcolumn	8	m
Drainage	Single	L	8	m
Total settlement		Δs_{tot}	0,048	m
LCC influence radius		R=0.55*c/c	0,55	m
Radius of the column		r	0,3	
Relationship between influence radius and LCC radius		n=R/r	1,8	
Vertical cofficient of consolidation		Cvv	8,55E-09	m2/s
Horizontal coefficient of consolidation		Cvh	1,71E-08	m2/s
Permability of the clay soil (average)		k_{clay}	1,76E-09	
Permability of the LCC		k_{col}	2,93E-07	
Permability of the LCC soil block (Report 15)		k_{block}	8,41E-08	
Function		f(n)	0,46	

Time (days)	$-2*C_{vh}*t$ t(s)	$R^2*f(n)$	$\exp\left[\frac{-2*C_{vh}*t}{R^2*f(n)}\right]$	U (%)	Settlement (mm)	Remaining Settlement (mm)	Time (month)
0	0,000			0	0	0	
1	-0,003	0,14	0,98	2	1,0	46,8	
7	-0,021	0,14	0,86	14	6,6	41,1	
14	-0,041	0,14	0,74	26	12,4	35,4	
30	-0,089	0,14	0,53	47	22,6	25,2	1,0
60	-0,177	0,14	0,28	72	34,5	13,3	2,0
90	-0,266	0,14	0,15	85	40,8	7,0	3,0
180	-0,532	0,14	0,02	98	46,8	1,0	6,0
270	-0,797	0,14	0,00	100	47,6	0,1	9,0
365	-1,078	0,14	0,00	100	47,8	0,0	12,2
720	-2,127	0,14	0,00	100	47,8	0,0	24,0
1080	-3,190	0,14	0,00	100	47,8	0,0	36,0
1260	-3,721	0,14	0,00	100	47,8	0,0	42,0
1800	-5,316	0,14	0,00	100	47,8	0,0	60,0
14600	-43,122	0,14	0,00	100	47,8	0,0	486,7

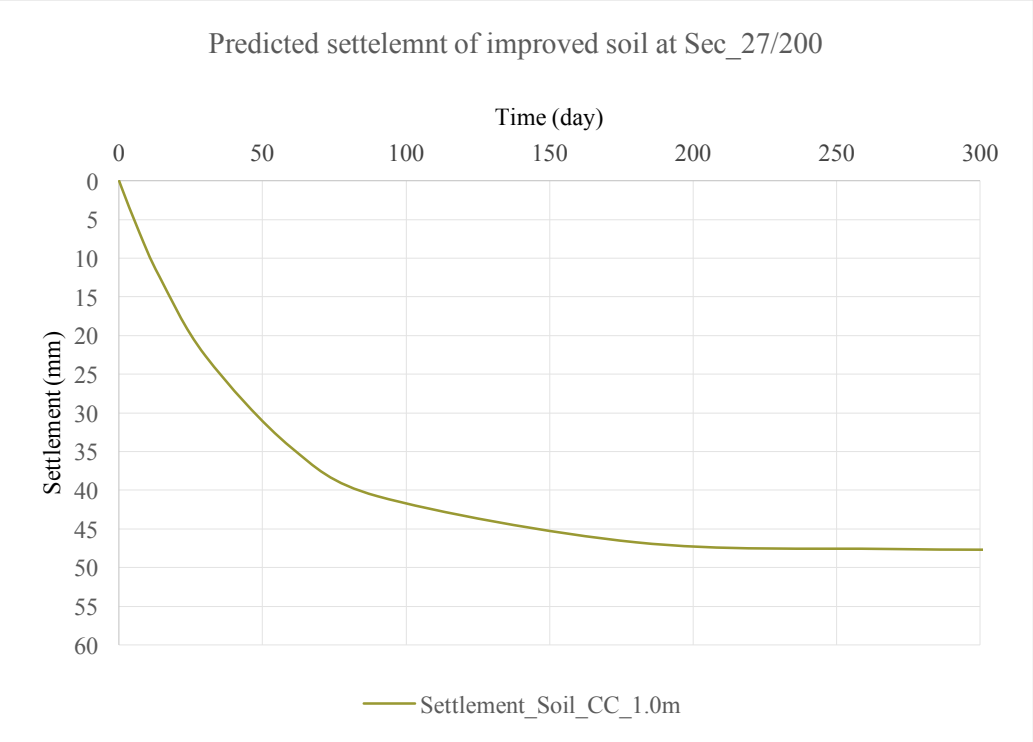

Time dependent Consolidation settlement improved soil at section 27/220

Column Length		Lcolumn	7,5	m
Drainage	Single	L	7,5	m
Total settlement		Δs_{tot}	0,046	m
LCC influence radius		R=0.55*c/c	0,55	m
Radius of the column		r	0,3	
Relationship between influence ardius and LCC radius		n=R/r	1,8	
Vertical cofficient of consolidation		Cvv	8,99E-09	m2/s
Horizontal coefficient of consolidation		Cvh	1,80E-08	m2/s
Permability of the clay soil (average)		k_{clay}	1,84E-09	
Permability of the LCC		k_{col}	9,21E-07	
Permability of the LCC soil block (Report 15)		k_{block}	2,62E-07	
Function		f(n)	1,07	

Time (days)	$-2*C_{vh}*t$ t(s)	$R^2*f(n)$	$\exp\left[\frac{-2*C_{vh}*t}{R^2*f(n)}\right]$	U (%)	Settlement (mm)	Remaining Settlement (mm)	Time (month)
0	0,000			0	0	0	
1	-0,003	0,32	0,99	1	0,4	46,0	
7	-0,022	0,32	0,93	7	3,0	43,4	
14	-0,044	0,32	0,87	13	5,9	40,6	
30	-0,093	0,32	0,75	25	11,7	34,8	1,0
60	-0,186	0,32	0,56	44	20,4	26,1	2,0
90	-0,280	0,32	0,42	58	27,0	19,5	3,0
180	-0,559	0,32	0,18	82	38,3	8,2	6,0
270	-0,839	0,32	0,07	93	43,0	3,4	9,0
365	-1,134	0,32	0,03	97	45,1	1,4	12,2
720	-2,237	0,32	0,00	100	46,4	0,0	24,0
1080	-3,356	0,32	0,00	100	46,5	0,0	36,0
1260	-3,915	0,32	0,00	100	46,5	0,0	42,0
1800	-5,594	0,32	0,00	100	46,5	0,0	60,0
14600	-45,370	0,32	0,00	100	46,5	0,0	486,7

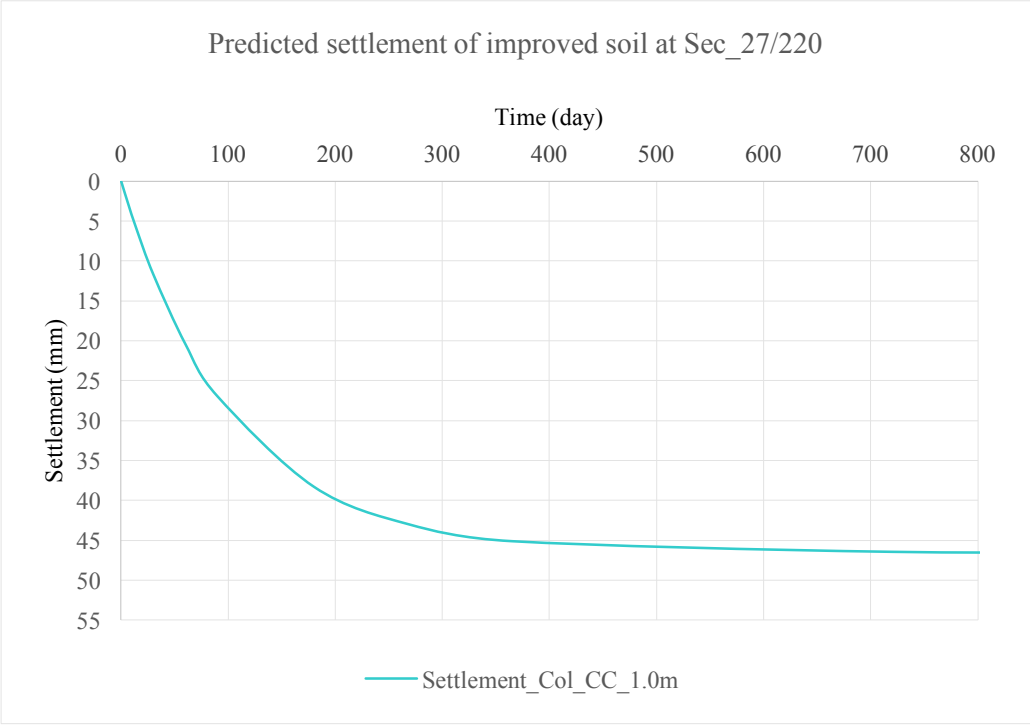

Analytical Method_2

Predicted settlement of improved soil at section 27/180 cc_col 0.8m

Equilibrium Method:		Upper half Column	Lower half Column
Area of the column	$A_c[m^2]$	0,28	
Area of the column and the surrounding soil	$A[m^2$	0,64	
Area Improvement ratio	a	0,44	
Stress in the column	$\sigma_c[kPa]$	119,80	
Stress in the soil	$\sigma_s[kPa]$	9,98	
Modular Ratio	m	12,00	13,50
Total applied stress	$\sigma[kPa]$	58,50	
Ratio of stress in the column to average stress	μ_c	2,048	
Ratio of stress in the soil to average stress	μ_s	0,171	0,153
Coefficent of volume compressibility of the column	m_{vc}	3,33E-05	2,96E-05
Coefficent of volume compressibility of the soil	m_{vs}	0,0004	0,0004
Poissnoes ratio of the soil	υ	0,30	
Thickness of the soft soil	$H[m]$	4,50	
Settlement of clay	$S_0(m)$	0,105	0,105
Settlement upper and lower column	$S[m]$	0,018	0,016
Final settlement	$S[m]$	0,034	
Settlement Reduction ratio	β	0,171	0,153

Cr	1,70E-08	P1	2,69E-01
H	4,5	P2	0,00
ns	12,00	P3	0,16
n	2,67	P4	1,09
kr	1,74E-09	Fm	1,52E+00
ks	1,74E-09		
kc	2,89E-07		
rs	0,4448		
rc	0,3		
dc	0,60		
s	1,48		
de	1,6		
Crm	4,32E-08		

Time (day)	Trm	EXP(-8*Trm/Fm)	Ur (%)	Tv	Uv (%)	Uvr (%)	Settlement (mm)	Remaining Settlement (mm)
0	0,000	1,000	0	0,00	0	0	0	34
1	0,001	0,992	1	0,01	14	14	5	29
7	0,010	0,948	5	0,10	36	40	14	21
14	0,020	0,898	10	0,21	52	56	19	15
30	0,044	0,794	21	0,45	73	79	27	7
60	0,088	0,631	37	0,89	91	94	32	2
90	0,131	0,501	50	1,34	97	99	34	1
180	0,263	0,251	75	2,68	100	100	34	0
270	0,394	0,126	87	4,03	100	100	34	0
365	0,533	0,061	94	5,44	100	100	34	0
720	1,050	0,004	100	10,73	100	100	34	0
1080	1,576	0,000	100	16,10	100	100	34	0
1260	1,838	0,000	100	18,79	100	100	34	0
1800	2,626	0,000	100	26,84	100	100	34	0
14600	21,300	0,000	100	217,67	100	100	34	0

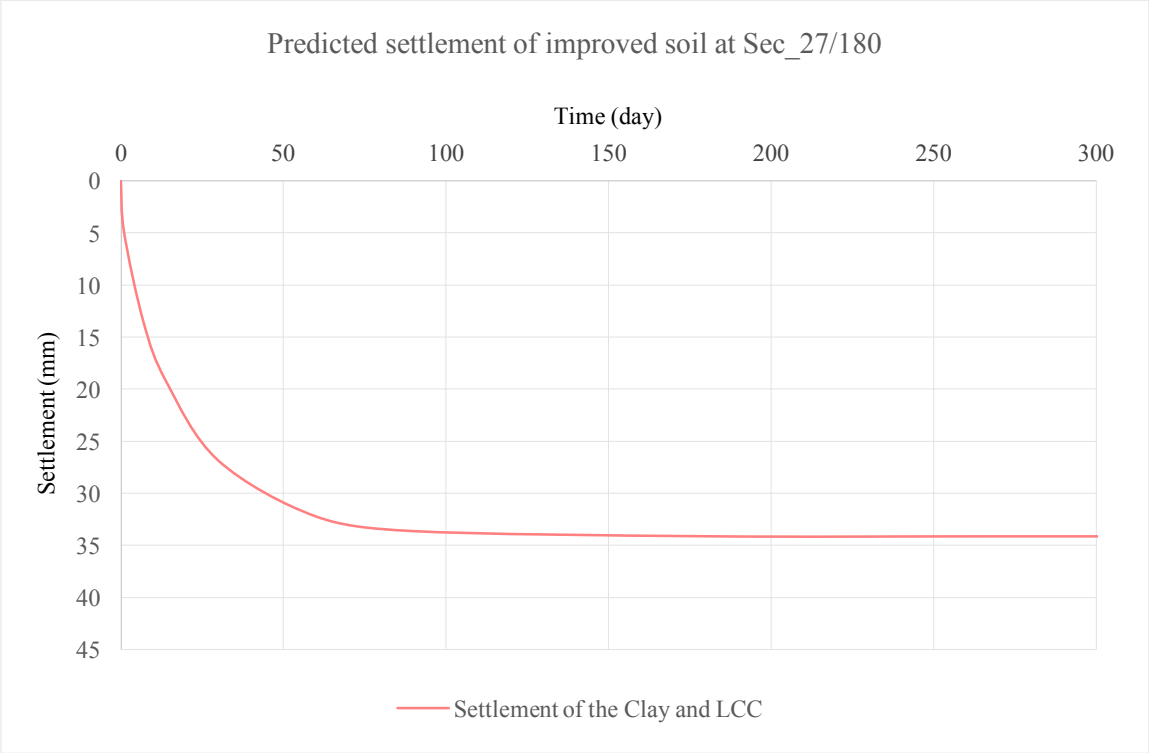

Settelemnt of improved clay soil at section 27/200 cc_col 1.0m

Equilibrium Method:		Upper part	Lower part
Area of the column	$A_c[m^2]$	0,28	
Area of the column and the surrounding soil	$A[m^2$	1,00	
Area Improvement ratio	a	0,28	
Stress in the column	$\sigma_c[kPa]$	170,80	
Stress in the soil	$\sigma_s[kPa]$	14,23	
Modular Ratio	m	12,00	13,50
Total applied stress	$q[kPa]$	58,50	
Ratio of stress in the column to average stress	μ_c	2,920	
Ratio of stress in the soil to average stress	μ_s	0,243	0,221
Coefficent of volume compressibility of the column	m_{vc}	3,33E-05	2,96E-05
Coefficent of volume compressibility of the soil	m_{vs}	4,00E-04	0,0004
Poissnoes ratio of the soil	v	0,30	
Thickness of the soft soil	$H[m]$	4,50	
Settlement of clay	$S_0(m)$	0,105	0,105
Settlement	$S[m]$	0,026	0,023
Final settlement	$S[m]$	0,049	
Settlement Reduction ratio	β	0,243	0,221

Cr	1,80E-08	P1	2,69E-01
H	4	P2	0,00
ns	12,00	P3	0,16
n	2,67	P4	0,86
kr	1,84E-09	Fm	1,29E+00
ks	1,84E-09		
kc	3,07E-07		
rs	0,4448		
rc	0,3		
dc	0,60		
s	1,48		
de	1,6		
Crm	3,66E-08		

Time(day)	Trm	EXP(-8*Trm/Fm)	Ur (%)	Tv	Uv (%)	Uvr (%)	Settlement (mm)	Remaining Settlement (mm)
0	0,000	1,000	0	0,00	0	0	0	43
1	0,001	0,992	1	0,01	14	14	6	37
7	0,010	0,948	5	0,10	36	40	17	26
14	0,020	0,898	10	0,21	52	56	25	19
30	0,044	0,794	21	0,45	73	79	34	9
60	0,088	0,631	37	0,89	91	94	41	2
90	0,131	0,501	50	1,34	97	99	43	1
180	0,263	0,251	75	2,68	100	100	43	0
270	0,394	0,126	87	4,03	100	100	43	0
365	0,533	0,061	94	5,44	100	100	43	0
720	1,050	0,004	100	10,73	100	100	43	0
1080	1,576	0,000	100	16,10	100	100	43	0
1260	1,838	0,000	100	18,79	100	100	43	0
1800	2,626	0,000	100	26,84	100	100	43	0
14600	21,300	0,000	100	217,67	100	100	43	0

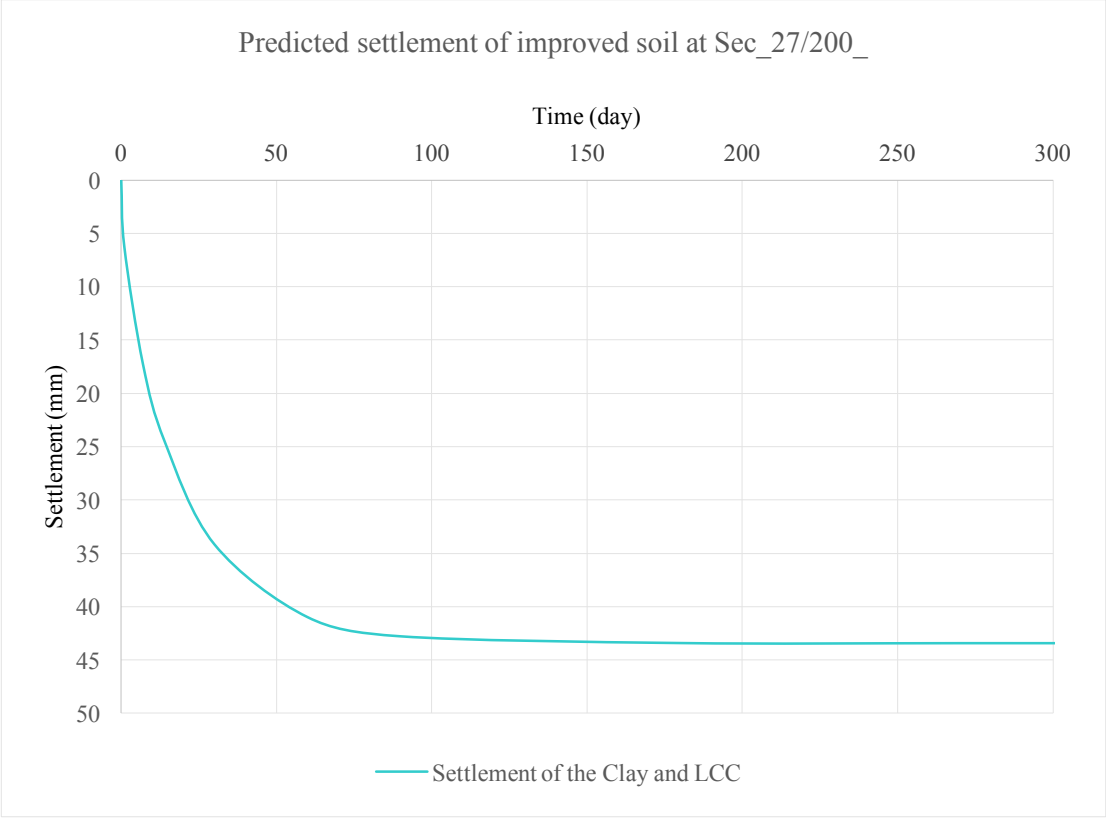

Settlement of improved clay soil at section 27/220 cc_col 1.0m

Equilibrium Method:		Upper part	Lower part
Area of the column	$A_c[m^2]$	0,28	
Area of the column and the surrounding soil	$A[m^2$	1,00	
Area Improvement ratio	a	0,28	
Stress in the column	$\sigma_c[kPa]$	170,80	
Stress in the soil	$\sigma_s[kPa]$	14,23	
Modular Ratio	m	12,00	13,50
Total applied stress	$q[kPa]$	58,50	
Ratio of stress in the column to average stress	μ_c	2,920	
Ratio of stress in the soil to average stress	μ_s	0,243	0,221
Coefficent of volume compressibility of the column	m_{vc}	3,33E-05	2,96E-05
Coefficent of volume compressibility of the soil	m_{vs}	4,00E-04	0,0004
Poissnoes ratio of the soil	v	0,30	
Thickness of the soft soil	$H[m]$	4,00	
Settlement of clay	$S_0(m)$	0,094	0,094
Settlement	$S[m]$	0,023	0,021
Final settlement	$S[m]$	0,043	
Settlement Reduction ratio	β	0,243	0,221

Cr	1,80E-08	P1	2,69E-01
H	3,5	P2	0,00
ns	12,00	P3	0,16
n	2,67	P4	0,66
kr	1,84E-09	Fm	1,09E+00
ks	1,84E-09		
kc	3,07E-07		
rs	0,4448		
rc	0,3		
dc	0,60		
s	1,48		
de	1,6		
Crm	2,76E-08		

Time(day)	Trm	EXP(-8*Trm/Fm)	Ur (%)	Tv	Uv (%)	Uvr (%)	Settlement (mm)	Remaining Settlement (mm)
0	0,000	1,000	0	0,00	0	0	0	38
1	0,001	0,992	1	0,01	14	14	5	33
7	0,010	0,948	5	0,10	36	40	15	23
14	0,020	0,898	10	0,21	52	56	21	17
30	0,044	0,794	21	0,45	73	79	30	8
60	0,088	0,631	37	0,89	91	94	36	2
90	0,131	0,501	50	1,34	97	99	37	1
180	0,263	0,251	75	2,68	100	100	38	0
270	0,394	0,126	87	4,03	100	100	38	0
365	0,533	0,061	94	5,44	100	100	38	0
720	1,050	0,004	100	10,73	100	100	38	0
1080	1,576	0,000	100	16,10	100	100	38	0
1260	1,838	0,000	100	18,79	100	100	38	0
1800	2,626	0,000	100	26,84	100	100	38	0
14600	21,300	0,000	100	217,67	100	100	38	0

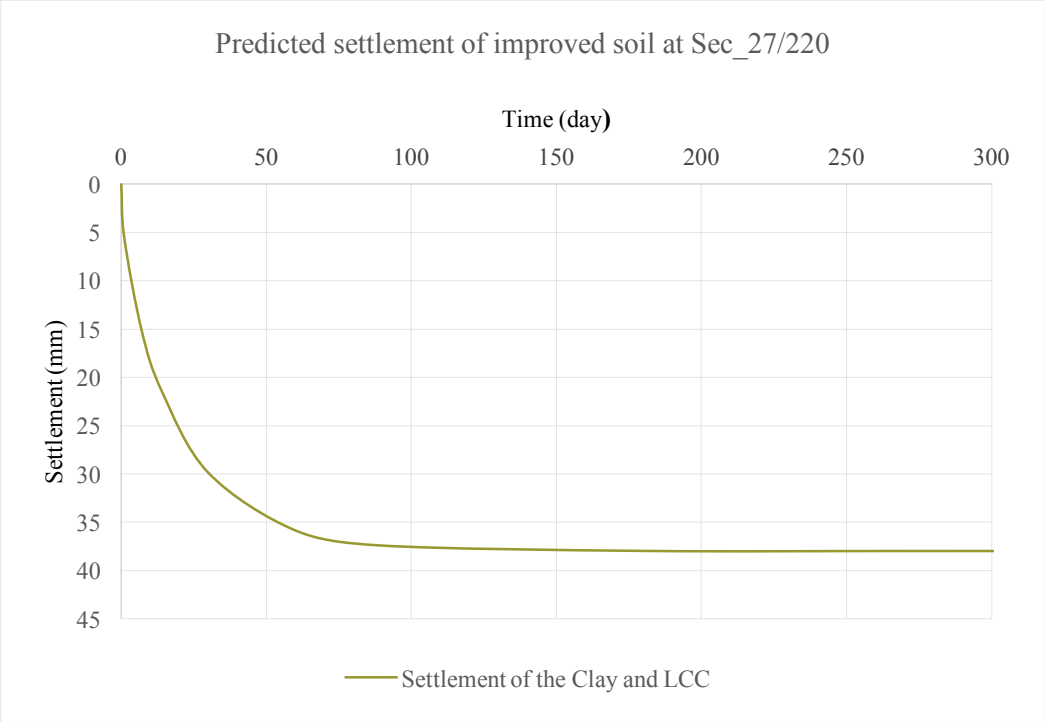
Predicted settlement of improved soil at Sec_27/220
Time (day)
0
50
100
150
200
250
300
Settlement (mm)
0
5
10
15
20
25
30
35
40
45
Settlement of the Clay and LCC

Appendix C

Input data for numerical analysis

C_1 Input data for Plaxis simulation

In the numerical analysis of 2D Plaxis simulation different material models had been used for the clay soil and the LCC. The basic input parameters used in the simulation are presented in the table. Three different methods were applied in relation to the conversion of the axisymmetric model to the 2D plane strain model. Plane strain method one is a parameter matching, plane strain method two is the geometry matching and the third one is the combined matching.

Input data for plane strain method_ Geometry Matching

Material type	Material Model	Drainage type	E_{50}^{u} (kPa)	c' (kPa)	φ' (deg)	λ^*	k^*	v'	k_h (m/day)	k_v (m/day)	γ_{sat} kN/m3)	γ_{unsat} kN/m3)
Clay	Soft soil	Undrained (A)	-	2	30	0,12	0,018	0,3	1,50E-04	5,00E-05	16,5	15
Lime/cement column_1	Mohr-Coulomb	Undrained (A)	30000	55	35	-	-	0,3	1,50E-03	5,00E-04	17	17
Lime/cement column_2	Mohr-Coulomb	Undrained (A)	33750	62	35	-	-	0,3	1,50E-03	5,00E-04	17	17

Material type	Material Model	Drainage type	E_{50}^{u} (kPa)	c' (kPa)	φ' (deg)	v'	k_h (m/day)	k_v (m/day)	γ_{sat} (kN/m3)	γ_{unsat} (kN/m3)
Clay	Mohr-Coulomb	Undrained (A)	2500	2	30	0,3	1,50E-04	5,00E-05	16,5	15
Lime/cement column	Mohr-Coulomb	Undrained (A)	30000	55	35	0,3	1,50E-03	5,00E-04	17	17
Lime/cement column	Mohr-Coulomb	Undrained (A)	33750	62	35	0,3	1,50E-03	5,00E-04	17	17

Material type	Material Model	Drainage type	c' (kPa)	φ' (deg)	λ^*	k^*	v'	k_h (m/day)	k_v (m/day)	γ_{sat} (kN/m3)	γ_{unsat} (kN/m3)
Clay	Soft soil	Undrained (A)	2	32	0,12	0,018	0,3	1,50E-04	5,00E-05	16,5	15
Lime/cement column	Soft soil	Undrained (A)	55	35	0,16	0,006	0,3	1,50E-03	5,00E-04	17	17
Lime/cement column	Soft soil	Undrained (A)	65	35	0,16	0,006	0,3	1,50E-03	5,00E-04	17	17

Input data for plane strain method Combined Matching

Material type	Material Model	Drainage type	E_{50}^{u} (kPa)	c' (kPa)	φ' (deg)	λ^*	k^*	v'	k_h (m/day)	k_v (m/day)	γ_{sat} (kN/m3)	γ_{unsat} (kN/m3)
Clay	Soft soil	Undrained (A)	2500	2	30	0,12	0,018	0,3	1,22E-03	4,06E-04	16,5	15
Lime/cement column_1	Mohr-Coulomb	Undrained (A)	24089	55	35	-	-	0,3	1,22E-02	4,06E-03	17	17
Lime/cement column_2	Mohr-Coulomb	Undrained (A)	27044	62	35	-	-	0,3	1,22E-02	4,06E-03	17	17

Material type	Material Model	Drainage type	E_{50}^{u} (kPa)	c' (kPa)	φ' (deg)	v'	k_h (m/day)	k_v (m/day)	γ_{sat} (kN/m3)	γ_{unsat} (kN/m3)
Clay	Mohr-Coulomb	Undrained (A)	2500	2	30	0,3	1,22E-03	4,06E-04	16,5	15
Lime/cement column	Mohr-Coulomb	Undrained (A)	24089	55	35	0,3	1,22E-02	4,06E-03	17	17
Lime/cement column	Mohr-Coulomb	Undrained (A)	27044	62	35	0,3	1,22E-02	4,06E-03	17	17

Material type	Material Model	Drainage type	c' (kPa)	φ' (deg)	λ^*	k^*	v'	k_h (m/day)	k_v (m/day)	γ_{sat} (kN/m3)	γ_{unsat} (kN/m3)
Clay	Soft soil	Undrained (A)	2	32	0,12	0,018	0,3	1,22E-03	4,06E-04	16,5	15
Lime/cement column	Soft soil	Undrained (A)	55	35	0,16	0,006	0,3	1,22E-02	4,06E-03	17	17
Lime/cement column	Soft soil	Undrained (A)	62	35	0,16	0,006	0,3	1,22E-02	4,06E-03	17	17

Curve fitting was performed based on the CRS test results run in Plaxis in order to determine the modified swelling K^* and compression λ^* indices. The resulted curves are presented below.

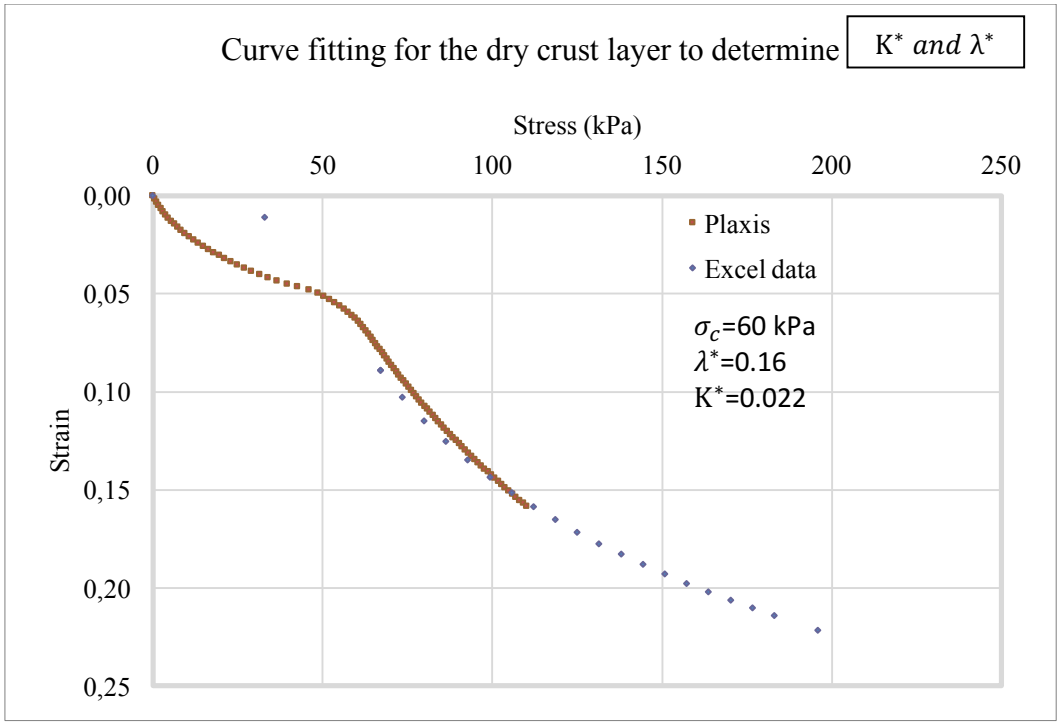

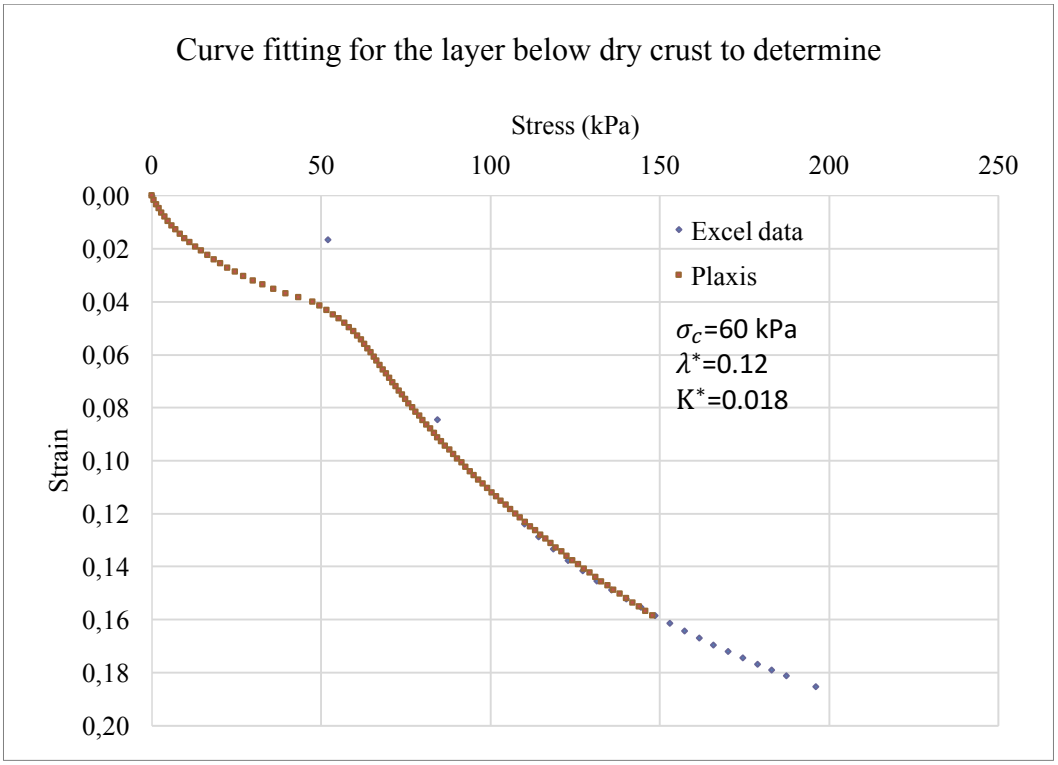

In put data for numerical calculation derived based on the CRS test results.

					Clay		Lime/ cement column				
Material	Depth [m]	ρ[t/m^3]	σ_c' [kPa]	σ_{vo}' [kPa]	w_L	K_o	w_L	K_o	OCR_{K_o}	OCR	e_{int}
Dry crust	0,0	1,76	38,0	0,00	0,425	0,47	0,379	0,44	1,44	8,72	0,64
Dry crust	0,5	1,76	33,0	8,80	0,420	0,47	0,374	0,43	1,30	7,37	0,64
Dry crust	1,0	1,76	33,0	17,60	0,420	0,47	0,374	0,43	1,20	6,38	0,64
Dry crust	1,5	1,76	33,0	26,40	0,420	0,47	0,374	0,43	1,12	5,62	0,64
clay	2,0	1,60	33,0	34,40	0,420	0,47	0,370	0,43	1,05	5,08	0,63
clay	2,5	1,60	33,0	37,40	0,420	0,47	0,370	0,43	1,03	4,90	0,63
clay	3,0	1,60	33,0	40,40	0,420	0,47	0,370	0,43	1,01	4,73	0,63
clay	3,5	1,64	57,5	43,58	0,510	0,53	0,451	0,49	1,13	4,57	0,77
clay	4,0	1,61	36,0	46,63	0,600	0,59	0,530	0,54	1,23	4,42	0,90
clay	4,5	1,62	60,0	49,73	0,560	0,57	0,495	0,52	1,16	4,28	0,84
clay	5,0	1,65	41,0	52,98	0,540	0,55	0,479	0,51	1,11	4,14	0,81
clay	5,5	1,55	57,5	55,73	0,510	0,53	0,448	0,49	1,05	4,03	0,76
clay	6,0	1,66	38,0	59,03	0,500	0,52	0,443	0,48	1,02	3,91	0,75
clay	6,5	1,48	39,0	61,43	0,505	0,53	0,441	0,48	1,01	3,82	0,75
clay	7,0	1,48	39,0	63,83	0,505	0,53	0,441	0,48	0,99	3,74	0,75
clay	7,5	1,67	63,0	67,18	0,465	0,50	0,412	0,46	0,94	3,63	0,70
clay	8,0	1,67	67,0	70,53	0,455	0,49	0,403	0,45	0,91	3,53	0,69
clay	8,5	1,70	69,0	74,03	0,480	0,51	0,427	0,47	0,93	3,43	0,73
clay	9,0	1,70	69,0	77,53	0,480	0,51	0,427	0,47	0,91	3,33	0,73
clay	9,5	1,68	82,0	80,93	0,480	0,51	0,426	0,47	0,90	3,24	0,72
clay	10,0	1,68	82,0	84,33	0,480	0,51	0,426	0,47	0,89	3,16	0,72

In the numerical calculation, the settlement of the column and the clay are plotted in one to make a comparison between them. The figure shows that higher settlement of clay soil in between column when the column spacing and the depth of clay are higher. In this case the clay and the column have different deformation.

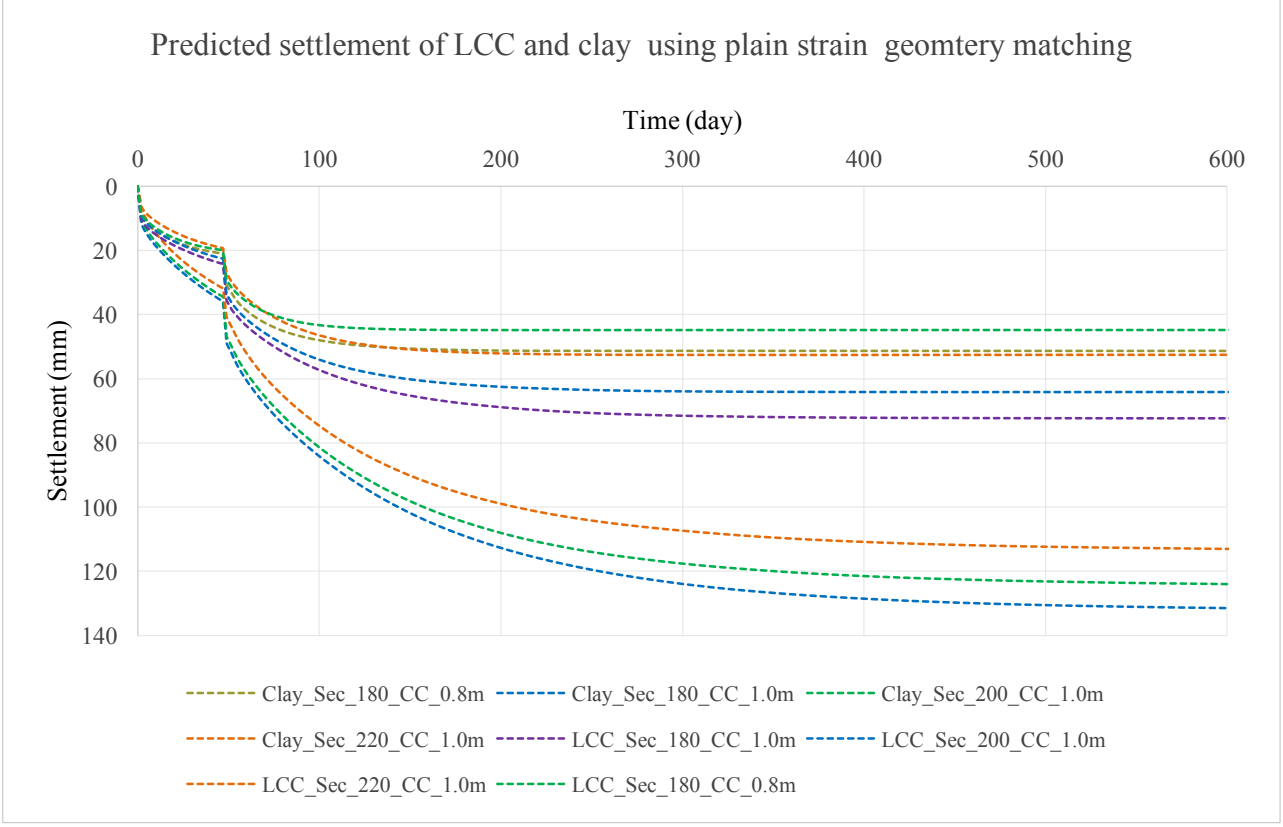

Figure C_1 Predicted settlement of the LCC and the clay in between the LCC

The Plaxis simulation also performed to analyze the vertical displacement of improved clay soil and how the excess pore water development looks through depth.

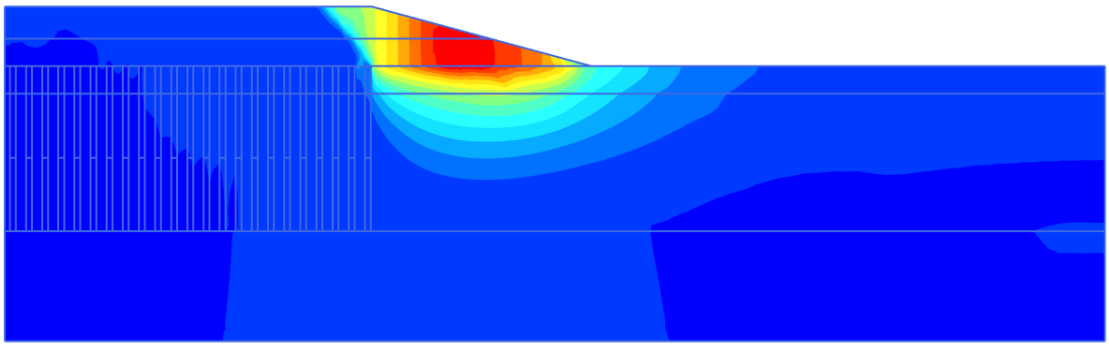

Figure C_2 Simulated vertical displacement of the improved clay soil

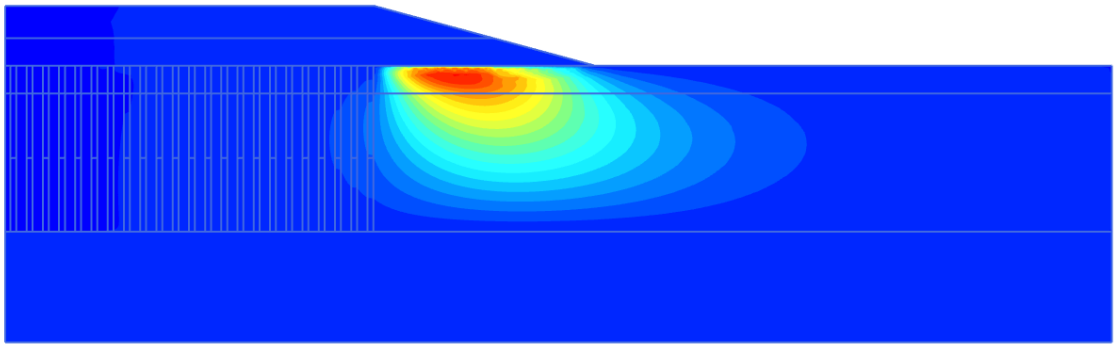

Figure C_3 Simulated excess pore water pressure developed due to the application of the over load

Results on sensitivity analysis run to check the influence of the permeability of the LCC and the clay soil on the vertical deformation of the improved soil. This analysis was performed using the geometry matching model at section 200.

Plaxis Sensitivity Analysis & Parameter variation

Settings | Select parameters | **Sensitivity analysis** | Parameter variation

Type	Material	Parameter	Min	Ref	Max	SensiScore
Soil	Clay	k_x	0,1220E-3	1,220E-3	0,01220	30
Soil	Clay	k_y	0,04060E-3	0,4060E-3	0,04060	19
Soil	LC column	k_x	1,220E-3	0,01220	0,1220	1
Soil	LC column	k_y	0,4060E-3	4,060E-3	0,04060	50

The second sensitivity analysis was preformed to check the most influencing parameter on the vertical deformation of the improved clay soil.

Plaxis Sensitivity Analysis & Parameter variation

Settings | Select parameters | **Sensitivity analysis** | Parameter variation

Type	Material	Parameter	Min	Ref	Max	SensiScore
Soil	Clay	λ* (lambda*)	0,1000	0,1200	0,1400	8
Soil	Clay	κ* (kappa*)	0,01600	0,01800	0,02000	0
Soil	Clay	k_x	0,1220E-3	1,220E-3	0,01220	3
Soil	Clay	k_y	0,04060E-3	0,4060E-3	4,060E-3	1
Soil	Clay	c'_{ref}	1,500	2,000	2,500	0
Soil	LC column	E'	20,00E3	22,28E3	25,00E3	84
Soil	LC column	c'_{ref}	65,00	69,00	75,00	0
Soil	LC column	k_x	1,220E-3	0,01220	0,1220	0
Soil	LC column	k_y	0,4060E-3	4,060E-3	0,04060	4

Appendix D

Field measurements

Datum	Mätning	P01	P02	P03	P04	P05	P06	P07	P08	P09	P10	P11	P12	P13	P14	P15	P16	P17	P18	P19	P20	P21	P22	P23
2017-06-22	0	0	0	0	0	0	0	0	0	0	0	0	0	0	0	0	0	0	0	0	0	0	0	0
2017-06-26	2	-3	-1	-2	1	2	-0	0	0	-0	-1	-1	-0	0	-2	-1	5	-1	1	1	-2	0	-1	-0
2017-06-29	3	-4	-3	-3	-1	-3	-2	-2	-2	-3	-2	-3	-2	-5	-5	-4	-4	-4	-3	-3	-4	-3	-4	-3
2017-07-03	4	-3	-4	-6	-2	-3	-5	-4	-1	-4	-5	-10	-6	-7	-7	-6	-3	-5	-4	-5	-4	-4	-5	-5
2017-07-06	5	-4	-3	-7	-4	-1	-2	-4	-3	-4	-4	-6	-5	-8	-8	-2	-3	-3	-5	-5	-5	-4	-6	-4
2017-07-10	6	-5	-3	-3	-2	-1	-1	1	-1	-2	-3	-5	-7	-5	-1	-1	1	-4	-3	-1	-2	-1	0	1
2017-07-13	7	-7	-7	-5	-5	-3	-3	-3	-3	-3	-7	-6	-10	-23	-13	-9	-4	-6	-7	-6	-11	-13	-13	-14
2017-07-17	8	-11	-10	-55	-4	-10				-4	-7	-11	-15	-26	-16	-12	-5	-9	-7	-8	-14	-18	-17	-14
2017-07-20	9	-10	-21	-60	-13	-13	-15	-4	-4	0	-20	-23	-29	-33	-20	-16	-2	-22	-21	-20	-26	-21	-18	-24
2017-07-24	10	-10	-23	-63	-17	-18	-29	-14	-5		-18	-31	-36	-43	-27	-19	-11	-21	-21	-20	-33	-24	-21	-17
2017-07-27	11	-21	-26	-66	-21	-17	-28	-16	-19	-15	-23	-34	-38	-45	-30	-21	-11	-25	-25	-18	-33	-25	-20	-19
2017-07-31	12	-23	-28	-67	-20	-19	-28	-20	-23	-21	-29	-35	-42	-48	-31	-25	-11						-19	-17
2017-08-03	13	-25	-32	-70	-23	-23	-30	-22	-25	-28	-33	-44	-51	-53	-33	-25	-13	-41	-7	-23		-20	-30	-15
2017-08-10	14	-22	-29	-72	-23	-20	-31	-23	-26	-15	-30	-40	-49	-54	-36	-26	-13	-33	-22	-26	-33	-29	-25	-3
2017-08-18	15	-24	-31	-74	-25	-21		-21	-25	-19	-32	-44	-51	-56	-35	-26	-10	-33	-24	-28	-37	-29	-23	0
2017-08-24	16	-25	-30	-73	-24	-21	-30	-20		-18	-32	-44	-52	-57	-37	-25	-12	-32	-23	-28	-35	-25	-21	1
2017-09-01	17				-27	-23					-28	-43					-11					-37	-30	5
2017-09-07	18			-30	-27	-23	-34	-25				-43								-45			-41	-2
2017-09-14	19			-33	-28		-34	-25			-29	-44		-59	-43	-36	-13	-37	-40	-51	-84	-49	-53	-20
2017-09-21	20			-31	-29	-24	-34				-28	-45		-61	-46	-36	-14	-37	-40	-50	-94	-53	-58	-24
2017-09-28	21			-34	-29		-34	-24			-30	-46		-62	-46	-34	-13	-39	-43		-96	-54	-59	-20
2017-10-05	22			-32	-28	-24	-34	-25			-29	-44		-60	-47	-35	-12	-39	-41	-50	-99	-56	-60	-22
2017 10 12	23			-26	-23	-19					-23	-41		-58	-45	-31	-10	-31	-34	-46	-97	-51	-58	-17